2016

Starch structures and properties affected by genetics and by environment

Hanyu Yangcheng
Iowa State University

Starch structures and properties affected by genetics and by environment

by

Hanyu Yangcheng

A dissertation submitted to the graduate faculty

in partial fulfillment of the requirements for the degree of

DOCTOR OF PHILOSOPHY

Major: Food Science and Technology

Program of Study committee:
Jay-lin Jane, Major Professor
Zhiyou Wen
Buddhi Lamsal
Paul Scott
Michael Blanco

Iowa State University

Ames, Iowa

2016

TABLE OF CONTENTS

ACKNOWLEDGEMENTS

I would like to express my sincere gratitude and respect to the following:

To my major professor, Dr.Jay-lin Jane, for her guidance, encouragement, and providing me with insight that will help me to succeed in my future career;

To my committees, Drs.Michael Blanco, Paul Scott, Zhiyou Wen, and Buddhi Lamsal for their valuable time, patience, advices, and help;

To my colleagues and co-workers, Drs. Candice Gardner, Hongxin Jiang, Yongfeng Ai, Jelena Medic, Steve Cannon, Vikas Belamkar, Xuehong Li, and Lingxiao Gong, and Mr.Michael Reed, Mr.Samuel Moore, for their generous time and kind help;

To Department of Food Science and Human Nutrition for the numerous assistance;

To my friends in Ames, for all the great time and encouragement;

Finally, I want to give thanks to my family, for their understanding, encouragement, and endless support during my Ph.D. study.

ABSTRACT

Functionalities of starch for food and non-food applications are dependent on the starch structures and properties, which are affected by both the genetics and the growing conditions of the crop. Objectives of this dissertation research were to 1) Understand the unique properties of Tibetan hull-less barley starches, their structures, and the impacts of growing conditions; and 2) Understand dosage effects of waxy gene on the contents and structures of amylose and amylopectin and properties of corn starch; and 3) Understand the starch physicochemical properties of *Apios* mother and child tuber and the mechanism of starch development.

Tibetan hull-less barley varieties, BQ and KQ, were grown at two locations with different growing temperatures and rainfall. The BQ starches displayed significantly lower onset-gelatinization temperature, larger gelatinization-temperature range, and higher peak viscosities than the KQ starches. The differences in starch thermal and pasting properties between BQ and KQ starches were attributed to the annealing of starch and enhanced amylose-lipid complex formation, resulting from higher growing temperature and more rainfall during the development of the KQ starches.

Reciprocal crossing of isogenic normal and waxy corn lines was conducted to develop hybrids with different dosages of waxy gene (3, 2, 1, 0) in the endosperm. The amylose content of starch and proportion of extra-long branch-chains negatively correlated with dosages of the *waxy* gene. The proportion of short chains (DP < 17) positively correlated, whereas that of intermediate chains (DP 17-30) negatively correlated with dosages of the *waxy* gene. The conclusion gelatinization-temperature and gelatinization temperature-range of the starch were positively correlated with the waxy-gene dosage, indicating that amylose facilitates gelatinization of the surrounding crystallites of amylopectin.

Apios americana is a wild legume bearing edible tubers. Domestication of *Apios* is in process because of the superior nutritional value of the tuber. The harvested *Apios* tuber can be planted in the following year as the mother tuber to further grow and produce child tubers. The *Apios* mother-tuber starch displayed higher degree of crystallinity, greater gelatinization enthalpy-change, longer branch-chain length of amylopectin, and lower pasting viscosity than the counterpart child-tuber starch. The mother-tuber starch of *Apios* 2127 showed two peaks of gelatinization, which was attributed to two groups of starch granules having different structures and gelatinization temperatures. The group of starch granules with a higher gelatinization-temperature was carried over from the previous year and went through a longer annealing process during the two-year growing of the tuber. These results of this dissertation research demonstrated significant effects of both genetics and the growing conditions on starch structures and properties.

DISSERTATION ORGANIZATION

The dissertation consists of a general introduction and four chapters. The first chapter of the dissertation is a review of literature on the background knowledge and information relating to the research topics. The second chapter, "Physicochemical properties of Tibetan hull-less barley starch," has been published in *Carbohydrate Polymers* (Vol.137, pp 525-531); The third chapter, "Dosage effects of *waxy* gene on the structures and properties of corn starch," has been submitted to *Carbohydrate Polymers*; The fourth chapter, "Characterization and development mechanism of *Apios americana* tuber starch," has been submitted to *Carbohydrate Polymers*. Literature cited in the Literature Review is listed in the alphabetical order of the first author's last name.

GENERAL INTRODUCTION

Starch is the second most abundant carbohydrate on earth next to cellulose. Starch is produced in green plants through photosynthesis and complex reactions and is found in different organs of the plant, including seed, root, tuber, fruit, stem, and leaf for energy storage. Native starch is present in the granular form, and starch granules vary in shapes (spherical, oval, polygonal, disk, etc.) and sizes (from <1 to >100 μm), depending on the botanical origin and stage of development of the starch. Starch consists of two polysaccharides: amylose and amylopectin. Amylose is primarily a linear molecule comprised of D-glucopyranose units linked by α-1,4 glycosidic bonds with a few branches. Amylopectin has a highly branched structure, consisting of short chains of α-1,4 linked D-glucopyranose units, connected by α-1,6 glycosidic bonds. The content and structures of amylose and amylopectin determine the properties of starch, including thermal and pasting properties. Native starch also consists of minor components, such as phospholipids and phosphate monoesters, which significantly affect starch properties.

Composition and structures of starch molecules are controlled by many genes. For example, the biosynthesis of amylose is determined by the *Waxy* gene, which encodes granule-bound starch synthase I (GBSSI). GBSSI is the exclusive enzyme responsible for the biosynthesis of amylose and has also been reported to synthesize extra-long branch-chains of amylopectin. In the *waxy* mutant of corn, GBSSI is defective and the waxy corn starch is essentially free of amylose. Dosage effects of the *waxy* gene on the structures and properties of corn starch, however, are not fully understood, and effects of GBSSI on the biosynthesis of extra-long branch-chains are still being debated. In the study of "Dosage effects of *waxy* gene on the structures and properties of corn starch," reciprocal crossing of isogenic normal and waxy corn was conducted to develop hybrids with different dosages (3, 2, 1, 0) of the *waxy*

gene in the endosperm. The corn starch with different dosages of the *waxy* gene was characterized to elucidate dosage effects of the *waxy* gene on starch structures and properties and to understand the function of GBSSI in the biosynthesis of amylose and amylopectin.

Starch structures and properties are also affected by the environment during the development of starch granules, such as growing temperature and rainfall. Starch biosynthetic enzymes are sensitive to temperature, and the enzyme activity drastically decreases under heat stress. The defective enzyme activity, in turn, leads to changes in granule size, amylose content, branch-chain length distribution of amylopectin, and starch properties. In addition to the impacts on the activities of starch biosynthetic enzymes, high growing temperatures and moisture also cause annealing of the starch molecules, resulting in increased onset gelatinization-temperature, decrease gelatinization temperature-range, and restricted swelling of the starch. In the study of "Physicochemical properties of Tibetan hull-less barley starch," starches isolated from two hull-less barley varieties, Beiqing (BQ) and Kangqing (KQ), were characterized. The BQ barleys were grown at a location with a lower temperature and less rainfall than the KQ barleys. The BQ starches displayed significantly lower onset gelatinization-temperatures and greater peak-viscosities than the KQ starches, despite the amylose and lipid contents and branch-chain length of amylopectin were similar between the BQ and KQ starches. The differences in starch thermal and pasting properties were attributed to the annealing of the KQ starch, resulting from higher growing temperature and more rainfall during the development of the KQ starch.

In general, less mature starch-granules display smaller granule sizes, less amylose contents, and lower onset gelatinization-temperatures than starch granules with a greater maturity. In the study of "Characterization and development mechanism of *Apios americana* tuber starch," the starch of *Apios americana* tubers was characterized and the mechanism of the development of starch granules in the tuber was studied. The *Apios* is a wild legume-

bearing plant with edible tuber and is currently under domestication as a potential food crop because of its superior nutritional values. The harvested *Apios* tuber can be planted in the following year as the mother (seed) tuber to further grow and produce child (progeny) tubers. The mother tubers were growing for two years, and the starch went through a further growth and was subjected to a longer annealing process. In general, the mother-tuber starch had larger granule-size, greater crystallinity, higher onset gelatinization-temperature, and greater enthalpy-change. Starch granules located in the periphery of the mother tuber displayed smaller granule-sizes, less amylose-contents, and lower gelatinization-temperatures than that located in the center of the mother tuber.

CHAPTER 1

LITERATURE REVIEW

1. Structures of starch granule

Starch is the major energy-reserving polysaccharide produced by green plants and can be found in different organs of the plant, including seeds (e.g. corn and barley grain), stems (e.g. trunk of sago palm tree), leaves (e.g. tobacco leaf, duckweed), fruits (e.g. green banana), tubers (e.g. potato) and roots (e.g. cassava root). Native starch is present in the granular form and has semi-crystalline structures. Starch granules vary in shapes (spherical, oval, polygonal, disk, elongated, etc.), sizes (ranging from submicron to more than 100μm), and structures (e.g. amylose / amylopectin ratio, amylopectin branch-chain length, phospholipid and phosphate monoester), depending on the botanical origins of the starch (Alcazar-Alay & Meireles 2015; Buleon et al., 1998; Fredriksson et al., 1998; Hoover, 2001; Jane et al., 1994; Srichuwong et al., 2005; Tester et al., 2004), the organ of the plants (Fasahat et al. 2014; Yu et al. 2015), and the stage of development (Huang et al., 2006; Li et al., 2007; Zeng et al. 2015). The composition and molecular structures of the starch determine starch properties.

1.1 Structures of amylose and amylopectin

Starch consists of two major polysaccharides: amylose and amylopectin. Amylose is primarily a linear molecule comprised of D-glucopyranose units linked by α-1,4 glycosidic bonds and a few branches linked by α-1,6 glycosidic bonds (French 1972; Perez and Bertoft, 2010; Taketa et al., 1987; Vamadevan and Bertoft 2015). Amylopectin has a highly branched structure consisting of short branch-chains of D-glucopyranose units, which are connected by α-1,6 glycosidic bonds (~5% of the total glycosidic bonds) (Banks and Greenwood, 1975; Hizukuri, 1986; Seetharaman and Bertoft 2013; Vamadevan and Bertoft 2015). Normal (wild

type) starches consist of 15-35% amylose, depending on the botanical origin and the stage of development (Hasjim et al. 2009; Jane et al. 1999; Li et al. 2007; Yoo et al. 2009; Zeng et al. 2015). Waxy starches consist of almost exclusively amylopectin, whereas high-amylose starches consist of 40% or more amylose (Campbell et al. 2007; Li et al., 2008; Perez and Bertoft, 2010; Schirmer et al. 2013; Shi et al., 1998).

1.1.1 Structures and properties of amylose

Although amylose molecules are generally considered to be linear, amylose isolated from various botanical sources cannot be completely hydrolyzed by β-amylase (an exo-enzyme that hydrolyzes α-1,4 glycosidic linkages from the non-reducing end of polysaccharide chains). The β-amylolysis limit of amylose varies from 72 to 95% (Banks and Greenwood 1967; Hizukuri et al. 1981; Shao et al. 2007). With a concurrent action of β-amylase and pullulanase (a debranching enzyme that hydrolyzes α-1,6 glycosidic linkages and releases the branch chains), however, amylose can be completely hydrolyzed, indicating the presence of α-1,6 linked branches in amylose molecule (Hizukuri et al. 1981; Takeda et al. 1987). The branching frequency of amylose is about 3-11 branches per molecule, and each branch-chain consists of 200-700 glucopyranose units (Hanashiro et al. 2013; Hizukuri 1993; Hizukuri et al., 1981; Mua and Jackson 1997; Tester and Karkalas 2002).

Average molecular weights of amylose are in the order of 10^4-10^6 g/mol, or a degree of polymerization by number (DPn) of 300-9000, depending on the botanical origin of the starch (Chung and Liu 2009; Hizukuri et al., 1981; Hizukuri 1993; Jane 2004; Mua and Jackson 1997; Mukejea and Robyt 2010; Takeda et al. 1987; Wang et al. 2014). In general, amylose of cereal starch has smaller molecular-size than that of tuber and root starch (Jane 2006; Mukerjea and Robyt 2010; Takeda et al. 1987).

Amylose has a strong tendency to complex with either a suitable complexing agent (e.g. 1-butanol or fatty acids) to form a single-helical inclusion complex (Ryno et al 2014;

Takeo et al. 1973; Cao et al. 2015) or with another amylose or amylopectin branch-chain to form a double helix (Jiang et al. 2010a; Miles et al. 1984; Wen et al. 2014). Amylose single-helical inclusion complex is usually left-handed, with the hydrophobic side of the amylose molecule facing the cavity of the helix, interacting with the non-polar moiety of the complexing agent (Lopez et al. 2012; Obiro et al. 2012; Takeo et al. 1973). The single-helix of amylose complex usually consists of six to eight glucosyl units per turn, depending on the cross-section diameter of the complexing agent (Jane and Robyt 1984; Nishiyama et al. 2010; Obiro et al. 2012; Putaux et al. 2011; Yamashita and Monobe 1971). Without the presence of a complexing agent, amylose molecules associate with one another and form double helices. A minimum chain length of DP 10 or DP 12 is required for the formation of double helices in a pure oligosaccharide solution, although shorter chains (e.g. DP 6) can co-crystallize with longer chains (Ciric et al. 2013; Gidley and Bulpin 1987; Wild and Blanshard 1986; Xu et al. 2012). Amylose molecules with a chain length of DP 90-110 display the greatest retrogradation rate (Gidley 1989; Gidley and Bulpin 1989; Pfannemuller et al., 1971).

1.1.2 Structures and properties of amylopectin

Amylopectin is a much larger molecule with a molecular weight in the order of 10^8–10^9 g/mol (Buleon et al., 1998; Mendez-Montealvo et al. 2015; Oh and Shin 2015; Yoo and Jane, 2002). Amylopectin is a highly branched molecule, and the branch chains of amylopectin, except the extra-long branch chains, are much shorter than that of amylose. The individual branch-chains can be classified into “A”, “B”, or “C” chains in terms the position of the branch chain within the amylopectin molecule (Peat et al. 1952; Hizukuri 1986; Vamadevan and Bertoft 2015). Each amylopectin molecule consists of only one C chain that carries the sole reducing end of the molecule and the B and A chains. The A chains (usually with a chain length of DP 6-12) are those attached to B or C chains through α-1,6 linkages carrying no other chains. All A-chains are external chains (Vamadevan and Bertoft, 2015).

The B chains carry A or other B chains and are further grouped into B1 (DP 13-24), B2 (DP 25-36), B3 (> DP 37) chains (Hanashiro et al. 1996). The average branch-chain lengths of normal starches are usually 18-31 DP, depending on the botanical origin of the starch (Bertoft et al., 2008; Hanashiro et al., 2002; Hizukuri, 1986; Mua and Jackson, 1997; Kallman et al. 2015; Ketthaisong et al. 2015; Takeda, et al., 2003; Waterschoot et al. 2015). Classification of amylopectin branch-chains is shown in **Figure 1**.

The actual architecture of amylopectin is still not fully understood, but the Cluster model, independently proposed by French (1972) and Nikuni (1978), is the most widely accepted model to describe the structure of amylopectin. It is proposed that branch-chains of amylopectin form double helices and the double helices are organized in parallel to form crystallites in clusters (Bertoft 2013; Chauhan and Seetharaman 2013; French 1972; Gallant et al. 1997; Nikuni 1978). The double helices are stabilized by hydrophobic interaction and hydrogen bonds, and the cluster structure is stabilized by hydrogen bonds and van de Waals forces between the adjacent double helices (Imberty et al. 1988; Seetharaman and Bertoft 2013). As shown in **Figure 1**, adjacent amylopectin branch-chains (usually 9 to 17 double helical strands) are closely packed to form clusters (Gallant et al. 1997). For wheat, corn, barley, rice, potato, and tapioca starches, the amylopectin molecule consists of alternative crystalline and amorphous lamellae, with a constant repeating distance of 8.7-9.2 nm (Cardoso and Westfahl 2010; Jenkins et al. 1993; Witt et al. 2012), indicating that a complete cluster consists of 27-28 glucosyl units (Gernat et al. 1990). The chain-lengths of the A and B1 chains are usually < DP 24 and, thus, both the A and B1 chains extend within a single cluster. The B2 and B3 chains with longer branch-chain length extend through two and three clusters, respectively (Hizukuri 1986; Witt et al. 2012), and the clusters are connected by the B2 or B3 chains.

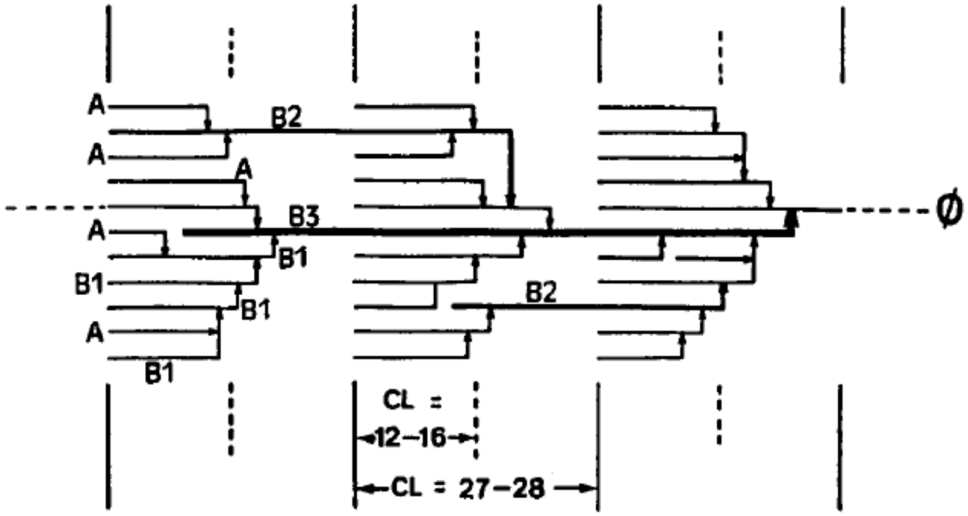

Figure 1. Cluster model and classification of amylopectin. (Adapted from Hizukuri 1986).

1.2 Organization of starch granule:

In a starch granule, amylopectin and amylose molecules are radially oriented from the hilum to the periphery, which is manifested by the Maltese cross of starch granules as viewed under a polarized-light microscope (Chen et al. 2015; Jane 2007; Munoz et al. 2015). Crosslinking studies using normal corn and potato starch showed that cross-linkages were only found between amylose and amylopectin molecules but not between amylose molecules (Jane et al., 1992; Kansemsuwan and Jane, 1994). These results indicate that, in normal starch granules, amylose molecules are interspersed among amylopectin molecules and are not in close proximity to other amylose molecules, as shown in **Figure 2**. Surface-gelatinization study using normal corn and potato starch indicated that amylose molecules were more concentrated at the periphery of starch granule (Jane and Shen 1993; Pan and Jane 2000). The amylose molecules intertwine with amylopectin and contribute to maintaining the integrity of the granular structure (Jane et al. 1986; Pan and Jane 2000).

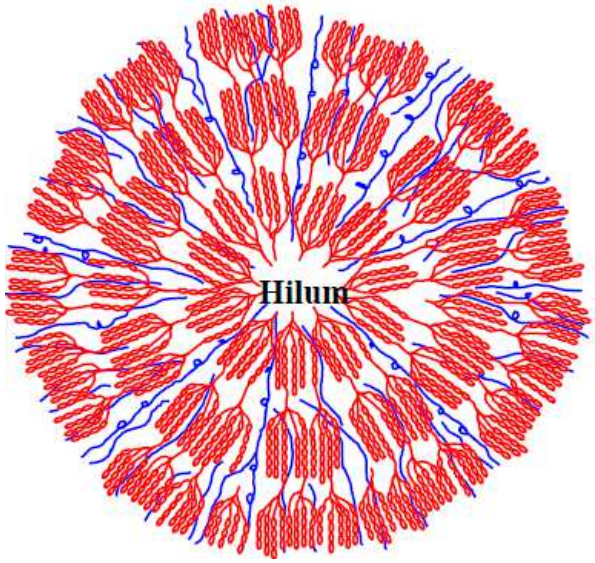

Figure 2. Schematic of the cross section of a starch granule. Amylopectin molecules are shown in red color and amylose molecules are shown in blue color.

In high-amylose corn starch with a higher concentration of amylose molecules in the granule, amylose molecules can form double helices with one another and with the long chains of amylopectin and the intermediate components (Jiang et al. 2010a). The presence of the long-chain double helical crystallites of amylose and intermediate components was reflected by the high gelatinization conclusion-temperature measured using a DSC (up to 130 °C), which was not affected after defatting of the starch (Jiang et al. 2010b).

The double helices of the branch chains of amylopectin are packed in two different polymorphs, A- and B-type. The unit cell of the A-type polymorph is monoclinic consisting of eight water molecules per unit cell, whereas that of the B-type polymorph is hexagonal consisting of thirty six water molecules per unit cell (Buleon et al. 1998; Popov et al., 2009; Wu and Sarko, 1978) (**Figure 3**). The packing of the double helices within the A-type polymorph is compact, whereas the B-type polymorph has a more open structure (**Figure 3**). The more compact packing of the A-type polymorph likely contributes to the higher gelatinization temperature and lower digestibility of A-type polymorphic spherulites than the

B-type spherulites (Cai and Shi 2013, 2014; Whittam et al., 1990). The branch-chain length of amylopectin has been found to be the key factor determining the polymorphic type of the starch. The B-type polymorphic starches, such as potato and amylomaize VII starches, consist of amylopectin with longer branch-chains than the A-type polymorphic starches, such as normal and waxy corn, wheat, tapioca, and taro starches (Hizukuri 1985; Jane 1994, 2004; Lin et al. 2016; Waterschoot et al. 2015). Some starches (e.g. pea or green banana starches) display a C-type polymorph, which is a mixture of A- and B-type polymorphs within a starch granule (Bogracheva et al. 1998; Buleon et al. 1998; Hung et al. 2013; Jiang et al. 2015). The distribution of the A- and B- polymorphic starch in the C-type polymorphic starch granules, however, are different among the botanical origins, likely depending on the granular shape and geographic location of the hilum in the granule. For the pea starch having an oval shape with the hilum located at the geographic center of the starch granule, the B-polymorphic starch is located essentially at the center of the granule, whereas A-polymorphic starch is located at the periphery of the granule (Bogracheva et al. 1998; Cai and Wei 2013). For the lotus rhizome starch having a rod shape with the hilum located at one end of the granule, the B-polymorphic starch is located close to the distal end from the hilum, whereas A-polymorphic starch is essentially located close to the hilum end (Cai et al. 2014; Cai and Wei 2013).

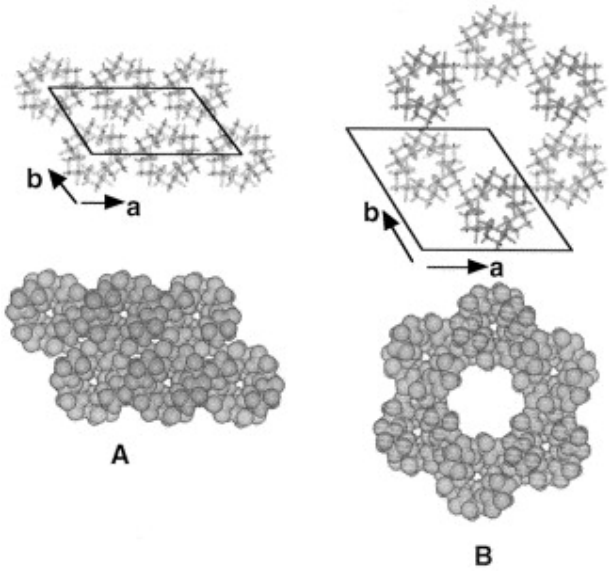

Figure 3. Crystalline packing of double helices of amylopectin in A-type and B-type polymorphs (Adapted from Buleon et al. 1998).

2. Properties of Starch

2.1 Thermal properties of starch

The crystalline structure of starch granules is a result of hydrophobic interaction and hydrogen bonds to form double helices and lamellae. When these interactions are overcame, e.g. by heating starch in the presence of water, the starch transforms from a semi-crystalline structure to an amorphous state, which is accompanied with disruption of starch granules, loss of crystallinity and birefringence (disappearance of Maltese cross), and dissociation of double helices (Jane 2004; Schirmer et al. 2015). The process is known as starch gelatinization, which is an endothermic reaction and is irreversible.

Starch gelatinization can be achieved by heating starch in the presence of a plasticizer (e.g. water or glycerol) or by non-heating approaches, such as mixing starch in alkaline solutions (Hu et al. 2016; Nadiha et al. 2015; Ragheb et al., 1995) or some neutral salt solutions (Huang et al. 2014; Jane 1993; Zhao et al. 2015). Hydroxide ions in the alkaline

solution can remove protons from the hydroxyl group and leave a negative charge on the glucose unit. The glucan chains bearing negative charges repel one another, resulting in dissociation of the double helices. Neutral salt solutions consist of cations with large charge-densities (such as Li^+ and Ca^{2+}), which interact with the hydroxyl groups of starch and release heat to destabilize and dissociate double helices of starch (Jane 1993; Jane and Shen 1993; Pan and Jane 2000). For food and industrial applications, gelatinization of starches is normally achieved by heating starch in the presence of water. The thermal properties of starch, including the gelatinization temperature and enthalpy change, are commonly measured using a differential scanning calorimeter (DSC).

Thermal properties of the native starch are determined by many factors, including structures of the starch (amylopectin structures and amylose content), minor components of starch (e.g. phosphate monoesters and lipids), and moisture content (or available water). In general, starch consisting of amylopectin with larger proportion of short branch-chains (DP 6-12) displays a lower gelatinization-temperature and a smaller enthalpy-change because the short-chain double-helix is dissociated at a lower temperature (Brummell et al. 2015; Jane et al. 1997; Jane et al. 1999; Oh and Shin 2015; Srichuwong et al. 2005). Among the normal starches, contradictory results were reported with regard to the effect of amylose on gelatinization temperatures: the normal starches showed lower, higher, or similar gelatinization temperature compared with the waxy starches (Cai et al. 2015; Chen et al. 2015; Fredriksson et al. 1998; Sasaki et al. 2000; Vandeputte et al. 2003; Yu et al. 2015). In the high-amylose corn starch, the peak and conclusion gelatinization-temperatures increase with the increase in the amylose content, resulting from double-helical structures formed by the long chains of amylose/intermediate components (Li et al., 2008; Jiang et al., 2010a). The presence of negatively charged phosphate-monoester derivatives decreases starch gelatinization temperature resulting from the charge-repulsion (Cai and Shi 2010; Jane et al.

1999). For example, potato starch displays a lower onset, peak, and conclusion gelatinization-temperature than corn and rice starches because of the presence of phosphate-monoester derivatives in the amylopectin of potato starch, although the amylopectin of potato starch has longer branch-chains than that of corn and rice starches (Alvani et al. 2011; Xu et al. 2013). In the presence of sugars or salts (e.g. NaCl or KCl), starch gelatinization-temperature and enthalpy change increase because sugars or salts bind with water and induce hydrogen-bond formation between water molecules, reducing free-water content (Ahmed 2012; Bogracheva et al. 1998; Li et al. 2015; Tomasik et al. 1995). In the presence of anions with a hydrophobic moiety and small charge-density (e.g. SCN^-), however, starch displays lower gelatinization-temperature and smaller enthalpy-change because a structure-breaking effect of the anions increases free-water content and solution power. Starch chains can also form single helical-complex with the anions to reduce the free energy of dissociated double-helices and reduce the gelatinization temperature and enthalpy change (Jane 1993).

2.2 Pasting properties of starch

When the gelatinized starch is continuously heated in excess water, starch pasting occurs, which is accompanied with a considerable increase in the swelling of starch granules, some dispersion, development of viscosity, and even complete disruption of the starch granule (Atwell et al. 1988). Starch pasting properties are usually measured using a Rapid Visco-Analyzer (RVA) or a Brabender Amylograph (Himeda et al. 2012; Jane et al. 1999; Okechukwu and Rao 1996; Suh and Jane 2003; Waterschoot et al. 2014).

Swelling of starch granules is primarily contributed by amylopectin molecules, whereas amylose and amylose-lipid complex intertwine with amylopectin and restrict its swelling (Gerits et al. 2015; Jane 2006; Tester and Morrison 1992). Therefore, starches having greater contents of amylose and lipids (especially phospholipids) usually display higher pasting-temperatures and lower peak-viscosities (Collado et al. 1999; Jane et al. 1999;

Li et al. 2014; Yoo and Jane 2002; Wang et al. 2014). After the lipids are removed from starch, the starch displays a substantial increase in peak viscosity and decrease in pasting temperature compared with the native starch (Debet and Gidley 2006; Gerits et al. 2015; Yangcheng et al. 2016). Normal starch displays a higher setback-viscosity than the waxy starch, which is attributed to the entanglement between amylose and amylopectin upon cooling of the starch paste. In the presence of phosphate-monoester derivatives (e.g. potato starch), the repulsion force between the negatively-charged phosphate-monoesters facilitates swelling of the granule and results in substantially lower pasting temperature and higher peak viscosity of the starch.

2.3 Gelling properties of starch

Gelling of the starch is the process by which the gelatinized and dispersed starch molecules re-associate, form a three-dimensional network, and fill up the space during the cooling of the starch paste. The network holds water molecules in the structure, which is a result of the interaction between the amylose and amylopectin molecules in the swollen granule. Starch gel has a defined shape with no fluidity, whereas starch paste has certain fluidity (Belitz et al. 2009). Amylopectin molecules can form gels at a much slower rate and at a substantially higher concentration than amylose molecules (Biliaderis and Izydorczyk 1992), indicating that amylose facilitates the network and gel formation. Swollen starch granules maintaining higher integrity tend to form starch gels with a greater firmness. The native potato and tapioca starch does not form a gel or forms a weak gel, whereas lightly cross-linked or heat-moisture treated potato starch forms a stronger gel at the same concentration (Jyothi et al. 2010; Keetels et al. 1996; Klein et al. 2013; Zavareze et al. 2012). This is attributed to the increased integrity of swollen starch-granules after these treatments of the potato starch. The gelling properties of starch are also significantly affected by the formation of amylose-lipid complex in the starch. Native tapioca starch hardly forms a gel,

whereas wheat and corn starch at the same concentration form firm gels after cooking and storage, resulting from the presence of endogenous lipids in the wheat and corn starch (Debet and Gidley 2006). Tapioca starch, however, can form a gel when tapioca starch is cooked in the presence of lipids (e.g. corn oil or linoleic acid), which is likely resulted from the amylose-lipid complex formation in the tapioca starch with the added lipids (Ai et al. 2013). Amylose-lipid complex in the starch reduces swelling of starch granule and prevents the dispersion of the swollen granule (Srichuwong and Jane 2007), contributing to the gel formation of the starch.

2.4. Retrogradation of starch

Upon cooling and during storage, gelatinized starch molecules in the paste and gel tend to recrystallize by forming double helices. The process is known as starch retrogradation (Jane 2004). Amylose molecules in an aqueous medium retrograde fast and form crystallites with a high dissociation-temperature (130-170 °C) (Sievert and Pomeranz 1990; Jane et al. 1999; Yu et al. 2014). Amylopectin molecules, however, retrograde in a much slower rate and form crystallites with a lower dissociation-temperature (40-60 °C) (Sievert and Pomeranz 1990; Wang et al. 2015; Yu et al. 2014).

Starch retrogradation is significantly affected by the structures and minor components of the starch. Generally, retrogradation rate positively correlates with the amylopectin branch-chain length (Chang and Lin 2007; Jane et al. 1999; Perera et al. 2001; Singh et al. 2010; Yoo et al. 2009). The presence of amylose and/or amylose-lipid complex facilitates starch retrogradation, resulting from the restricted swelling of starch granule during cooking, which keeps the starch molecules in a close proximity and facilitates retrogradation (Jane et al. 1999). The presence of phosphate-monoesters in potato starch, however, retards starch retrogradation because of the repulsion force between the negatively-charged phosphate monoesters (Jane et al. 1999; Nwokocha et al. 2014; Thygesen et al. 2003).

3. Starch Biosynthesis

Starch molecules are cooperatively synthesized in the chloroplast or amyloplast by four classes of core enzymes, including ADP-glucose pyrophosphorylase, starch synthases, starch-branching enzymes, and starch-debranching enzymes (James et al. 2003; Jeon et al. 2010; Smith 2001; Tetlow 2006, 2011).

The substrate for starch biosynthesis is ADP-glucose, which is synthesized from glucose-1-phosphate and ATP in a reaction catalyzed by ADP-glucose pyrophosphorylase (AGPase) (Jeon et al. 2010; Martin and Smith 1995; Saripalli and Gupta 2015). The production of ADP-glucose by AGPase is considered as the rate-limiting step because it is the first committed step in the pathway of starch biosynthesis (Smith 2001). The catalytic activity of AGPase is positively regulated by 3-phosphoglycerate (3-PGA) and negatively regulated by inorganic orthophosphate (Pi) (James et al. 2003; Saripalli and Gupta 2015). Both up- and down-regulations of AGPase lead to proportional increase and decrease in the rates of starch biosynthesis. For example, the maize mutants of *brittle 2* (*bt2*) and *shrunken2* (*sh2*) display a 70% reduction in starch content because they have less enzymatic activity of AGPase in their endosperm tissues. However, the revertant of *sh2* mutant having increased AGPase activity or overexpression of AGPase displays an overproduction of starch in cereal endosperms (Buleon et al. 1998; Kang et al. 2013).

The ADP-glucose is utilized by starch synthases (SSs) to elongate the linear chains of amylose and branch chains of amylopectin by transferring glucose units from ADP-glucose to the non-reducing end of a growing α-1,4-linked glucan (Jeon et al. 2010; Smith 2001). Cereal endosperms consist of at least five SS isoforms including granule-bound starch synthase I (GBSSI), SSI, SSII, SSIII, and SSIV. GBSSI is responsible for the biosynthesis of amylose and extra-long branch-chains of amylopectin (Hanashiro et al. 2008; James et al. 2003; Yoo and Jane 2002). Although the *in vivo* mechanism of synthesis of amylose and amylopectin by

GBSSI remains unclear, the *in vitro* studies have reported that GBSSI incorporates glucose both in amylopectin and amylose molecules depending on the conditions used in these experiments. In the absence or with a low concentration of malto-oligosaccharides, the product synthesized *in vitro* by GBSSI is confined to the amylopectin fraction. In the presence of a high concentration of malto-oligosaccharides, however, GBSSI massively incorporates glucose into amylose-like glucans (Denyer et al. 1996). A mechanism has been proposed that GBSSI synthesizes amylose by elongating the malto-oligosaccharide primers (Denyer et al. 2001).

Other SS isoforms (SSI, II, III, IV) are exclusively involved in amylopectin biosynthesis. SSI is primarily responsible for the synthesis of the shortest chains with DP<10. With the increase in the length of the substrate linear-chains, SSI binding affinity increases but its catalytic activity decreases (Commuri and Kelling 2001; James et al. 2003). Two SSII enzymes have been identified: SSIIa and SSIIb. SSIIa predominates in cereal endosperms, whereas SSIIb predominates in photosynthetic tissues and the function of SSIIb in starch biosynthesis is unknown (Tetlow 2006, 2011). SSIIa is responsible for the biosynthesis of branch chains with a DP 12-24 by elongating short chains of DP<10. In mutants lacking SSIIa activities (e.g. *sugary 2* corn), the starch displays a decrease in the amylopectin content (Jobling 2004) and an increase in the proportion of short branch-chains with DP<12 (Perera et al. 2001). SSIII is responsible for the elongation of longer branch-chains with DP>25 (Jame et al. 2003), whereas the function of SSIV in starch biosynthesis remains unclear (Tetlow 2006).

The branch chains are introduced by starch branching enzymes (SBE), which cleaves α-1,4 linkages and transfers the released glucan residues to C6 hydroxyl groups (Jame et al. 2003; Nakamura et al. 2010; Smith 2001). In corn, there are two SBE isoforms, SBEI and SBEII, and SBEII is further classified to SBEIIa and SBEIIb. SBEIIa is the dominant

branching enzyme in the endosperms of wheat and barley, whereas SBEIIb is dominant in the endosperms of rice and corn (Regina et al. 2010). All the SBE isomers differ in terms of affinities to different substrates and capabilities of transferring glucan-chains. Typically, SBEI preferentially branches amylose-like linear glucans, whereas SBEII has a higher capacity for branching highly branched glucans (e.g. amylopectin) (Nakamura et al. 2010; Tetlow and Emes 2014).

The debranching enzymes (DE) are responsible for the trimming of the amylopectin structure. The DE selectively removes branches inappropriately positioned and is required for the maintenance of the cluster structure of the amylopectin (James et al. 2003; Tetlow 2011). Deficiency of DE, for example, in *sugary-1* (*su*-1) mutants of corn, rice, and barley, leads to an accumulation of over-branched, water-soluble phytoglycogen at the expense of amylopectin (Hamada et al. 2014; Szymanek et al. 2015). Although the precise functions of DE are still not clear, it is for certain that the final structure of amylopectin is determined by a balance between the activities of debranching and branching enzymes (Martin and Smith 1995).

4. Waxy corn

The waxy mutants of corn, barley, wheat, and sorghum have been known for many years, but only waxy corn is grown on a commercial scale (Jobling 2004). Waxy corn starch is essentially free of amylose, and, therefore, the physicochemical properties of waxy corn starch are quite different from normal corn starch. In general, waxy corn starch displays greater gelatinization enthalpy-change, slower retrogradation rate, lower pasting temperature, higher peak viscosity, and lower set-back viscosity than normal corn starch (Ai and Jane 2015; Kibar et al. 2011; Wang et al. 1992; Jane et al. 1999; Yu et al. 2015). Waxy corn starch-paste displays a high viscosity, stringy texture, little cloudiness, and a low tendency to

gel, which is similar to tapioca starch-paste (BeMiller 2009). Because of the unique pasting properties of waxy corn starch, it is preferred in many food and non-food applications over normal corn starch. In food applications, waxy corn starch is used to improve the uniformity, viscosity, freeze-thaw stability, and appearance of the food products (Fergason 1994). In non-food applications, because of the higher hydrolysis rate of waxy corn starch, waxy corn displays higher feed conversion-efficiency when used as a livestock feed (Collins et al. 2003) and higher starch-ethanol conversion-efficiency when used for ethanol production (Yangcheng et al. 2013). Waxy corn starch is preferred in producing adhesives and textiles because of its clear film-forming properties (Fergason 1994; Wang et al. 2012).

Paste of native/unmodified waxy corn starch, however, is too stringy and cohesive and easy to break down under shear, which is not desirable for many food applications. Therefore, modification of the waxy corn starch (e.g. cross-linking) is usually necessary to improve the quality and endurability of waxy corn starch during processing (BeMiller 2009). Recent studies on partial-waxy wheat and durum wheat starches, however, may provide a new approach to improve the processing properties of waxy corn starch. Partial-waxy wheat and durum wheat starches, having a reduced amylose-content, improve the texture and quality of pasta and Japanese white salted noodle, whereas the full waxy starches give a poor quality (Ishada et al. 2003; Sharma et al. 2002). It is possible that amylose in the partial-waxy starches, although at a reduced concentration, improve the integrity of the swollen starch-granule without causing much decrease in the paste viscosity. It is of great interest to understand the functionalities of partial-waxy corn starch, which may provide a new approach to improve the endurability and processing quality of waxy corn starch without applying chemical modifications.

5. Effects of Growing Conditions on Starch Physicochemical Properties

In the cereal endosperm, the maximum rate of starch accumulation occurs between 12 and 35 days after pollination (DAP), which is knowns as grain-filling period (Thitisaksakul et al. 2012). Transcription of different isoforms of AGPase, SSs, SBEs, and SDEs are present at distinct times during the grain-filling stage (Ohdan et al. 2011; Stamova et al. 2009; Toyota et al. 2006), and changes in even one enzyme isoform could profoundly affect the starch structures and properties (Keeling and Myers 2010).

Starch biosynthetic enzymes are sensitive to temperature changes, and the enzyme activity decreases drastically under heat stress. The optimal temperature for SSs in wheat is around 20-25 °C (Keeling et al. 1993), the enzyme activity drastically decreases when the temperature is above 35°C. GBSSI is also affected by heat, although not to the same extent as the SSs, and the susceptibility of GBSSI to high temperature is the dependent on a single nucleotide polymorphism (SNP) in its DNA sequence. For example, the GBSSI of Indica rice is more susceptible to heat stress than Japonica rice, resulting from the difference in a single nucleotide of its DNA sequence between the Indica and Japonica rice (Inukai and Hirayama 2010; Yamakawa et al. 2007). The optimal temperature for SBEIIb in rice and corn is around 25°C and 15-20 °C, respectively, and decreased activities of SBEs under heat stress may contribute to the changes in the branch-chain length of starch (Ohdan et al. 2011).

5.1 Effects of Growing Temperature on Starch Structures and Properties

The effect of growing temperature on starch physicochemical properties has been intensively studied in many plant species. In barley and wheat, the elevated temperature is associated with reduced starch accumulation in the grain, smaller granule-size, larger proportion of small B-granules, increased lipid contents in the starch, similar or slightly increased amylose contents (Lu et al. 2014; Matsuki et al. 2003; Shi et al. 1994; Tester et al. 1991). The percentage of short branch-chains (DP < 12) of amylopectin decreases and that of

long branch-chains (DP > 35) increases with the increase in the growing temperature of wheat (Matsuki et al. 2003). The yield and physicochemical properties of sorghum starch display similar changes to wheat at high growing temperatures (Li et al. 2013).

Corn and rice starches, however, display decreased amylose content at high growing temperatures (Asaoka et al. 1985; Lu et al. 1996). The rice starch developed at high temperatures displays increased proportion of long and intermediate B-chains and decreased proportion of short branch-chains (Asaoka et al. 1985; Cao et al. 2015; Inouchi et al. 2000). Lu et al. (1996) reported that the changes in the branch-chain length distribution of normal dent corn starch in response to the growing temperature were variety-dependent: one variety displayed increased proportion of intermediate branch-chains and decreased proportions of short and long branch-chains, whereas the other variety displayed increased proportion of intermediate and long branch-chains and decreased proportions of short branch-chains. The waxy corn starch developed at high growing-temperatures displays an increased iodine-binding capacity, indicating that the waxy corn starch has longer branch-chains in response to the high growing temperature (Lu et al. 2014; Yang et al. 2015). These studies indicate that the activity of starch-biosynthetic enzymes and starch structures and properties are affected in different ways in response to the elevated growing temperature, which is dependent on the botanical origins and genetic backgrounds of the plant (Thitisaksakul et al. 2012).

5.2 Annealing of starch during the crop development

Annealing of starch is defined as a physical treatment that involves incubation of starch granules in excess water (usually above 60%) for a certain period of time at a temperature above the glass transition temperature but below the onset-gelatinization temperature (Jacobs and Delcour 1998; Tester and Debon 2000; Jayakody and Hoover 2008). It is possible that commercial corn, wheat, and barley starches are annealed during the isolation process because the grains are steeped at ~50 °C for 48-72 hr prior to milling.

It has been widely accepted that annealing of starch improves alignment and structure of double helices within the crystalline lattice and perfection of the existing crystallites without increasing the number of double helices in normal or waxy starches (Gomand et al. 2012; Tester and Debon 2000). Nevertheless, it is likely that new double helices form within the high-amylose potato starch after annealing (Gomand et al. 2012; Tester and Debon 2000). Thermal and pasting properties of the starch significantly change after annealing. It has been reported that, despite of starch sources, annealed starches display a higher onset-gelatinization temperature and a reduced gelatinization temperature-range (Jacobs and Delcour 1998; Jayakody and Hoover 2008; Zavareze and Dias 2011; Gomand et al. 2012). The gelatinization enthalpy-change either remains unchanged (Vermeylen et al. 2006; Wang et al. 1997) or slightly increases after annealing (Hoover and Vasanthan 1994; Jayakody and Hoover 2008; Vamadevan et al. 2013). The annealed starches also display decreased swelling power, increased pasting temperature, and decreased peak viscosity compared with the un-annealed starches (Jacobs and Delcour 1998; Jayakody and Hoover 2008; Song et al. 2014; Tester and Debon 2000).

During the development of starch granules of the crop, there is an environmentally driven *in vivo* annealing of starch granules, especially when the starch granules develop at a high growing temperature. Debon et al. (1998) investigated the starch physicochemical properties of potato tubers grown at 10, 16, and 24 °C. The authors reported increased onset-gelatinization temperature and decreased gelatinization-temperature range with increase in the growing temperature, although the amylopectin branch-chain length distribution was not affected by the growing temperature. Similar results were reported on waxy, normal, and high-amylose barley cultivars grown at a temperature ranging 7-20 °C (Kiseleva et al. 2004). The authors reported increased onset-gelatinization temperature and decreased gelatinization-temperature range with increase in the growing temperature for all the barley cultivars and

the change in gelatinization enthalpy-change did not show a clear trend. These findings indicate that, apart from the direct impact of growing temperature on the activities of starch biosynthetic enzymes, a high growing temperature facilitates *in vivo* annealing of starch during the development of starch granules and results in different properties of the starch.

References

Ai, Y., Hasjim, J., Jane, J. (2013). Effects of lipids on enzymatic hydrolysis and physical properties of starch. Carbohydr. Polym. 92, 120-127.

Ai, Y. & Jane, J. (2015). Gelatinization and rheological properties of starch. Starch 67, 213-224.

Ahmed, J. (2012). Rheometric non-isothermal gelatinization kinetics of mung bean starch slurry: effect of salt and sugar. J. Food Engineering 109, 321-328.

Alcazar-Alay, S.C. & Meireles, M.A.A. (2015). Physicochemical properties, modifications and applications of starches from different botanical sources. Food Sci. Tech. 35, 215-236.

Alvani, K. et al. (2011). Physico-chemical properties of potato starches. Food Chem. 125, 958-965.

Asaoka, M., Okuno, K., Fuwa, H. (1985). Effect of environmental temperature at the milky stage on amylose content and fine structure of amylopectin of waxy and nonwaxy endosperm starches of rice. *Agric.Biol. Chem*. 49, 373-379.

Atwell, W. A., Hood, L. F., Lineback, D. R., Varriano-Marston, E., and Zobel, H. F. (1988). The terminology and methodology associated with basic starch phenomena. *Cereal Food World,* 33,306-310.

Banks, W., Geenwood, C.T. (1967). Physicochemical Studies on Starches Part XXXII. The Incomplete β-Amylolysis of Amylose: A Discussion of its Cause and Implications**.** *Starch*, 19,197–206.

Banks, W., Greenwood, C.T. (1975). Starch and its components. University Press, Edinburg, UK.

Belitz, H.D., Grosch, W., Schieberle, P. (2009). Food Chemistry. Springer: Berlin-Heidelberg.

BeMiller, J.N. (2009) One hundred years of commercial food carbohydrates in the United States. J. Agric. Food Chem. 57, 8125-8219.

Bertoft, E. (2013). On the building block and backbone concepts of amylopectin structure. Cereal Chem. 90, 294-311.

Bertoft, E., Koch, K. (2000). Composition of chains in waxy-rice starch and its structural units. Carbohydr. Polym. 41, 121-132.

Bertoft, E., Piyachomkwan, K., Chatakanonda, P., Sriroth, K. (2008). Internal unit chain composition in amylopectins. Carbohydr. Polym. 74, 527-543.

Biliaderis CG and Izydorczyk MS. (1992). In: Phillips GO, Wedlock DJ, Williams PA, eds. Gums and Stabilizers for the Food Industry 6. Oxford, UK. IRL Press; pp 227.

Brummell, D.A. et al. (2015). Overexpression of starch branching enzyme II increases short-chain branching of amylopectin and alters the physicochemical properties of starch from potato tuber. BMC Biotechnol. 15, 28.

Bogracheva, T., Morris, V. J., Ring, S. G., Hedley, C. L. (1998). The granular structure of C-type pea starch and its role in gelatinization. 45, 323-332.

Buleon, A., Colonna, P., Planchot, V., Ball, S. (1998). Starch granules: Structure and biosynthesis. *Int J Bio. Macromol.* 23(2), 85-112.

Cai, C.; Cai, J.; Man, J.; Yang, Y.; Wang, Z.; Wei, C. (2014). Allomorph distribution and granule structure of lotus rhizome C-type starch during gelatinization. Food Chem. 142, 408-415.

Cai, C. & Wei, C. (2013). In situ observation of crystallinity disruption patterns during starch gelatinization. Carbohydr. Polym. 92, 469-478.

Cai, J.W. et al. (2015). Relationship between structure and functional properties of rice starches with different amylose contents. Carbohydr. Polym. 125, 35-44.

Cai, L. & Shi, Y. (2010). Structure and digestibility of crystalline short-chain amylose from debranched waxy wheat, waxy maize, and waxy potato starches, Carbohydrate Polymers, 79, 1117-1123

Cai, L. & Shi, Y. (2013). Self-assembly of short linear chains to A- and B-type starch spherulites and their enzymatic digestibility. J Agric. Food Chem. 61, 10787-10797.

Cai, L. & Shi, Y. (2014). Preparation, structure, and digestibility of crystalline a- and b-type aggregates from debranched waxy starches. Carbohydr. Polym. 105, 341-350.

Cao, Z.; Woortman, A.J.; Rudolf, P.; Loos, K. (2015). Facile synthesis and structural characterization of amylose-fatty acid inclusion complexes. Macromol. Biosci. 15, 691-697.

Cao, Z.Z., Pan, G., Wang, F.B., Wei, K.S., Li, Z.W., Shi, C.H., Cheng, F.M. (2015) Effect of high temperature on the expressions of genes encoding starch synthesis enzymes in developing rice endosperms. J Integrative Agric. 14, 642-659.

Campbell, M.R., Jane, J., Pollak, L., Blanco, M, O'Brien, A. (2007). Registration of maize germplasm line GEMS-0067. J Plant Registration, 1, 60-61.

Cardoso, M.B. & Westfahl, H. (2010). On the lamellar width distributions of starch. Carbohydr. Polym. 81, 21-28.

Chang, Y.H. and Lin, J.H. (2007). Effects of molecular size and structure of amylopectin on the retrogradation thermal properties of waxy rice and waxy corn starches. Food Hydrocolloids 21, 645-653.

Chauhan, F. & Seetharaman, K. (2013). On the organization of chains in amylopectin. Starch 65, 191-199.

Chen, P. et al. (2015). Phase transition of waxy and normal wheat starch granules during gelatinization. Intnl. J. Polym. Sci. 397128.

Chung, H.J. & Liu, Q (2009). Impact of molecular structure of amylopectin and amylose on amylose chain association during cooling. Carbohydr. Polym. 77, 807-815.

Ciric, J. et al. (2013). Physical properties and structure of enzymatically synthesized amylopectin analogs. Starch 65, 1061-1068.

Collado, L.S., Mabesa, R.C., Corke, H. (1999). Genetic variation in the physical properties of sweet potato starch. J Agric. Food Chem. 47, 4195-4201.

Collins, N.E.; Moran, E.T.; & Stillborn, H.L. 2003. Performance of broilers fed normal and waxy corn diets formulated with chick and rooster derived apparent metabolizable energy values for the grains. *J. Appl. Poult. Res*. 12, 196-206.

Commuri, P.D. and Keeling, P.L. (2001). Chain-length specificities of maize starch synthase I enzyme: studies of glucan affinity and catalytic properties. Plant J. 25, 475-486.

Debet, M. R. and Gidley, M. J. 2006. Three classes of starch granule swelling: Influence of surface proteins and lipids. Carbohydrate Polymers 64:452-465.

Debon, S.J.J., Tester, R.F., Millam, S., Davies, H.V. (1998). Effect of temperature on the synthesis, composition and physical properties of potato microtuber starch. *J Sci. Food Agric*. 76, 599-607.

Denyer K, Clarke B, Hylton C, Tatge H and Smith AM (1996). The elongation of amylose and amylopectin chains in isolated starch granules. Plant J. 10, 1135-1143.

Denyer, K., Johnson, P., Zeeman, S., Smith, A.M. (2001) The control of amylose synthesis. J. Plant Physiol. 158, 479-487.

Fasahat, P.; Rahman, S.; Ratnam, W. (2014). Genetic controls on starch amylose content in wheat and rice grains. J. Genetics 93, 279-292.

Fergason, V. (1994) High amylose and waxy corns. Pages 55-77. In: *Specialty Corns*, 1st ed., Hallauer, A.R. Eds., CRC Press, Inc., Boca Raton, Florida.

Fredriksson, H., Silverio, J., Andersson, R., Eliasson, A.C. Aman, P. (1998). The influence of amylose and amylopectin characteristics on gelatinization and retrogradation properties of different starches. Carbohydrate Polymers 35, 119-134.

French, D. (1972). Fine structure of starch and its relationship to the organization of starch granules. *J. Japan. Soc. Starch Sci*., 1972, 19, 8-25.

Gallant, D.J. et al. (1997). Microscopy of starch: Evidence of a new level of granule organization. Carbohydr. Polym. 32, 177-191.

Gerits, L.R.; Pareyt, B.; Declour, J.A. (2015). Wheat starch swelling, gelatinization and pasting: Effects of enzymatic modification of wheat endogenous lipids. LWT-Food Sci. Technol. 63, 361-366.

Gernat, C., Radosta, S., Damaschun, G., Schierbaum, F. (1990). Supramolecular Structure of Legume Starches Revealed by X-Ray Scattering., 42, 175-178.

Gidley, M. J. (1989). Molecular mechanisms underlying amylose aggregation and gelation. Macromolecules 22, 351-358.

Gidley, M. J., Bulpin, P. V. (1987). Crystallisation of malto-oligosaccharides as models of the crystalline forms of starch: minimum chain-length requirement for the formation of double helices. *Carbohydr. Res.*, 161, 291–300.

Gidley, M. J., Bulpin, P. V. (1989). Aggregation of amylose in aqueous systems: the effect of chain length on phase behavior and aggregation kinetics. Macromol. 22, 341-346

Gomand SV, Lamberts L, Gommes CJ, Visser RGF, Delcour JA. (2012). Molecular and morphological aspects of annealing-induced stabilization of starch crystallites. *Biomacromol.* 13, 1361–70

Gray, J.A. & BeMiller, J.N. (2004). Development and utilization of reflectance confocal laser scanning microscropy to locate reaction sites in modified starch granules. Cereal Chem. 81, 278-286.

Hamada, S.; Suzuki, K.; Suzuki, Y. (2014). Development of a new selection method and quality improvement of sugary-1 rice mutants. Breeding Sci. 63, 461-467.

Hanashiro, I., Abe, J., Hizukuri, S. (1996). A periodic distribution of the chain length of amylopectin as revealed by high-performance anion-exchange chromatography, Carbohydrate Research, 283, 151-159.

Hanashiro, I.; Sakaguchi, I.; Yamashita, H. (2013). Branched structures of rice amylose examined by differential fluorescence detection of side-chain distribution. J Applied Glycosci. 60, 79-85.

Hanashiro, I., Tagawa, M., Shibahara, S., Iwata, K., Takeda, Y. (2002). Examination of molar-based distribution of A, B and C chains of amylopectin by fluorescent labeling with 2-aminopyridine. Carbohydr. Res. 337, 1211-1215.

Hasjim, J., Srichuwong, S., Scott, M.P., Jane, J. (2009). Kernel composition, starch structure, and enzyme digestibility of opaque-2 maize and quality protein maize. J Agric. Food Chem. 57, 2049-2055.

Himeda, M., Yanou, N.N., Nguimbou, R.M., Mbofung C.M.F. (2012). Physicochemical, rheological, and thermal properties of taro starch harvested at different maturity stages. *Int. J. Biosci*. 2, 14-27.

Hizukuri, S. (1986). Polymodal distribution of the chain lengths of amylopectins and its significance. *Cabohydrate Research, 147*, 342.

Hizukuri, S., Takeda, Y., Yasuda, M., Suzuki, A. (1981). Multibranched nature of amylose and the action of de-branching enzymes. *Carbohydr. Res.,* 94, 205–213.

Hoover, R. (2001). Composition, molecular structure, and physicochemical properties of tuber and root starches: A review. *Carbohydr. Polym.,* 45, 253–267.

Hu, J.B. et al. (2016). Dissolution of starch in urea/NaOH aqueous solutions. J. Applied Polym. Sci. 133, 26-32.

Huang, J.R. et al. (2014). Comparison of waxy and normal potato starch remaining granules after chemical surface gelatinization: Pasting behavior and surface morphology. Carbohydr. Polym. 102, 1001-1007.

Hung, P.V. et al. (2013). Characterization of Vietnamese banana starch and its resistant starch improvement. Intnl. Food Res. J. 20, 205-211.

Imberty, A., Chanzy, H., Perez, S., Buleon, A., and Tran, V. (1988). The double-helical nature of the crytalline part of A-starch. *J. Mol. BIo. 201*, 365-378.

Inouchi, N., Ando, H., Fuwa, H. (2000). The effect of environmental temperature on distribution of unit chains of rice amylopectin. *Starch* 52, 8-12.

Inukai, T. and Hirayama, Y. (2010) Comparison of starch levels reduced by high temperature during ripening in japonica rice lines near-isogenic for the Wx locus. J Agronomy Crop Sci. 196, 296-301.

Ishada, N., Miura, H., Noda, T., Yamauchi, H. (2003) Physical properties of white salted noodles from near-isogenic wheat lines with different wax protein-deficiency. Starch 55, 390-396.

Jacobs H. & Delcour, J.A. (1998). Hydrothermal modifications of granular starch, with retention of the granular structure: A review. *J Agri. Food Chem*. 46, 2895-2905.

James, M.G., Denyer, K., Myers, A.M. (2003). Starch synthesis in the cereal endosperm. Current Opinion in Plant Biology. 6:215-222.

Jane, J. (1993). Mechanism of starch gelatinization in neutral salt-solutions. Starch 45, 161-166.

Jane, J. (2004). Starch: structure and properties. In P. Tomasik. *Chemical and Functional Properties of Food Saccharides* pp. 81-101. New York: CRC Press.

Jane, J. (2006). Current understanding on starch granule structure. *J. Appl. Glycosci.* 53, 205-213.

Jane, J. (2007). Structure of starch granules. *The Japanese Society of Applied Glycoscience,* 54, 31-36.

Jane, J., Chen, Y.Y., Lee, L.F., McPherson, A. E., Wong, K-S., Radosavljevic, M., Kasemsuwan, T. (1999). Effects of amylopectin branch chain length and amylose content on the gelatinization and pasting properties of starch. *Cereal Chem*., 76, 629-637.

Jane, J., Kasemsuwan, T., Leas, S., Zobel, H., Robyt, J. F. (1994). Anthology of starch granule morphology by scanning electron microscopy. *Starch,* 46, 121-129.

Jane, J. & Shen, J. (1993). Internal structure of the potato starch granule revealed by chemical gelatinization. Carbohydr. Res. 247, 279-290.

Jane, J., Wong, K-S., McPherson, A.E. (1997). Branch-structure difference in starches of A- and B-type X-ray patterns revealed by their Naegeli dextrins. *Carbohydrate Research* 300, 219-227.

Jane, J., Xu, A., Radosavljevic, M., Seib, P. A. (1992). Location of Amylose in Normal Starch Granules. I. Susceptibility of Amylose and Amylopectin to Cross-Linking Reagents. 69, 405-409.

Jayakody L, and Hoover R. (2008). Effect of annealing on the molecular structure and physicochemical properties of starches from different botanical origins—a review. *Carbohydr. Polym.* 74, 691–703

Jenkins, P. J., Cameron, R. E. and Donald, A. M. (1993). A universal feature in the structure of starch granules from different botanical sources. *Starch* 45, 417-420.

Jeon, J.S. et al. (2010). Starch biosynthesis in cereal endosperm. Plant Physiol. Biochem. 48, 383-392.

Jiang, H.; Lio, J.; Blanco, M.; Campbell, M.; Jane, J. (2010). Resistant-starch formation in high-amylose maize starch during kernel development. J. Agri. Food Chem. 58, 8043-8047.

Jiang, H.H., et al. (2015). Digestibility and changes to structural characteristics of green banana starch during in vitro digestion. Food Hydrocolloids 49, 192-199.

Jobling, S. (2004) Improving starch for food and industrial applications. *Current Opinion in Plant Biology* 7, 210-218.

Jyothi, A.N. et al. (2010). Hydrothermal modifications of tropical tuber starches. 1. Effect of heat-moisture treatment on the physicochemical, rheological and gelatinization characteristics. Starch 62, 28-40.

Kallman, A. et al. (2015). Starch structure in developing barley endosperm. Intnl. J. Biol. Macromol. 81, 730-735.

Kang, G.Z. et al. (2013). Increasing the starch content and grain weight of common wheat by overexpression of the cytosolic AGPase large subunit gene. Plant Physiol. Biochem. 73, 93-98.

Kasemsuwan, T. and Jane, J. (1994). Location of Amylose in Normal Starch Granules. II. Locations of Phosphodiester Cross-Linking Revealed by Phosphorus-31 Nuclear Magnetic Resonance. 71, 282-287.

Keeling, P.L., and Myers, A. (2010) Biochemistry and genetics of starch synthesis. Annual Review of Food Science and Technology 1, 271-303.

Keetels, C. J. A. M., vanVliet, T. and Walstra, P. 1996. Gelation and retrogradation of concentrated starch systems .1. Gelation. Food Hydrocolloids 10:343-353.

Ketthaisong, D. et al. (2015). Physicochemical and morphological properties of starch from fresh waxy corn kernels. J. Food Sci. Tech. 52, 6529-6537.

Kiseleva, V.I., Genkina, N.K., Tester, R., Wasserman, L.A., Popov, A.A., Yuryev, V.P. (2004) Annealing of normal, low and high amylose starches extracted from barley cultivars grown under different environmental conditions. Carbohydr. Polym. 56, 157-168.

Kibar, E.A.A. et al. (2011). Modeling of retrogradation of waxy and normal corn starches. Intnl. J. Food Properties 14, 954-967.

Klein, B. et al. (2013). Effect of single and dual heat-moisture treatments on properties of rice, cassava, and pinhao starches. Carbohydr. Polym. 98, 1578-84.

Li, E., Hasjim, J., Singh, V., Tizzotti, M., Godwin, I.D., Gilbert, R.G. (2013). Insights into sorghum starch biosynthesis from structure changes induced by different growth temperatures. *Cereal Chem*. 90, 223-230.

Li, L., Blanco, M., & Jane, J. (2007). Physicochemical properties of endosperm and pericarp starches during maize development. *Carbohydr.Polym.* 67, 630-639.

Li, L.; Jiang, H.; Campbell, M.; Blanco, M.; Jane, J. (2008). Characterization of maize amylose-extender (*ae*) mutant starches. Part I: Relationship between resistant starch contents and molecular structures. *Carbohydr.Polym.* 74, 396-404.

Li, Q.; Li, H.; Gao, Q.Y. (2015). The influence of different sugars on corn starch gelatinization process with digital image analysis method. Food Hydrocolloids 43, 803-811.

Li, Z. et al. (2014). Physicochemical properties of high-amylose maize starch. J Northwest A & F University 42, 53-60.

Lin, L. et al. (2016). Relationships between amylopectin molecular structures and functional properties of different-sized fractions of normal and high-amylose maize starches. Food Hydrocolloids 52, 359-368.

Liu, Q., Weber, E., Currie, V., Yada, R. (2003). Physicochemical properties of starches during potato growth. *Carbohydr. Poly.* 51, 213-221.

Lopez, C.A.; de Vries, A.H.; Marrink, S.J. (2012). Amylose folding under the influence of lipids. Carbohydr. Res. 364, 1-7.

Lu, D.L., Cai, X.M., Yan, F.B., Sun, X.L., Lu, W.P. (2014) Effects of high temperature after pollination on physicochemical properties of waxy maize flour during grain development. J Sci. Food Agric. 94, 1416-1421.

Lu, H.F. et al. (2014). Starch composition and its granules distribution in wheat grains in relation to post-anthesis high temperature and drought stress treatments. Starch 66, 419-428.

Lu, T., Jane, J., Keeling, P.L., Singletary, G.W. (1996). Maize starch fine structures affected by ear developmental temperature. *Carbohydr. Res*. 282, 157-170.

Martin, C.; Smith, A.M. (1995). Starch biosynthesis. The Plant Cell. 7: 971-985.

Matsuki, J., Yasui, T., Kohyama, K., Sasaki, T. (2003). Effects of environmental temperature on structure and gelatinization properties of wheat starch. *Cereal Chem*. 80, 476-480.

Mendez-Montealvo, G. et al. (2015). Structural features of banana starches using HPSEC-MALLS-RI. 14, 293-302.

Miles, M. J., Morris, V. J., Ring, S. G. (1984). Some recent observations on the retrogradation of amylose. *Carbohydr. Polym.*, 4, 73–77.

Mua, J.P. and Jackson, D.S. (1997). Fine structure of corn amylose and amylopectin fractions with various molecular weights. J Agri. Food Chem. 45, 3840-3847.

Mukerjea, R. & Robyt, J.F. (2010). Isolation, structure, and characterization of the putative soluble amyloses from potato, wheat, and rice starches. Carbohydr. Polym. 345, 449-451.

Munoz, L.A. et al. (2015). Loss of birefringence and swelling behavior in native starch granules: Microstructural and thermal properties. J. Food Engineering 152, 65-71.

Nadiha, MZN. et al. (2015). Comparative susceptibilities of sago, potato, and corn starches to alkali treatment. Food Chem. 121, 1053-1059.

Nakamura Y., Utsumi Y., Sawada T., Aihara S., Utsumi C., Yoshida M., Kitamura S. (2010). Characterization of the reactions of starch branching enzymes from rice endosperm. Plant Cell Physiol. 51(5):776-794.

Nikuni, Z. (1978). Studies on starch granules. *Starch*, 30 (4), 105-111.

Nishiyama, Y. et al. (2010). Molecular and crystal structure of 7-fold V-amylose complexed with 2-propanol. Macromol. 43, 8628-8636.

Nwokocha, L.M. (2014). A comparative study of properties of starches from Irish potato (Solanum Tuberosum) and sweet potato (Ipomea batatas) grown in Nigeria. Starch 66, 714-723.

Obrio, W.C.; Ray, S.S.; Emmambux, M.N. (2012). V-amylose structural characteristics, methods of preparation, significance, and potential applications. Food Review Intln. 28, 412-438.

Oh, S.M. & Shin, M. (2015). Physicochemical properties and molecular structures of Korean waxy rice starches. Food Sci. Biotech. 24, 791-798.

Ohdan, K., Sawada, T., Nakamura, Y. (2011) Effect of temperature on starch branching enzyme properties of rice. J Applied Glycoscience 58, 19-26.

Okechukwu, P.E., and Anandha Rao. M. (1996). Kinetics of Cowpea Starch Gelatinization Based on Granule Swelling. 48, 43-47.

Pan, D.D. & Jane, J. (2000). Internal structure of normal maize starch granules revealed by chemical surface gelatinization. Biomacromolecules 1, 126-132.

Peat, S., Whelan, W. J., Thomas,G. J. (1952). Evidence of multiple branching in waxy maize starch. *J. Chem. Soc. Chem. Commun.* , 4546–4548.

Perera, C., Lu, Z., Sell, J., Jane, J. (2001). Comparison of physicochemical properties and structures of sugary-2 cornstarch with normal and waxy cultivars. *Cereal Chem.,* 78, 249.

Perez, S., & Bertoft, E. (2010). The molecular structures of starch components and their contribution to the architecture of starch granules: A comprehensive review. *Starch*, 62, 389-420.

Pfannemuller, B., Mayerhofer, H., Schultz, R.C. (1971). Conformation of amylose in aqueous solution: optical rotatory dispersion and circular dichroism of amylose-iodine complexes and dependence on chain length of retrogradation of amylose. Biopolymers 10, 243-261.

Putaux, J.L.; Nishiyama, Y.; et al. (2011). Helical conformation in crystalline inclusion complexes of V-amylose: A historical perspective. Macromolecular Symposia 303, 1-9.

Ragheb, A.A., Elthalouth, I.A., Tawfik, S. (1995) Gelatinization of starch in aqueous alkaline-solutions. Starch 47, 338-345.

Regina, A., Kosar-Hashemi, B., Ling, S., Li, Z.Y., Rahman, S., Morell, M. (2010) Control of starch branching in barley defined through differential RNAi suppression of starch branching enzyme IIa and IIb. J Experimental Botany 61, 1469-1482.

Robyt, J. F. (1998). *Essentials of Carbohydrate Chemistry*, Springer-Verlag, New York.

Ryno, L.M.; Levine, Y.; Iovine, P.M. (2014). Synthesis, characterization, and comparative analysis of amylose-guest complexes prepared by microwave irradiation. Carbohydr. Res. 383, 82-88.

Sasaki, T., Yasui, T., Matsuki, J. (2000). Effect of amylose content on gelatinization, retrogradation, and pasting properties from waxy and nonwaxy wheat and their F1 seeds. Cereal Chem. 77, 58-63.

Saripalli, G. & Gupta, P.K. (2015). AGPase: its role in crop productivity with emphasis on heat tolerance in cereals. Theoretical and Applied Genetics 128, 1893-1916.

Seetharaman, K. & Bertoft, E. (2013). Perspectives on the history of research on starch Part V: On the conceptualization of amylopectin structure. Starch 65, 1-7.

Schirmer, M.; Hochstotter, A.; Jekle, M.; Arendt, E.; Becker, T. (2013). Physicochemical and morphological characterization of different starches with variable amylose/amylopectin ratio. Food Hydrocolloids 32, 52-63.

Schirmer, M.; Jekle, M.; Becker, T. (2015). Starch gelatinization and its complexity for analysis. Starch 67, 30-41.

Shao, Y.; Tseng, Y.; Chang, Y.; Lin, J.; Li, C. (2007). Rheological properties of rice amylose gels and their relationships to the structures of amylose and its subfractions. Food Chem. 103, 1324-1329.

Shi, Y.C., Capitani, T., Trzasko, P., &Jeffcoat, R. (1998). Molecular structure of a low-amylopectin starch and other high-amylose maize starches. J Cereal Sci. 27, 289-299.

Shi, Y.C., Seib, P.A., Bernardin, J.E. (1994). Effects of temperature during grain-filling on starches from six wheat cultivars. *Cereal Chem*. 71, 369-383.

Sharma, R., Sissons, M.J., Rathjen, A.J., Jenner, C.F. (2002) The null-4A allele at the waxy locus in durum wheat affects pasta cooking quality. J Cereal Sci. 35, 287-297.

Singh, S., Singh, N., Isono, N., Noda, T. (2010). Relationship of granule size distribution and amylopectin structure with pasting, thermal, and retrogradation properties in wheat starch. J Agri. Food Chem. 58, 1180-1188.

Smith, A.M. (2001). The biosynthesis of starch granules. Biomacromolecules 2, 335-341.

Song HY, Lee SY, Choi SJ, Kim MK, Kim JS, et al. (2014) Digestibility and physicochemical properties of granular sweet potato starch as affected by annealing. *Food Sci. Biotechnol.* 23, 23–31

Srichuwong, S., Sunarti, T. C., Mishima, T., Isono, N., Hisamatsu, M. (2005). Starches from different botanical sources I: Contribution of amylopectin fine structure to thermal properties and enzymes digestibility. *Carbohydr. Polym.,* 60, 529-538.

Stamova, B.S., Laudencia, D., Beckles, D.M. (2009) Transcriptional analysis of starch biosynthesis in the developing grain of hexaploid wheat. Intel. J Plant Genomics, 23.

Suh, D.S. and Jane, J. (2003). Comparison of starch pasting properties at various cooking conditions using the Micro-Visco-Amylose-Graph and the Rapid Visco Analyzer. Cereal Chem. 80, 745-749.

Szymanek, M.; Tanas, W.; Kassar, F.H. (2015). Kernel carbohydrate concentration in sugary-1, sugary enhanced and shrunken sweet corn kernels. Agriculture and Agricultural Science Procedia 7, 260-264.

Takeda, Y., Hizukuri, S., Takeda, C., Suzuki, A. (1987). Structures of branched molecules of amyloses of various origins, and molecular fractions of branched and unbranched molecules. *Carbohydr. Res.*, 164, 139-145.

Takeda, Y., Shitaozono, T., Hizukuri, S. (1988). Molecular structure of corn starch. *Starch*, 40, 51–54.

Takeda, Y., Shibahara, S., Hanashiro, I. (2003). Examination of the structure of amylopectin molecules by fluorescent labeling. Carbohydr. Res. 339, 471-475.

Takeo, K., Tokumura, A., Kuge, T. (1973). Complexes of starch and its related materials with organic compounds. X. X-ray diffraction of amylose-fatty acid complexes. *Starch*, 35, 357-362.

Tester, R.F. (1997). Influence of growth conditions on barley starch properties. *Int. J Biol. Macromol*. 21, 37-45.

Tester, R.F. & Debon S.J.J. (2000). Annealing of starch - A review. *Int. J. Biol. Macromol*. 27, 1-12.

Tester, R.F. and Karkalas, J. (2002). Starch. In: Steinbuchel, A. (Series Ed.) Vandamme, E.J., De Baets. S., Steinbuchel, A. Biopolymers, vol. 6. Polysaccharides. II. Polysaccharides from Eukaryotes, Wiley-VCH, Weinheim, pp. 381-438.

Tester, R. F., Karkalas, J., Qi, X. (2004). Starch-composition, fine structure and architecture. *J. Cereal Chem.* 39, 151-165.

Tester, R. F. and Morrison, W. R. (1992). Swelling and Gelatinization of Cereal Starches. III. Some Properties of Waxy and Normal Nonwaxy Barley Starches. 69, 654-658.

Tester, R.F., South, J.B., Morrison, W.R., Ellis, R.P. (1991). The effects of ambient temperature during the grain-filling period on the composition and properties of starch from four barley genotypes. *J Cereal Sci*. 13, 113-127.

Tetlow, I.J. (2006). Understanding storage starch biosynthesis in plants: a means to quality improvement. Canadian Journal of Botany 84, 1167-1185.

Tetlow, I.J. (2011). Starch biosynthesis in developing seeds. Seed Sci. Res. 21, 5-32.

Thitisaksakul, M., Jimenez, R.C., Arias, M.C., Beckles, D.M. (2012). Effects of environmental factors on cereal starch biosynthesis and composition. *J Cereal Sci*. 56, 67-80.

Thygesen, L.G., Blennow, A., Engelsen, S.B. (2003). The effects of amylose and starch phosphate on starch gel retrogradation studied by low-field H-1 NMR relaxometry. Starch 55, 241-249.

Tomasik, P., Wang, Y.J., Jane, J. (1995). Complexes of starch with low-molecular saccharides. Starch 47, 185-191.

Toyota, K., Tamura, M., Ohdan, T., Nakamura, Y. (2006) Expression profiling of starch metabolism-related plastidic translocator genes in rice. Planta 223, 248-257.

Vamadevan V, Bertoft E, Soldatov DV, Seetharaman K. (2013) Impact on molecular organization of amylopectin in starch granules upon annealing. *Carbohydr. Polym.* 98, 1045–55

Vamadevan, V. and Bertoft, E. (2015). Structure-function relationships of starch components. Starch 67, 55-68.

Vandeputte, G.E., Vermeylen, R., Geeroms, J., Delcour, J.A. (2003). Rice starches. I. Structural aspects provide insight into crystallinity characteristics and gelatinization behavior of granular starch. J Cereal Sci. 38, 43-52.

VermeylenR,Goderis B,Delcour JA. (2006) An X-ray study of hydrothermally treated potato starch. *Carbohydr. Polym.* 64, 364–75

Wang, K.; Hasjim, J.; Wu, A.C.; Henry, R.J.; Gilbert, R.G. (2014). Variation in amylose fine structure of starches from different botanical sources. J Agri. Food Chem. 62, 4443-4453.

Wang, S.J. et al. (2014) A comparative study of annealing of waxy, normal and high-amylose maize starches: The role of amylose molecules. Food Chem. 164, 332-338.

Wang, S.J. et al. (2015). Starch retrogradation: A comprehensive review. Comprehensive Reviews in Food Science and Food Safety 14, 568-585.

Wang WJ, Powell AD, Oaks CG. (1997). Effect of annealing on the hydrolysis of sago starch granules. *Carbohydr. Polym.* 33, 195–202

Wang, Y.J., White, P., Pollak L. (1992). Thermal and gelling properties of maize mutants from the OH43 inbred line. Cereal Chemistry 69(3):328-334.

Wang, Z.; et al. (2012). Preparation, characterization and properties of starch-based wood adhesive. Carbohydr. Polym. 88, 699-706.

Waterschoot, J. et al. (2015). Production, structure, physicochemical and functional properties of maize, cassava, wheat, potato, and rice starches. Starch 67, 14-29.

Waterschoot, J. et al. (2014). Pasting properties of blends of potato, rice and maize starches. Food hydrocolloids 41, 298-308.

Wen, Y.; Kang, H.; Wang, D.; Qiu, X.; Lian, X.; Li, L. (2014). The salt-induced crystallization behavior of potato amylose. Starch 66, 857-864.

Whittam, M.A., Noel, T.R., Ring, S.G. (1990). Melting behavior of A- and B-type crystalline starch. Int. J. Biol. Macromol. 12, 359-362.

Wild, D.L., & Blanshard, J.M.V. (1986). The relationship of the crystal structure of amylose polymorphs to the structure of the starch granule, *Carbohydr. Poly*. 6, 121-143

Witt, T. et al. (2012). Relations between molecular, crystalline, and lamellar structures of amylopectin. Biomacromol. 13, 4273-4282.

Wu, H. C. H., & Sarko, A. (1978). The double-helical molecular structure of crystalline A-amylose. *Cabohydrate Research, 61*, 27-40.

Xu, J. et al. (2012). Comparative study of spring dextrin impact on amylose retrogradation. J. Agric. Food Chem. 60, 4970-4976.

Xu, Y.X. et al. (2013). Resistant starch content, molecular structure and physicochemical properties of starches in Virginia-grown corn, potato and mungbean. J. Cereals Oilseeds 4, 10-18.

Yamakawa, H., Hirose, T., Kuroda, M., Yamaguchi, T. (2007) Comprehensive expression profiling of rice grain filling-related genes under high temperature using DNA microarray. Plant Physiol. 144, 258-277.

Yamashita, Y., Monobe, K. (1971). Single crystals of amylose V complexes. III. Crystal 81 helical configuration. *J. Polym. Sci., Part A: Polym. Chem.*, 4, 1471–1481.

Yang, H. et al. (2015). Heat stress at different grain filling stages affects fresh waxy maize grain yield and quality. Cereal Chem. 92, 258-264.

Yangcheng, H.; Gong, L., Zhang, Y., Jane, J. (2016). Physicochemical properties of Tibetan hull-less barley starch. Carbohydr. Polym. 137, 525-531.

Yangcheng, H.; Jiang, H.; Blanco, M.; & Jane, J. (2013). Characterization of normal and waxy corn starch for bioethanol production. *J. Agric. Food Chem*. 61, 379-386.

Yoo, S. H., Jane, J. (2002). Structural and physical characteristics of waxy and other wheat starches. *Carbohydr. Polym.* 49, 297.

Yoo, S.H., Perera, C., Shen, J., Ye, L. Suh, D.S., Jane, J. (2009). Molecular structure of selected tuber and root starches and effect of amylopectin structure on their physical properties. J Agric. Food Chem. 57, 1556-1564.

Yu, S.F. et al. (2014). Relationship between intrinsic viscosity, thermal, and retrogradation properties of amylose and amylopectin. Czech J. Food Sci. 32, 514-520.

Yu, X.R.; Zhang, J.; Shao, S.S.; Yu, H.; Wang, Z. (2015). Morphological and physicochemical properties of bulb and bulbil starches from Lilium lancifolium. Starch 67, 448-458.

Yu, X.R. et al. (2015). Endosperm structure and physicochemical properties of starches from waxy, normal, and super-sweet maize. Intnl. J. Food Properties 18, 2825-2839.

Zavareze ED, Dias ARG. (2011). Impact of heat-moisture treatment and annealing in starches: a review. *Carbohydr. Polym.* 83, 317–28

Zavareze, ED. et al. (2012). Development of oxidized and heat-moisture treated potato starch film. Food Chem. 132, 344-350.

Zeng, S.X.; Xu, L.B.; Guo, Z.B.; Chen, B.Y.; Zheng, B.D. (2015). Physicochemical properties of lotus-seed starch obtained from different maturity stages. Current Topics in Nutraceutical Research 13, 231-234.

Zhao, J.W. et al. (2015). Distribution of phosphorus and hydroxypropyl groups within starch granules of modified sweet potato starches as determined after chemical peeling. Carbohydr. Polym. 132, 630-637.

CHAPTER 2

PYSICOCHEMICAL PROPERTIES OF TIBETAN HULL-LESS BARLEY STARCH

A paper published in *Carbohydrate Polymers (Vol.137, pp 525-531)*

Hanyu Yangcheng [a], Lingxiao Gong [b], Ying Zhang [b], Jay-lin Jane [a,*]

[a] Department of Food Science and Human Nutrition, Iowa State University, Ames 50011, Iowa, USA.

[b] Department of Food Science and Nutrition, College of Biosystems Engineering and Food Science, Zhejiang University, Hangzhou 310058, Zhejiang Province, China.

[*] **Corresponding author**: Jay-lin Jane

Tel: 01 515-294-9892; Fax: 01 515-294-8181;

E-mail address: jjane@iastate.edu (J.Jane)

ABSTRACT

Objectives of this study were to 1) determine the starch physicochemical properties of two commercial Tibetan hull-less barley varieties, Beiqing (BQ) and Kangqing (KQ); and 2) understand the relationship between unique properties of the starches, their structures, and impacts of growing conditions. The BQ barleys were grown at a location with lower temperature and less rainfall compared with the KQ barleys. The BQ starches showed significantly lower onset-gelatinization temperature (54.1-54.9 °C), larger gelatinization-temperature range (9.4-10.6 °C), and higher peak-viscosities (138.9-153.9 RVU) than the KQ starches (55.1-56.1°C, 7.4-8.8 °C, and 63.4-64.7 RVU, respectively). After a treatment with 2% sodium-dodecyl-sulphate solution, the KQ starches showed substantially greater increases in peak viscosities than the BQ starches. Annealing of starch and enhanced amylose-lipid complex formation, resulting from higher growing temperature during the development of the KQ starches, likely contributed to the differences in thermal and pasting properties between the BQ and KQ starches.

Keywords: Tibetan hull-less barley; Thermal properties; Pasting properties; Annealing effects

1. Introduction

Barley is the fourth largest cereal crop produced worldwide, following maize, rice, and wheat (FAOSTAT, 2012). Barley grain is mainly used for the production of alcoholic beverage and livestock feed (Li, Vasanthan, Rossnagel, & Hoover, 2001a). Hull-less barley, also known as naked barley, is different from hulled barley because kernels of hull-less barley can easily detach from the hull during threshing. This is attributed to a recessive gene, *nud*, expressed in hull-less barley varieties, which inhibits the development of husks and caryopsis (Franckowiack & Konishi, 1997). Compared with hulled barley, hull-less barley needs less space for storage and transportation and can avoid the loss of vitamins and minerals resulting from the peeling operation (Liu et al., 1996).

Hull-less barley usually has greater starch, protein, and β-glucan contents than the hulled barley because hull-less barley does not have the fibrous hull (Bhatty, 1999). Applications of hull-less barley have been studied, including for swine and poultry feeds (Darroch, Aherne, Helm, Sauer, & Jaikaran, 1996; Liu et al., 1996), production of bran and flour for food ingredients (Bhatty, 1995a), extraction of β-glucan for food applications (Bhatty, 1995b), and production of fuel ethanol (Ingledew, Jones, Bhatty, & Rossnagel, 1995; Tomas, Dhas, Rossnagel, & Ingledew, 1995). Different genotypes of hull-less barley, including normal (25-30% amylose), waxy (1-5% amylose), zero-amylose (0%), and high-amylose (35-45%) varieties, have been developed through traditional breeding practices (Bhatty & Rossnagel, 1997; Li et al., 2001a). Starches isolated from these hull-less barley varieties showed diverse physicochemical properties, such as pasting temperature and pasting viscosity, paste clarity, and freeze-thaw stability (Li, Vasanthan, Rossnagel, & Hoover, 2001b; Song & Jane, 2000; Zheng, Han, & Bhatty, 1998), which extends the potential of using hull-less barley starch for various food and industrial applications.

As a traditional staple food for Tibetan people, hull-less barley is a major food crop grown on the Tibetan Plateau, representing 64% of the total crop production in Tibet (Zou et al., 2008). The recent growing interest in Tibetan hull-less barley (THLB) has been sparked by its high nutritional values and health benefits. The low incidence of hyperlipidemia and diabetes in Tibetan population has been associated with the consumption of hull-less barley (Gou, Li, & Guo, 2005). Studies have shown that, among 164 barley cultivars collected from China, Canada and Australia, THLB has the largest β-glucan content, up to 8.62% (average 5.25%) (Zhang, Wang, & Chen, 2002). The bran of THLB is a good source of linoleic acid and palmitic acid (Qian, Jiang, Su, & Gao, 2009). THLB is also a rich source of soluble phenolic compound, which displays an excellent radical-scavenging capacity in plasma (Gong, Cheng, Wu, Wu, & Zhang, 2012). The THLB extracts inhibit lipid oxidation in rat tissues (Li, Yan, & Zhong, 2005) and increase the survival time of rats under hypoxia conditions (Zhang et al., 2007).

Beiqing (BQ) and Kangqing (KQ) hull-less barley are the most important commercial varieties grown in Tibet area (Feng, Yang, Liu, Gou, &Tang, 2005; Ma 2011). The production yields of BQ (1518-1822 kg/acre) and KQ varieties (1570-1744 kg/acre) are 10-20% higher than other commercial varieties (Feng et al., 2005; Ma 2011). The two THLB varieties, however, have quite different eating quality. Starch is the major component of hull-less barley grain (59-64%) (Li et al., 2001a), which affects the eating quality of the grain. In contrast to abundant literature on health-promoting values of THLB, there is a scarcity of information on its starch physicochemical properties and the impacts on the eating quality and value-added applications (Li et al., 2014).

Objectives of this study were to 1) determine the starch physicochemical properties of two commercial THLB varieties, Beiqing (BQ) and Kangqing (KQ); and 2) understand the relationship between unique properties of the starches, their structures, and impacts of

growing conditions. Results obtained from this study will unveil the mechanism of the variations in starch properties of THLB and are important for development of value-added utilization of the THLB starch.

2. Materials and methods

2.1 Materials

Six Tibetan spring hull-less barley varieties (*Hordeum vulgare L. var. nudum hook. f.*) were used in this study. Three of the six barley varieties, Beiqing 4 (BQ4), Beiqing 6 (BQ6), and Beiqing 7 (BQ7), were grown in Tibetan autonomous prefecture of Haibei, Qinghai province (N36°58', E100°52', ~3,110 m altitude). The other three varieties, Kangqing 3 (KQ3), Kangqing 6 (KQ6), and Kangqing 7 (KQ7), were grown in Tibetan autonomous prefecture of Ganze, Sichuan province (N30°04', E101°95', ~3,500 m altitude). The growing season of the six THLB varieties was from May to September. The average temperature and accumulated rainfall of the growing season in the Beiqing location were 7.4 °C and 27.0 cm, respectively, whereas that in the Kangqing location were 13.3 °C and 58.9 cm, respectively (Public Weather Service Center of CMA, 2014). THLB kernels were coarsely crushed before shipping to Iowa State University.

Pseudomonas isoamylase (EC 3.2.1.68, 280 U/mg) was purchased from Megazyme International Ireland (Wicklow, Ireland). Porcine pancreatic α-amylase (EC 3.2.1.1, 21.6 U/mg) and *A. niger* amyloglucosidase (EC 3.2.1.3, ≥300 U/ml) were from Sigma-Aldrich Co. (St. Louis, MO). All other chemicals were reagent grade and were purchased from either Sigma-Aldrich Co. (St. Louis, MO) or Fisher Scientific (Pittsburgh, PA) and used without further purification.

2.2 Starch Isolation by Wet-milling

Starches were isolated from the coarsely-crushed THLB kernels using a wet-milling method reported by Li, Jiang, Campbell, Blanco, & Jane (2008).

2.3 Scanning Electron Microscopy

Scanning electron micrographs of isolated starch granules were taken using a scanning electron microscope (JEOL JSM-35, Tokyo, Japan) following the methods previously reported (Song & Jane, 2000). The average starch granule size was determined by measuring 200 granules using an Infinity Analyze software (version 6.1.0, Lumenera Corp., Canada).

2.4 X-ray Diffraction Pattern

X-ray diffraction patterns of starch samples were obtained using a diffractometer (Siemens D-500, Madison, WI) following the methods previously reported (Song & Jane, 2000). The copper tube was operated at 30 mA and 45 kV, and the scanning region of the two-theta angle (2θ) was from 4 to 40 degree. The crystallinity of the starch was calculated using a MDI JADE software (version 6.5, Materials Data Inc., Livermore, California, USA)

2.5 Amylose Content of Starch

The amylose content of the THLB starch was determined using an iodine potentiometric- autotitrator (702 SM Titrino, Brinkmann Instrument, Westbury, NY) (Song & Jane, 2000). Starch was defatted using 85% methanol in a Soxhlet extractor for 16 h prior to the analysis. The iodine affinity of amylose used for the calculation was 0.2 (Takeda & Hizukuri, 1987). The amylose content was calculated using the equation: Amylose (%) = 100% IA_s / 0.2, where IA_s was the iodine affinity of the starch.

2.6 Lipid Content of Starch

Lipid contents of the starches were determined using a Gas Chromatography-Flame Ionization Detection system (HP 5890 Series II, Hewlett-Packard, Palo Alto, CA), equipped

with a Supelco SP-2340 capillary column (Sigma-Aldrich Co., St. Louis, MO). The fatty acid methyl ester (FAME) was prepared directly using the native starch without prior lipid extraction. Starch (500 mg, dsb) was suspended in 4 ml of methanol : chloroform (1:1) containing 3% (v/v) sulfuric acid. Margaric acid (C17:0, 1 mg) was added as the internal reference. The mixture was incubated at 80 °C overnight to completely convert the lipids to FAME. The mixture was washed twice with deionized water, and the chloroform layer containing the FAME was collected. The chloroform was evaporated under nitrogen gas-flow, and the obtained FAME was re-dissolved in 0.5 ml of analytical-grade hexanes for gas-chromatography analysis. The oven temperature was programmed with an initial hold of 1 min at 100 °C, heating from 100 to 240 °C at 4 °C/min, and a final hold of 5 min (the total analysis time was 41 min). The lipid content was calculated following the equation:

$$\text{Lipid (\%)} = ((100\% - \text{Peak}_{C17:0}\%) / \text{Peak}_{C17:0}\% \times 1 \text{ mg}) / 500 \text{ mg}) \times 100\%$$

2.7 Phosphorus Analysis and Characterization

Total phosphorus contents of the THLB starches were determined using a colorimetric method after an ashing process (Singh & Ali, 1987). The chemical structure of phosphorus of the starch was characterized using a ^{31}P-NMR spectrometer (Bruker Instruments, Billerica, MA) following the method reported by Kasemsuwan & Jane (1996).

2.8 Amylopectin Branch-chain Length Distribution

Amylopectin of the THLB starch was separated from amylose and collected using a gel-permeation chromatographic column packed with Sepharose CL-2B gel. The isolated amylopectin was debranched using *Pseudomonas* isoamylase (Megazyme International Irelands, Wicklow, Ireland). The branch chains of the debranched amylopectin were labeled with 8-amino-1,3,6-pyrenetrisulfonic acid (0.2M in 15% acetic acid), and the branch-chain length distribution was analyzed using a fluorophore-assisted capillary electrophoresis

(Beckman Coulter, Fullerton, CA) following the methods previously reported (Jiang, Campbell, Blanco, & Jane, 2010; Morell, Samuel, & O'Shea, 1998).

2.9 Starch Thermal Properties

Thermal properties of the isolated starch were analyzed using a differential scanning calorimeter (DSC, Diamond, Perkin-Elmer, Norwalk, CT). Starch gelatinization onset (T_o), peak (T_p), and conclusion temperatures (T_c), and enthalpy change (ΔH) were obtained using a Pyris software (Perkin-Elmer). The gelatinized starch samples were stored at 4 °C for 7 days and then analyzed using the same parameters for their percentages retrogradation. The percentage retrogradation was calculated using the equation: Retrogradation (%) = 100% ΔH of dissociation of retrograded starch / ΔH of starch gelatinization.

2.10 Starch Pasting Properties

Pasting properties of both the native THLB starch and the starch treated with a sodium-dodecyl-sulphate (*sds*) solution were analyzed. Isolated starches were treated with a *sds* solution (2%, w/v) at room temperature for 30min following the method previously reported (Debet & Gidley, 2006; Nierle, Baya, Kersting, & Meyer, 1990).

Starch pasting properties were analyzed using a Rapid Visco-Analyzer (Newport Scientific, Sydney, Australia) following the method of Jane et al. (1999). The pasting temperature, and the peak, breakdown, and final viscosities were determined using the Thermocline software (Newport Scientific).

2.11 Starch Digestibility

Starch digestibility was analyzed following the Englyst's method (Englyst, Kingman, & Cummings, 1992) with modifications (Li, et al. 2008). Starch was suspended (5%, w/v) in a sodium-acetate buffer solution (0.1 M, pH 5.2) and heated in a boiling-water bath for 20 min with stirring. After cooling and equilibrating at 37 °C in a shaker water bath, the starch sample was hydrolyzed *in vitro* using porcine pancreatin extract and *A. niger*

amyloglucosidase (Sigma-Aldrich Co., St. Louis, MO) with continuous agitation. Starch that was hydrolyzed within 20 min incubation-time was defined as rapidly-digestible starch. Starch that was hydrolyzed between 20 and 120 min was defined as slowly-digestible starch, and the portion that was not hydrolyzed at the end of 120 min was defined as resistant starch.

2.12 Syneresis of Starch Gels after Freeze-Thaw Cycles

Starch paste (5%, w/w, dsb) was prepared following the same procedures for starch pasting properties. The resulting starch paste (1±0.1 g) was quantitatively transferred to a pre-weighed microcentrifuge tube, and allowed to cool down at room temperature for 4 h. Starch gels in the tubes were stored at -18 °C for 20 h followed by thawing at 30 °C for 4 h. The process was repeated up to five cycles. After the 1st, 3rd, and 5th freeze-thaw cycles, the tubes were centrifuged at 6,600 *g* for 10 min to remove the water released from the gel. Percentage syneresis was calculated as the weight percentage of the water released on the basis of the initial gel weight.

2.13 Statistical Analysis

Data were subjected to analysis of variance and Tukey's multiple comparison analysis using PROC ANOA procedure of SAS 9.2 (SAS Institute, Inc., Cary, NC).

3. RESULTS

3.1 Starch Granule Morphology and Crystalline Structure

THLB starch granules isolated from the BQ and KQ barley displayed typical bimodal size-distributions (**Figure 1**). Large granules (A granules) had a lenticular shape and granule diameters of 10-30 μm, and small granules (B granules) had a spherical shape and granule diameters of 1-5 μm. These results were in line with those reported in previous studies on hulled and hull-less barley starches (Jane, Kasemsuwan, Leas, Zobel, &Robyt, 1994; Li et al., 2001a; Song & Jane, 2000; Vasanthan & Bhatty, 1996). Average diameters of the BQ starch

A- and B- granules were 12.0-13.1 μm and 2.0-2.1 μm, respectively, which were smaller than that of the KQ starch granules, 13.3-14.0 μm and 2.2-2.3 μm, respectively (**Table 1**).

X-ray diffraction studies of the THLB starch showed a typical A-type diffraction pattern with strong peaks at 2θ of 15.1°, 16.8°, 17.8°, and 23.0° (**Figure 2**). The BQ starches showed slightly lower percentage crystallinity (20.8-21.3%) than the KQ starches (21.3-21.9%).

3.2 Amylose, Lipid, and Phosphorus Contents of Starch

Results of the amylose contents showed that the BQ starches had less amylose contents (24.0-25.0%) than the KQ starches (26.2-26.9%). Correlation analysis showed that amylose contents of the starches positively correlated with the granule diameters of the A granules for both the BQ and KQ starches (R^2=0.99, $p<0.01$ for the BQ starches and R^2=0.90, $p<0.05$ for the KQ starches, respectively). These results agreed with previous reports that the amylose content increases with the increase in starch granule-size (Duffus & Murdoch, 1979; Li, Blanco, & Jane, 2007). Lipid contents of the BQ starches ranged 0.41-0.45% (w/w), which were similar to that of the KQ starches (0.42-0.45%, w/w) (**Table 1**).

Starch phosphorus-contents of the six varieties ranged 0.045-0.050% (w/w) (**Table 1**). ^{31}P-NMR spectra of all the THLB starches showed signals at the chemical shift between -1 and 0 ppm (Data not shown), corresponding to phospholipids, and no signals appeared between 4 and 6 ppm, corresponding to phosphate monoester derivatives (Kasemsuwan & Jane, 1996; Lim, Kasemsuwan, & Jane, 1994). The results showed that the phosphorus in THLB starches was present exclusively in the form of phospholipids.

3.3 Amylopectin Branch-Chain Length Distribution

Amylopectin branch-chain length distributions of the THLB starches are shown in **Table 2**. Average branch-chain lengths of the BQ amylopectin molecules (DP 20.5 – 20.7)

were similar to that of the KQ amylopectin (DP 20.2 – 20.6). The results were in line with the previous findings (DP 17.6-22.6) (Vasanthan & Hoover, 2009).

3.4 Starch Thermal Properties

Thermal properties of the THLB starches are shown in **Table 3**. The BQ starches showed significantly lower ($p<0.05$) onset-gelatinization temperatures (T_o) (54.1-54.9 °C) than the KQ starches (55.1-56.1 °C). Gelatinization-temperature ranges (T_c-T_o) of the BQ starches (9.4-10.6 °C) were significantly ($p<0.05$) larger than that of the KQ starches (7.4-8.8 °C). Percentages retrogradation of the gelatinized KQ starches after storage at 4 °C for seven days (24.6-27.8%) were greater than that of the BQ starches (21.1-25.0%).

3.5 Starch Pasting Properties

Starch pasting properties are shown in **Figure 3**. Remarkable differences in starch pasting properties were observed between the BQ and KQ barley. The BQ starches showed significantly greater peak viscosities (138.9-153.9 RVU) but lower pasting temperatures (90.6-91.3 °C) than the KQ starches (63.4-64.7 RVU and 92.5-93.2 °C, respectively) (**Figure 3** (A)). The peak viscosities of the BQ starches were more than double of that of the KQ starches.

To investigate the effect of amylose-lipid complex on starch pasting properties, we analyzed the pasting properties of the THLB starches after being treated with a *sds* solution (2%, w/v). It is known that *sds*, as a surfactant, removes lipids from the starch, and *sds*-treatment is unlikely to cause damage to the starch granules (Debet & Gidley, 2006; Nierle et al., 1990). The *sds*-treated THLB starches showed significant reductions in the pasting temperature (70.3-72.5 °C) compared with that of the native starch (90.6-93.2 °C) (**Figure 3**). The peak viscosities of the *sds*-treated BQ starches (232.7-238.4 RVU) increased to ~1.6 times of that of the native BQ starches (138.9-153.9 RVU), whereas that of the *sds*-treated KQ starches (191.6-214.8 RVU) increased to more than 3 times of that of the native KQ

starches (63.4-64.7 RVU) (**Figure 3**). The KQ starches showed substantially greater increases in peak viscosities than the BQ starches after the *sds* treatment. Consequently, the differences in peak viscosities between the BQ and KQ starches were substantially reduced (from >2.1 times to <1.2 times) after the *sds* treatment.

3.6 Starch Digestibility

Digestibility of the THLB starch after cooking is shown in **Table 4**. The BQ starches contained more RDS (76.8-78.6%) but less SDS (11.7-14.2%) and RS (8.6-9.8%) than the KQ starches (74.6-75.6%, 14.1-16.0%, and 9.4-10.3%, respectively).

3.7 Freeze-Thaw Stability of Starch Gel

Freeze-thaw stability of the starch gel, determined after the 1st, 3rd, and 5th freeze-thaw cycles (FTC), is shown in **Table 5**. In general, the syneresis increased with increasing numbers of FTC. After the 1st FTC, corn, BQ4, and BQ7 starch gels showed good stability (<15% syneresis), whereas KQ starch gels had a syneresis ranging 46.3-49.8%. After the 3rd and 5th FTC, however, corn, BQ4, and BQ7 starch gels lost stability and reached ~50% of syneresis. The KQ starch gel showed larger syneresis than the BQ starch gel (**Table 5**), and the results were consistent with the greater retrogradation rate of the KQ starches (**Table 3**), both resulting from the restricted swelling of the starch granules.

4. DISCUSSION

The physicochemical properties of the starch isolated from two commercial THLB varieties, BQ and KQ, were compared in this study. The results showed significant differences in starch physicochemical properties between the BQ and KQ varieties, especially in starch thermal and pasting properties.

The BQ starches showed significantly lower onset-gelatinization temperature and larger gelatinization temperature-range than the KQ starches. The branch-chain lengths of

amylopectin, however, were similar between the BQ and KQ starches, which unlikely contributed to the differences in the starch thermal properties between the BQ and KQ varieties. It is known that gelatinization temperatures can also be affected by the growing conditions, including temperature and moisture during the development of starch granules (Lu, Jane, Kelling, &Singletary, 1996; Tester, 1997), which resembles the annealing process of starch *in vitro*. The average temperature and accumulated rainfall during the growing season of the KQ varieties (13.3°C and 58.9 cm, respectively) were substantially higher than that of the BQ varieties (7.4°C and 27.0 cm, respectively). The higher growing temperature and abundant moisture during the development of starch granules could cause annealing of starch and resulted in the higher onset-gelatinization temperatures and narrower gelatinization temperature-ranges of the KQ starches (Tester, Debon, & Sommerville, 2000).

The BQ starches showed significantly higher peak viscosities but lower pasting temperatures than the KQ starches. It is known that amylopectin is primarily responsible for granule swelling and viscosity (Tester & Morrison, 1990) and starch pasting properties are affected by amylose and lipid contents (Jane et al., 1999; Morrison, Tester, Snape, Law, & Gidley, 1993; Srichuwong, Sunarti, Mishima, Isono, & Hisamatsu, 2005). The insignificant difference in amylopectin branch-chain length and lipid contents and small differences in the amylose contents between the BQ and KQ starches were unlikely a convincing explanation of the significant differences in starch pasting properties. It has also been reported that starch granule swelling is significantly affected by the growing temperature of the plant during starch development (Tester, 1997). Elevated growing temperatures enhanced the development of double-helical crystalline structure as shown in **Figure 2**, which reduced the rate of starch hydration and restricted granule swelling (Tester, 1997; Tester et al., 2000). After removing lipids by *sds*-treatment, the KQ starches showed substantially greater increases in peak viscosities than the BQ starches. These results indicated that starch-lipid

interactions in the KQ starches could be enhanced by the high growing temperature and moisture during the development of starch granules, which in turn further restricted granule swelling of the KQ starches. The higher pasting temperatures and lower viscosities of the KQ starches were likely results of starch annealing and the enhanced amylose-lipid complex formation during the development of starch granules. The KQ starch granules had restricted swelling after cooking, which were less susceptible to enzyme hydrolysis (Singh, Dartois, & Kaur, 2010) and displayed less RDS contents but greater SDS and RS contents than the BQ starches.

5. CONCLUSIONS

The Tibetan hull-less barley starches contained 24.0-26.9% amylose, 0.41-0.45% lipids, and 0.045-0.050% (w/w) phosphorus, in the form of phospholipids. The BQ starches showed significantly lower onset-gelatinization temperature but larger gelatinization-temperature range than the KQ starches. The BQ starches showed significantly greater peak viscosities than the KQ starches. After a treatment with 2% sodium-dodecyl-sulphate solution, the starches showed significant decreases in pasting temperatures and increases in peak viscosities, and the KQ starches showed substantially greater increases in peak viscosities than the BQ starches. Annealing of starch and enhanced amylose-lipid complex formation, resulting from higher growing temperatures and more rainfall during the growth and development of the KQ starches, likely contributed to the differences in thermal and pasting properties between the BQ and KQ starches. The cooked KQ starches displayed less RDS content but more SDS and RS contents than the BQ starches, resulting from restricted swelling of the KQ starch granules compared with the BQ starch granules after cooking.

ACKNOWLEDGMENTS

The authors thank the Microscopy and NanoImaging Facility at Iowa State University for the microscopic study.

REFERENCES

Bhatty, R. S. (1995a). Hull-less barley bran: A potential new product from an old grain. *Cereal Foods World* 40, 819-824.

Bhatty, R. S. (1995b). Laboratory and pilot plant extraction and purification of β-glucans from hull-less barley and oat brans. *Journal of Cereal Science* 22, 163-170.

Bhatty, R. S. (1999). The potential of hull-less barley. *Cereal Chemistry* 76, 589-599.

Bhatty, R. S., & Rossnagel, B. G. (1997). Zero amylose lines of hull-less barley. *Cereal Chemistry* 74, 190-191.

Darroch, C. S., Aherne, F. X., Helm, J., Sauer, W. C., & Jaikaran, S. (1996). Effects of dietary level of barley hulls and fiber type on digestibilities of Condor hulless barley in growing swine. *Animal Feed Science and Technology* 61, 173-182.

Debet, M. R., & Gidley, M. J. (2006). Three classes of starch granule swelling: Influence of surface proteins and lipids. *Carbohydrate Polymers* 64, 452-465.

Duffus, C.M. & Murdoch, S.M. (1979). Variation in starch granule size distribution and amylose content during wheat endosperm development. *Cereal Chemistry* 56, 427-429.

Englyst, H. N., Kingman, S. M., & Cummings, J. H. (1992). Classification and measurement of nutritionally important starch fractions. *European Journal of Clinical Nutrition* 46, S33-50.

FAOSTAT, (2012). The Statistics Division of the Food and Agriculture Organization. (URL: http://faostat3.fao.org/faostat-gateway/go/to/download/Q/QC/E; Last accessed: 02/07/2014)

Feng, J., Yang, K., Liu, T., Gou, A., Tang, Y. (2005). Highland barley in Ganze prefecture of Sichuan province. *Barley Science* 3, 28-34.

Franckowiack, J. D. & Konishi T. (1997). Naked caryopsis. *Barley Genet. Newsletter* 26, 51–52.

Gong L., Cheng, J., Wu, L., Wu, X., & Zhang, Y. (2012). Tibetan hull-less barley (*Hordeum vulgare L.*) as a potential source of antioxidants. *Cereal Chemistry* 89, 290-295.

Gou, A. C., Li, L., & Guo, C. H. (2005). Discussion on the importance of highland barley production from Tibetan compatriot the food construction variety. *Chinese Agricultural Science Bulletin* 21, 142-145.

Ingledew, W. M., Jones, A. M., Bhatty, R. S., & Rossnagel, B. G. (1995). Fuel alcohol production from hull-less barley. *Cereal Chemistry* 72, 147-150.

Jane, J., Chen, Y. Y., Lee, L. F., McPherson, A. E., Wong, K. S., Radosavljevic, M., & Kasemsuwan, T. (1999). Effects of amylopectin branch-chain length and amylose content on the gelatinization and pasting properties of starch. *Cereal Chemistry* 76, 629-637.

Jane, J., Kasemsuwan, T., Leas, S., Zobel, H. F., & Robyt, J. F. (1994). Anthology of starch granule morphology by scanning electron microscopy. *Starch* 46, 121-129.

Jiang, H., Campbell, M., Blanco, M., & Jane, J. (2010). Characterization of maize amylose-extender (*ae*) mutant starches. Part II: Structures and properties of starch residues remaining after enzymatic hydrolysis at boiling-water temperature. *Carbohydrate Polymers* 80, 1-12.

Kasemsuwan, T., & Jane, J. (1996). Quantitative method for the survey of starch phosphorus derivatives and starch phospholipids by ^{31}P Nuclear Magnetic Resonance spectroscopy. *Cereal Chemistry* 73, 702-707.

Li, J. H., Vasanthan, T., Rossnagel, B., & Hoover, R. (2001a). Starch from hull-less barley: I. Granule morphology composition and amylopectin structure. *Food Chemistry* 74, 395-405.

Li, J. H., Vasanthan, T., Rossnagel, B., & Hoover, R. (2001b). Starch from hull-less barley: II. Thermal, rheological and acid hydrolysis characteristics. *Food Chemistry* 74, 407-415.

Li, L., Blanco, M., & Jane, J. (2007). Physicochemical properties of endosperm and pericarp starches during maize development. *Carbohydrate Polymers* 67, 630-639.

Li, L., Jiang, H., Campbell, M., Blanco, M., & Jane, J. (2008). Characterization of maize amylose-extender (*ae*) mutant starches. Part I: Relationship between resistant starch contents and molecular structures. *Carbohydrate Polymers* 74, 396-404.

Li,. W., Xiao, X., Zhang, W., Zheng, J., Luo, Q., Ouyang, S., & Zhang, G. (2014). Compositional, morphological, structural and physicochemical properties of starches from seven naked barley cultivars grown in China. *Food Research International* 58, 7-14.

Li, Y., Yan, E., & Zhong, L. (2005). The research of the antioxidants and lipid peroxidation from naked barley. *Acta Academiae Medicinae CPAPF* 14, 353-356.

Lim, S., Kasemsuwan, T., & Jane, J. (1994). Characterization of phosphorus in starch by ^{31}P-nuclear resonance spectroscopy. *Cereal Chemistry* 71, 488-493.

Liu, C. T., Wesenberg, D. M., Hunt, C. W., Branen, A. L., Robertson, L. D., Burrup, D. E., Dempster, K. L., & Haggerty, R. J. (1996). Hulless barley: A new look for barley in Idaho. University of Idaho Extension / CALS Publications and Multimedia. (URL: www.cals.uidaho.edu/edcomm/pdf/CIS/CIS1050.pdf)

Lu, T., Jane, J., Keeling, P. L., & Singletary, G. W. (1996). Maize starch fine structures affected by ear development temperature. *Carbohydrate Research* 282, 157-170.

Ma, C. (2011). Highland barley production in Haibei prefecture of Qinghai province and making use of the chosen breeding of No.Beiqing. *Tibetan Agricultural Technology* 33, 28-32.

Morell, M. K., Samuel, M. S., & O'Shea, M. G. (1998). Analysis of starch structure using fluorophore-assisted carbohydrate electrophoresis. *Electrophoresis* 19, 2603–2611.

Morrison, W. R., Tester, R. F., Snape, C. E., Law, R., & Gidley, M. J. (1993). Swelling and gelatinization of cereal starches. IV. Some effects of lipid-complexed amylose and free amylose in waxy and normal barley starches. *Cereal Chemistry* 70, 385-391.

Nierle, W., Baya, A. W. EI, Kersting, H. J., & Meyer, D. (1990). Lipids and rheological properties of starch. Part II: the effect of granule surface material on viscosity of wheat starch. *Starch* 42, 471-475.

Public Weather Service Center of CMA, (2014). (URL: http://www.weather.com.cn; Last accessed: 03/14/2014)

Qian, J., Jiang, S., Su, W., & Gao, P. (2009). Characterization of oil from hulless barley (*Hordeum vulgare L.*) bran from Tibet. *Journal of the American Oil Chemists' Society* 86, 1175-1179.

Singh, J., Dartois, A., & Kaur, L. (2010). Starch digestibility in food matrix: a review. *Trends in Food Science and Technology* 21, 168-180.

Singh, V., & Ali, S. Z. (1987). Estimation of phosphorus in native and modified starches. Improvement in the molybdovanadophosphoric acid method. *Starch* 39, 277-279.

Song, Y., & Jane, J. (2000). Characterization of barley starches of waxy, normal, and high amylose varieties. *Carbohydrate Polymers* 41, 365-377.

Srichuwong, S., Sunarti, T. C., Mishima, T., Isono, N., & Hisamatsu, M. (2005). Starches from different botanical sources II: Contribution of starch structure to swelling and pasting properties. *Carbohydrate Polymers* 62, 25-34.

Takeda, Y., & Hizukuri, S. (1987). Structures of rice amylopectins with low and high affinities for iodine. *Carbohydrate Research* 168, 79-88.

Tester, R. F. (1997). Influence of growth conditions on barley starch properties. *International Journal of Biological Macromolecules* 21, 37-45.

Tester, R. F., Debon, S. J. J., & Sommerville, M. D. (2000). Annealing of maize starch. *Carbohydrate Polymers* 42, 287-299.

Tester, R. F., Karkals, J., & Qi, X. (2004). Starch-composition, fine structure and architecture. *Journal of Cereal Science* 39, 151-165.

Tester, R. F., & Morrison, W. R. (1990). Swelling and gelatinization of cereal starches. I. Effects of amylopectin, amylose, and lipids. *Cereal Chemistry* 67, 551-557.

Thomas, K. C., Dhas, A., Rossnagel, B .G., & Ingledew, W. M. (1995). Production of fuel alcohol from hull-less barley by very high gravity technology. *Cereal Chemistry* 72, 360-364.

Vasanthan, T., & Bhatty, R. S. (1996). Physicochemical properties of small- and large-granule starches of waxy, regular, and high-amylose barleys. *Cereal Chemistry* 73, 199-207.

Vasanthan, T., & Hoover, R. (2009). Barley starch: production, properties, modification and uses. In J. BeMiller & R. Whistler, (Eds.) *Starch: chemistry and technology*. (pp. 601-628). Wiley-VCH: Academic Press: New York.

Zhang, G., Wang, J., & Chen, J. (2002). Analysis of β-glucan content in barley cultivars from different locations of China. *Food Chemistry* 79, 251-254.

Zhang, Y., Zhang, D., Ma, Y., Hao, L., Xiao, Z., Nie, H., & Xie, Y. (2007). Identification of chemical composition of fermented highland barley juice and evaluation of its antihypoxia effect. *Journal of Preventive Medicine-Chinese PLA* 25, 171-174.

Zheng, G. H., Han, H. L., & Bhatty, R. S. (1998). Physicochemical properties of zero amylose hull-less barley starch. *Cereal Chemistry* 75, 520-524.

Table 1. Amylose, lipid, and phosphorus contents, and average granule diameters of the hull-less barley starch [a]

	Amylose (w/w, %)	Lipid (w/w, %)	Total phosphorus (w/w, %)	Average granule diameter (μm)	
				A granules	B granules
BQ4	24.0**c**±0.1	0.42±0.01	0.049**a**±0.000	12.0**b**±3.9	2.0**b**±0.7
BQ6	25.0**bc**±0.7	0.42±0.02	0.048**bc**±0.000	13.1**ab**±4.4	2.1**ab**±0.8
BQ7	24.8**bc**±0.0	0.45±0.02	0.048**bc**±0.000	12.8**ab**±4.0	2.1**ab**±0.7
KQ3	26.9**a**±0.8	0.42±0.01	0.047**c**±0.000	14.0**a**±4.9	2.3**a**±1.0
KQ6	26.5**ab**±0.3	0.45±0.00	0.050**a**±0.000	13.8**a**±3.8	2.2**a**±1.0
KQ7	26.2**ab**±0.1	0.41±0.02	0.045**d**±0.000	13.3**a**±4.8	2.3**a**±0.9

[a] Values are means ± standard deviations of two replicates. Different letters following the mean values within the same columns indicate statistically different mean values ($p<0.05$).

Table 2. Amylopectin branch-chain length distributions [a] of hull-less barley starches [b]

	DP<12	DP13-24	DP25-37	DP>37	Ave.CL [c]
BQ4	30.4±0.3	47.0±0.2	10.7±0.6	11.9±0.1	20.7**a**±0.1
BQ6	30.3±0.6	46.2±0.7	12.0±2.1	11.5±0.8	20.5**a**±0.4
BQ7	30.9±0.3	47.3±0.4	10.1±0.1	11.7±0.1	20.5**a**±0.1
KQ3	31.8±0.6	47.5±0.1	9.4±0.4	11.3±0.1	20.2**b**±0.1
KQ6	30.7±0.1	46.9±0.3	10.6±0.1	11.8±0.3	20.6**a**±0.2
KQ7	30.7±0.5	47.2±0.2	10.3±0.4	11.8±0.1	20.6**a**±0.0

[a] Molar basis. [b] Values are means ± standard deviations of two replicates. Different letters following the mean values within the same columns indicate statistically different mean values ($p<0.05$). [c] Average branch-chain length of amylopectin.

Table 3. Thermal properties of the hull-less barley starches [a]

	Gelatinization				Dissociation of retrograded starch			
	T_o[b] (°C)	T_c(°C)	ΔH(J/g)	T_c-T_o(°C)	T_o(°C)	T_c(°C)	ΔH(J/g)	Retro.% [c]
BQ4	54.9**c**±0.0	64.3±0.0	10.6±0.1	9.4**b**±0.0	39.9±0.4	59.5±0.0	2.6±0.0	25.0**c**±0.2
BQ6	54.1**c**±0.1	63.6±0.0	10.5±0.1	9.5**b**±0.1	40.4±0.6	59.4±0.8	2.2±0.0	21.1**e**±0.1
BQ7	54.8**c**±0.1	65.4±0.0	10.9±0.1	10.6**a**±0.2	41.4±0.2	60.1±0.4	2.6±0.0	23.9**d**±0.2
KQ3	55.4**b**±0.0	63.1±0.0	10.1±0.1	7.7**d**±0.0	41.5±0.0	59.5±0.1	2.8±0.0	27.8**a**±0.0
KQ6	56.1**a**±0.0	63.5±0.0	10.3±0.0	7.4**d**±0.0	42.2±0.0	59.8±0.3	2.7±0.1	26.5**b**±0.6
KQ7	55.1**b**±0.0	63.9±0.2	10.5±0.2	8.8**c**±0.2	42.3±0.3	59.5±0.2	2.6±0.0	24.6**cd**±0.2

[a] Values are means and (standard deviations) of two replicates. Different letters following the mean values within the same columns indicate statistically different mean values ($p<0.05$). [b] T_o= onset gelatinization temperature, T_c= conclusion temperature, ΔH= enthalpy change. [c] Retrogradation (%) =100% ΔH of dissociation of retrograded starch/ΔH of starch gelatinization.

Table 4. Rapidly-digestible (RDS), slowly-digestible (SDS) and resistant starch (RS) contents of hull-less barley starches [a]

	RDS (%)	SDS (%)	RS (%)
BQ4	78.6**a**±0.0	12.8**bc**±0.3	8.6**b**±0.3
BQ6	76.8**ab**±1.2	14.2**ab**±0.3	9.0**b**±0.9
BQ7	78.5**a**±1.0	11.7**c**±1.5	9.8**ab**±0.5
KQ3	74.7**b**±0.1	15.5**a**±0.6	9.8**ab**±0.5
KQ6	75.6**ab**±0.9	14.1**ab**±0.7	10.3**a**±0.2
KQ7	74.6**b**±1.1	16.0**a**±0.8	9.4**ab**±0.3

[a] Values are means ± standard deviations of two replicates. Different letters following the mean values within the same columns indicate statistically different mean values ($p<0.05$).

Table 5. Syneresis (%) of maize, wheat, and hull-less barley starch gels (5%, w/w) [a]

	0 FTC [b]	1 FTC	3 FTC	5 FTC
Maize	0.1±0.0	10.9±1.0	46.6±1.5	53.6±1.2
Wheat	0.5±0.1	21.6±0.2	57.7±1.2	62.8±1.5
BQ4	0.1±0.0	14.4±0.2	49.3±0.6	50.3±0.2
BQ6	0.1±0.0	39.1±0.3	50.2±2.5	50.7±1.7
BQ7	0.1±0.1	12.1±0.6	51.8±0.1	51.2±0.7
KQ3	1.3±0.1	49.8±1.5	53.8±1.5	56.4±0.0
KQ6	0.2±0.0	47.7±2.2	54.5±4.3	54.7±2.0
KQ7	0.2±0.0	46.3±1.0	47.6±2.9	54.0±2.1

[a] Values are means ± standard deviations of two replicates. [b] FTC = Freeze-thaw cycle.

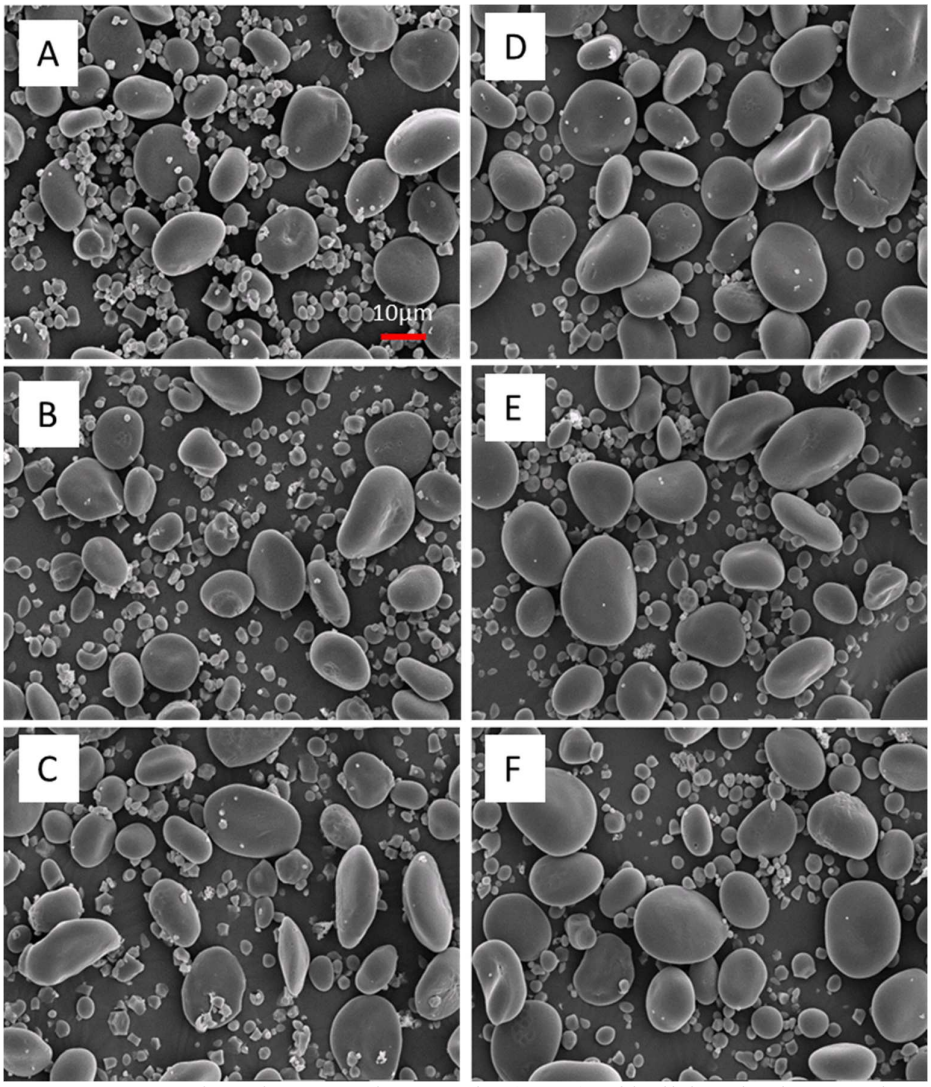

Figure 1. Scanning electron micrographs (SEM) of hull-less barley starch granules. A: BQ4; B: BQ6; C: BQ7; D: KQ3; E: KQ6; F: KQ7.

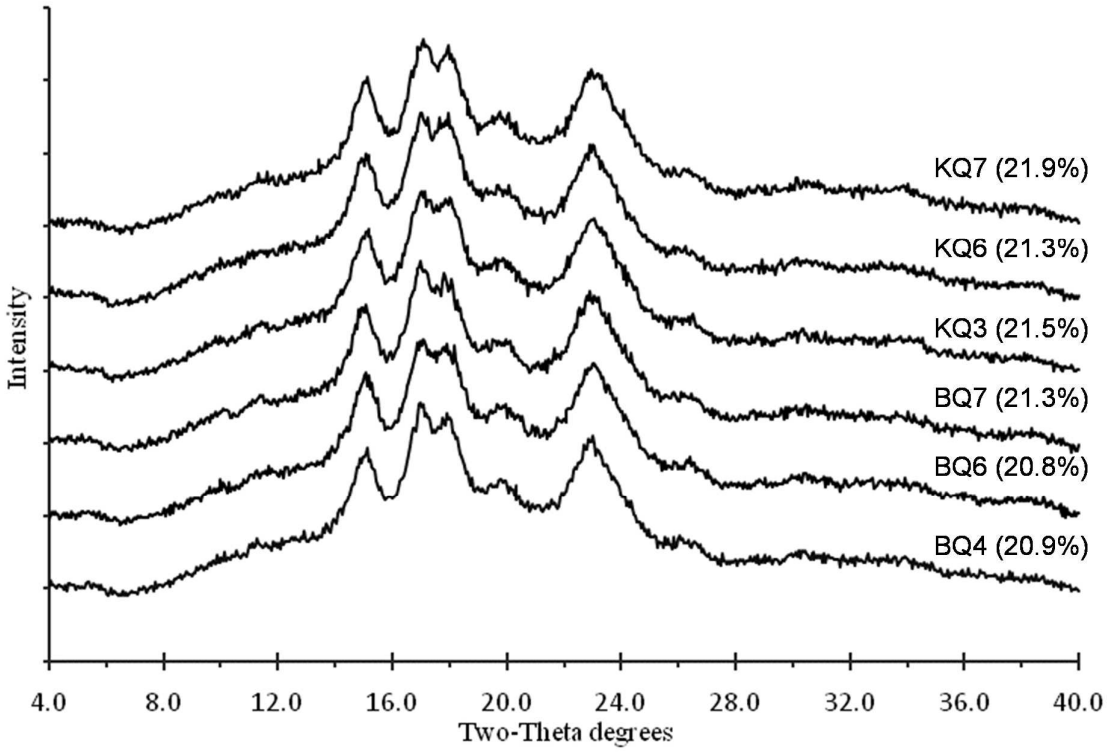

Figure 2. X-ray diffraction patterns and the numbers in the parentheses are percentages crystallinity of hull-less barley starches.

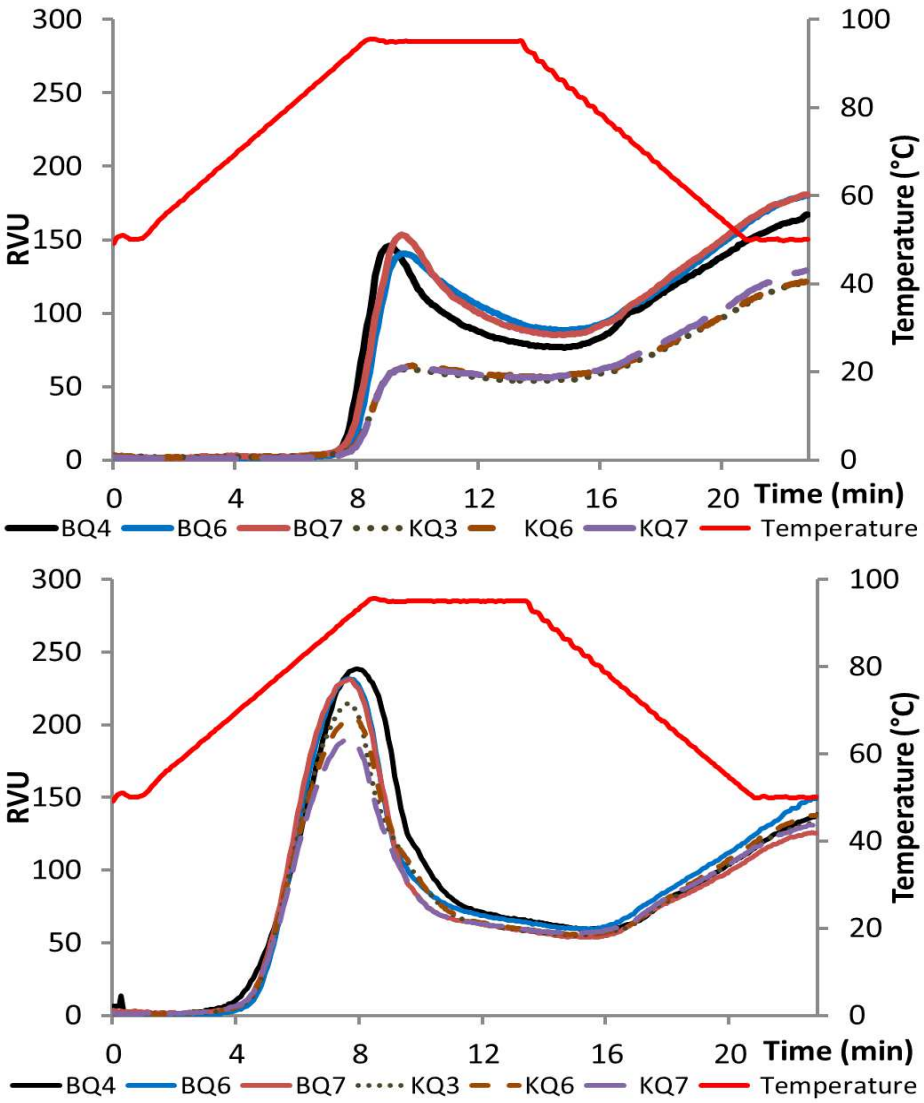

Figure 3. Pasting profiles of native (A) and sodium-dodecyl-sulphate-treated (B) hull-less barley starches.

CHAPATER 3

DOSAGE EFFECTS OF *WAXY* GENE ON THE STRUCTURES AND PROPERTIES OF CORN STARCH

A paper submitted to *Carbohydrate Polymers*

Hanyu Yangcheng,[1] Michael Blanco,[2] Candice Gardner,[2] Xuehong Li,[1,3] Jay-lin Jane [1,*]

[1] Department of Food Science and Human Nutrition, Iowa State University, Ames, IA 50011 USA;

[2] USDA-ARS Plant Introduction Research Unit, and Department of Agronomy, Iowa State University, Ames, IA 50011, USA;

[3] Department of Food Science and Bioengineering, Zhengzhou University of Light Industry, Zhengzhou, Henan, China

***Corresponding author:**

Tel: 01 515-294-9892; Fax: 01 515-294-8181;

E-mail address: jjane@iastate.edu (J.Jane)

Abstract

The objective of this study was to understand dosage effects of the *waxy* gene on the structures of amylose and amylopectin and on the properties of corn starch. Reciprocal crossing of isogenic normal and waxy corn lines was conducted to develop hybrids with different dosages (3, 2, 1, 0) of *waxy* gene in the endosperm. The amylose content of starch and proportions of branch chains of DP 17-30 and extra-long branch chains (DP > 100) of amylopectin were negatively correlated with the *waxy*-gene dosage. Proportions of short (DP < 17) and long branch-chains (DP 30-80), however, were positively correlated with the *waxy*-gene dosage. The gelatinization conclusion-temperature and temperature-range of the starch were positively correlated with the *waxy*-gene dosage, indicating that amylose facilitated dissociation of the surrounding crystalline regions. These results helped us understand the function of granule-bound starch synthase I in the biosynthesis of amylose and amylopectin and impacts of *waxy*-gene dosages on the properties of corn starch.

Keywords: waxy gene; dosage effects; branch-chain length distribution; starch properties

1. Introduction

Corn (*Zea mays L.*) is the largest crop produced worldwide, followed by rice and wheat (FAOSTAT, 2012). Most of the corn is used for livestock feed, and the remaining is processed for many food and industrial applications, including corn meal, corn starch, corn syrup and high-fructose corn syrup, alcoholic beverage, and fuel ethanol, etc. (USDA ERS, 2015). Starch is the major component of corn kernels (~72% by dry mass) and the energy source for food, feed, and ethanol fuel. Starch of normal (wild type) corn consists of two glucans: amylose and amylopectin. Amylose is primarily a linear polysaccharide of D-glucopyranose units connected by α-1,4 glycosidic bonds with few α-1,6 linked branches (Takeda, Tomooka, & Hizukuri, 1993). Amylopectin is a highly branched polysaccharide, in which the short linear-chains are connected by α-1,6 glycosidic branch linkages (Tester, Karkalas, & Qi, 2004).

Waxy corn is a naturally occurring corn mutant, and the starch of waxy corn consists of almost exclusively amylopectin. Compared with normal corn starch, waxy corn starch provides unique functions for many food and non-food applications. For example, waxy corn starch is preferably used in frozen foods to improve the freeze-thaw stability, and in textile, corrugating, and adhesive industries because of its clear film-forming property (Fergason, 1994). Waxy corn can be preferred as livestock feed because of its good feed-conversion efficiency resulting from the greater digestibility of the waxy starch (Collins, Moran, & Stillborn, 2003).

The endosperm of waxy corn kernels lacks the enzyme activity of granule-bound starch synthase I (GBSSI) encoded by the *waxy* gene (Denyer, Johnson, Zeeman, & Smith, 2001). The GBSSI, with a molecular weight of 58-60 kDa, is the only known enzyme responsible and required for the biosynthesis of amylose molecules in corn (Denyer et al. 2001). It has been reported that GBSSI is also involved in the biosynthesis of extra-long

branch-chains of amylopectin in various plants, such as wheat (Yoo & Jane, 2002a), rice (Hanashiro et al., 2008), and sweet potato (Kitahara et al., 2007). Some other studies using near-isogenic waxy and non-waxy wheat, however, showed contradictory results: non-waxy wheat starch consisted of no extra-long branch-chains and GBSSI showed no effects on the branch-chain length distribution of amylopectin (Miura, Wickramasinghe, Subasinghe, Araki, & Komae, 2002; Yasui, Ashida, & Sasaki, 2009). Yasui et al. (2009) argued that the extra-long branch-chains of amylopectin in normal or non-waxy starches were possibly contamination of amylose molecules resulting from incomplete separation of the amylose from amylopectin molecules.

The endosperm tissue of corn has three sets of chromosomes, two sets from maternal parent and one set from pollen parent (Darrah, McMullen, & Zuber, 2003). Therefore, for a single gene, there could be four different dosages (3, 2, 1, 0) in the endosperm. The dosage effects of *waxy* gene on the structures and properties of corn starch are not fully understood, and the effects of GBSSI on the biosynthesis of extra-long branch-chains are still being debated.

The objective of this study was to understand the dosage effects of *waxy* gene on the structures of amylose and amylopectin of corn starch and on starch properties. Results obtained from this study will add to the understanding of the physiological function of GBSSI in the biosynthesis of starch molecules and the properties of starch with different dosages of *waxy* gene. Understanding properties of starch with different *waxy*-gene dosages can facilitate developments of value-added utilizations of waxy and partial-waxy corn starch.

2. Materials and Methods

2.1 Materials

Isogenic normal and waxy corn lines were used in this study to minimize the interference of different genetic background. Two sets of isogenic normal and waxy corn lines were used as parent lines, and reciprocal crossing were conducted to develop corn lines with different dosages of the *waxy* gene in the endosperm: waxy × waxy (3 dosages), waxy × normal (2 dosages), normal × waxy (1 dosage), and normal × normal (0 dosage). The Set 1 samples included the pedigree DKXL370:N11a20-036-002, and the Set 2 samples included the pedigree AR16035:S02-615-001. All the corn lines were developed within the USDA-ARS Germplasm Enhancement of Maize (GEM) Project and grown at the North Central Regional Plant Introduction Station farm (Ames, IA) in 2014. Corn ears were harvested and dried to approximately 12% moisture and shelled. The pedigree, genotype, and the dosage of *waxy* gene in the endosperm of the corn lines are listed in **Table 1**.

Pseudomonas isoamylase (EC 3.2.1.68, 280 U/mg) was purchased from Megazyme International Ireland (Wicklow, Ireland). All other chemicals were reagent grade and were purchased from either Sigma-Aldrich Co. (St. Louis, MO) or Fisher Scientific (Pittsburgh, PA) and used without further purification.

2.2 Starch Isolation by Wet-Milling

Starches were isolated from the corn kernels using a wet-milling method reported by Li, Jiang, Campbell, Blanco, & Jane (2008).

2.3 Amylose Content of Starch

The amylose content of the corn starch was determined using an iodine potentiometric- autotitrator (702 SM Titrino, Brinkmann Instrument, Westbury, NY) using a method reported by Song & Jane (2000). Lipids of the starch were removed using 85% methanol in a Soxhlet extractor for 16 h prior to the analysis. The iodine affinity of amylose

used for the calculation was 0.2 (Takeda & Hizukuri, 1987). The amylose content was calculated using the equation:

Amylose (%) = 100% IA_s / 0.2, where IA_s was the iodine affinity of the starch.

2.4 Lipid Content of Starch

Lipids of the starch were extracted following the AOAC method 996.06 (2000). The lipid content of the starch was determined gravimetrically after removal of the solvent and calculated using the equation:

Lipid (%) = Weight of extracted lipids / Weight of the starch (db) × 100%.

2.5 Fractionation of Amylose

Amylose of the starch was separated from amylopectin using 1-butanol, following the method reported by Jane & Chen (1992) and Schoch (1942). Dispersed starch in an aqueous medium (1%, w/v) was mixed with 1-butanol (20%, v/v) and refluxed under mechanical stirring in a boiling-water bath for 1 hr. The mixture in a sealed flask was place in a Duwar flask filled with boiling water, and the Duwar flask was sealed and allowed to slowly cool down to room temperature over 24-30 hr. During the cooling process, amylose formed helical complex with 1-butanol, which crystallized and precipitated from the starch dispersion. Amylopectin molecules, however, remained in the supernatant.

2.6 Molecular Weight of Amylose

Molecular weight of the isolated amylose was determined using a high-performance size-exclusion chromatography (HPSEC) following the method of Jiang, Campbell, Blanco, & Jane (2010). The HPSEC system consisted of a Prostar 210 pump (Varian, Walnut Creek, CA), a refractive-index detector (Prostar 355, Varian, Walnut Creek, CA), and Shodex SB-804 and SB-803 analytical columns (Showa Denko K.K., Tokyo, Japan). The temperature of the columns was maintained at 50 °C in a column oven (Prostar 510, Varian, Walnut Creek, CA). The mobile phase was degassed and distilled-deionized water at a flow rate of 0.5

ml/min. Maltose, maltotriose, maltotetraose, maltohepaose, and pullulan standards (P10, P20, P100, Showa Denko K.K., Tokyo, Japan) were used as references to determine the molecular weight of amylose.

2.7 Molecular Weight and Gyration Radii of Amylopectin

Molecular weight and gyration radii of the amylopectin were determined using a HPSEC equipped with a multi-angle laser-light scattering detector (Dawn DSP-F, Wyatt Tech. Corp., Santa Barbara, CA) and a refractive-index detector (HP 1047A, Hewlett Packard, Valley Forge, PA) following the method of Yoo & Jane (2002b). Shodex SB-806 and SB-804 analytical columns (Showa Denko K.K., Tokyo, Japan) were used to separate amylopectin from amylose. The temperature of the columns was maintained at 50 °C using a CH-460 column heater and a TC-50 controller (Eppendorf, Madison, WI). The mobile phase was degassed and distilled-deionized water at a flow rate of 0.5 ml/min.

2.8 Amylopectin Branch-Chain Length Distribution

Amylopectin of the corn starch was separated from amylose using a gel-permeation chromatographic column packed with Sepharose CL-2B gel. The isolated amylopectin was debranched using *Pseudomonas* isoamylase (Megazyme International Irelands, Wicklow, Ireland) following the method of Li, et al. (2008). Branch-chain length distribution of the debranched amylopectin was analyzed using a HPSEC following the method of Jiang, et al. (2010). The HPSEC system consisted of a Prostar 210 pump (Varian, Walnut Creek, CA), a refractive-index detector (Prostar 355, Varian, Walnut Creek, CA), and a Shodex SB-803 analytical column (Showa Denko K.K., Tokyo, Japan). The temperature of the columns was maintained at 50 °C in a column oven (Prostar 510, Varian, Walnut Creek, CA). The mobile phase was degassed and distilled-deionized water at a flow rate of 0.5 ml/min.

2.9 Thermal Properties of the Starch

Thermal properties of the starch were analyzed using a differential scanning calorimeter (DSC, Diamond, Perkin-Elmer, Norwalk, CT). The gelatinization onset (T_o), peak (T_p), and conclusion temperatures (T_c) and enthalpy change (ΔH) of the starch were determined using a Pyris software (Perkin-Elmer).

2.10 Pasting Properties of the Starch

Pasting properties of the starch in an aqueous suspension (8%, w/w, db) were analyzed using a rapid visco-analyzer (Newport Scientific, Sydney, Australia) following the method of Jane, et al. (1999). The pasting temperature, and the peak, breakdown, and final viscosities were determined using the Thermocline software (Newport Scientific).

2.11 Statistical Analysis

Data were subjected to ANOVA and Tukey's multiple comparison analysis using PROC ANOVA procedure of SAS 9.4 (SAS Institute, Inc., Cary, NC). The normality of data for each variable was investigated using the PROC UNIVARIATE procedure. Because the dosage of *waxy* gene and most of the other variables were not normally distributed (data not shown), a Spearman correlation test was used to analyze correlations between the *waxy* gene dosage and the physicochemical properties of the starch. Statistical significance was declared at $p < 0.05$ if without further indication.

3. Results and Discussion

Amylose contents and amylose molecular-weights of starches from corn with different dosages of *waxy* gene are shown in **Table 2**. The amylose contents ranged from 1.6 to 27.9% for the Set 1 samples and from 0.0 to 26.6% for the Set 2 samples. The amylose content was negatively correlated with the dosage of *waxy* gene ($r = -0.98$, $p < 0.01$), which was in line with the effects of *waxy*-gene dosages on wheat starch (Miura et al. 2002;

Wichramasinghe & Miura, 2003). The increase in the amylose content, however, was not proportional to the decrease in the dosage of *waxy* gene in the endosperm. For example, the relative amylose content increased by 69 or 75%, using the amylose content of the isogenic normal corn starch as the reference (100%), when the *waxy*-gene dosage decreased from 3 to 2 in the endosperm, whereas further decrease in the *waxy*-gene dosage from 2 to 1 only showed small increase in the relative amylose content by 5 or 6% (**Table 2**). These results were in line with that previously reported (Tsai, 1974).

Molecular weight of the isolated amylose ranged from DP 629.8 to 651.3 for the Set 1 samples, and from DP 637.8 to 646.1 for the Set 2 samples (**Table 2**). There were no significant differences in the molecular weight of amylose between the starch samples with different dosages of the *waxy* gene in the endosperm, indicating that the *waxy* gene had little effects on the molecular weight of amylose.

Lipid contents of the starch samples are shown in **Table 2**. The waxy corn starches consisted of little lipids (0.24% for the Set 1 waxy corn and 0.10% for the Set 2 waxy corn). Lipid contents of the partial-waxy and normal corn starches ranged from 0.71 to 0.84% for the Set 1 samples and from 0.55 to 0.84% for the Set 2 samples. The correlation coefficient between the amylose and lipid contents of the starch samples was 0.75, although the correlation was not significant ($p = 0.086$).

The molecular-weight and gyration radii of amylopectin with different dosages of *waxy* gene are shown in **Table 3**. The amylopectin molecules of the waxy corn starch displayed larger molecular weights and gyration radii than the partial-waxy and normal isogenic corn lines containing 2 to 0 *waxy*-gene dosage(s). These results were consistent with that previously reported (Bello-Perez, Roger, Baud, & Colonna, 1998; Yoo & Jane, 2002b). The correlation coefficient between the molecular weights of amylopectin and amylose contents of the starch samples was -0.66, although the correlation was not significant ($p =$

0.063). For the partial-waxy and normal corn, biosynthesis of amylose competed with that of amylopectin for the substrate of adenosine-5'-diphosphate glucose (ADP-Glu), which resulted in smaller molecular weight of amylopectin than that of the waxy corn starch (Yoo & Jane, 2002a).

Branch-chain length distributions of the debranched amylopectin molecules determined using a HPSEC are shown in **Figure 1**, and the results are summarized in **Table 4**. Both sets of the samples showed the same trends in the branch-chain length distribution of amylopectin with different dosages of *waxy* gene. The chromatograms showed a major peak at DP ~22 and two minor peaks at DP ~13 and DP ~40 for both sets of samples. For the Set 1 samples, percentages of the extra-long branch chains (DP 100-287) increased from 0.2% to 2.0% ,and for the Set 2 samples, percentages of the extra-long branch chains (DP 100-256) increased from 0.3% to 1.8% with the decrease in the *waxy*-gene dosage from 3 to 0. Percentages of the extra-long branch chains were negatively correlated with the *waxy*-gene dosage ($r = -0.93$, $p < 0.01$). It has been reported that extra-long branch chains are present in partial-waxy and normal starches from various plants, including wheat, rice, and sweet potato (Yoo & Jane, 2002a; Kitahara, et al. 2007; Hanashiro, et al. 2008), and GBSSI is responsible for the biosynthesis of extra-long branch chains (Denyer, Clarke, Hylton, Tatge, & Smith, 1996; Hanashiro, et al. 2008). Yasui et al. (2009) postulated that amylose could have been eluted with amylopectin during the GPC separation and the presence of extra-long branch chains could be a result of contamination of the amylose. In this study, the largest detectable chain lengths of extra-long branch chains were DP 287 for the Set 1 samples and DP 256 for the Set 2 samples, which were substantially smaller than the average molecular weight of amylose (DP 629.8-651.3 for the Set 1 samples and DP 637.8-646.1 for the Set 2 samples, respectively) (**Table 2**). Therefore, the presence of extra-long branch chains was unlikely the contamination of amylose molecules. The negative correlation between the *waxy*-gene dosage

and the proportion of extra-long branch chains further supported that GBSSI was responsible for the biosynthesis of extra-long branch chains of amylopectin.

The HPSEC chromatograms showed that, for both sets of the samples, percentages of the short chains (DP < 17) (47.3-51.0% for the Set 1 samples and 46.1-49.9% for the Set 2 samples) (**Table 4**) were positively correlated with the *waxy*-gene dosage ($r = 0.94$, $p < 0.01$). Percentages of the intermediate chains of DP 17-30 (30.0-33.5% for the Set 1 samples and 31.2-37.4% for the Set 2 samples) were negatively correlated with the *waxy*-gene dosage ($r = -0.86$, $p < 0.01$). Percentages of the long branch-chains (DP 30-80) (16.2-17.9% for the Set 1 samples and 14.0-17.8% for the Set 2 samples) were positively correlated with the *waxy*-gene dosage ($r = 0.76$, $p < 0.05$). It was plausible that, with the presence of GBSSI in the partial-waxy and normal corn, the short chains (DP < 17) were elongated to the intermediate chains (DP 17-30). These results also suggested that GBSSI could synthesize the extra-long branch-chains by elongating the long branch-chains (DP 30-80), resulting in decreases in the proportion of the long branch-chains in the partial-waxy and normal corn starches. More studies are needed to understand the mechanisms of the effects of GBSSI on the elongation of amylopectin branch-chains.

Starch thermal properties are shown in **Table 5**. The gelatinization conclusion-temperature (74.4-77.0 °C for the Set 1 samples and 72.0-74.4 °C for the Set 2 samples) and temperature-range (8.8-11.2 °C for the Set 1 samples and 9.5-12.1 °C for the Set 2 samples) were negatively correlated with the amylose content of starch (**Table 2**). These results were in line with that reported on wheat starch (Sasaki, Yasui, & Matsuki, 2000). It is known that gelatinization of starch begins at the hilum of the granule and proceeds radially (Hoseney, Zeleznak, & Yost, 1986). Amylose is interspersed among amylopectin and is oriented from the hilum to the periphery, extending through multiple clusters of amylopectin molecules (Jane, 2006). During gelatinization of starch, amylose molecules facilitate dissociation of

surrounding crystalline clusters of amylopectin, proceeding from the hilum to the periphery, resulting in a lower gelatinization conclusion-temperature and a narrower gelatinization temperature-range (Hoseney, et al. 1986). The starch gelatinization enthalpy-change was positively correlated with the *waxy*-gene dosage, resulting from a larger amylopectin-content and a greater percentage-crystallinity of waxy starch (Jane, et al. 1999).

Starch pasting properties are shown in **Figure 2**, and the results are summarized in **Table 6**. Pasting temperatures of the starch (71.0-73.8 °C for the Set 1 samples and 69.0-72.5 °C for the Set 2 samples) had no correlation with the *waxy*-gene dosage but were positively correlated ($r = 0.81$, $p < 0.01$) with the lipid contents of the starch (**Table 2**). Although there was no correlation between the peak viscosity and the *waxy*-gene dosage, the breakdown viscosity was positively correlated with the *waxy*-gene dosage ($r = 0.83$, $p < 0.01$) and the setback viscosity was negatively correlated with the *waxy*-gene dosage ($r = -0.97$, $p < 0.01$). It has been reported that amylose intertwines with amylopectin and maintains the integrity of the starch granule (Hermansson & Svegmark, 1996; Jane, 2007), which reduces the breakdown of swollen starch-granules. Amylose participates in gel-network formation during the cooling of the starch paste, resulting in a higher setback viscosity (Deffenbaugh & Walker, 1989; Jane, et al. 1999; Sasaki, et al. 2000).

4. Conclusions

To our knowledge this is the first study to report dosage effects of the *waxy* gene on amylopectin branch-chain length distribution in isogenic corn starch. The negative correlation between the *waxy*-gene dosage and the percentage of extra-long branch chains supported that GBSSI was responsible for the biosynthesis of extra-long branch chains. GBSSI also increased the proportion of intermediate chains with DP 17-30 and decreased the proportion of short chains with DP < 17. The *waxy* gene showed dosage effects on the amylose content,

but no effects on the molecular weight of amylose. The conclusion gelatinization-temperature and gelatinization temperature-range of the starch were positively correlated with the *waxy*-gene dosage, indicating that amylose facilitates dynamic gelatinization of the crystalline structures of amylopectin. The breakdown viscosity of starch was positively correlated but the setback viscosity was negatively correlated with the *waxy*-gene dosage. These results showed that GBSSI was responsible for the biosynthesis of both amylose and amylopectin, which in turn affected the thermal and pasting properties of the starch.

Acknowledgements

The authors thank the USDA-ARS Plant Introduction Research Unit and the GEM project for providing the financial support and the nursery site for the study.

References

AOAC. (2000). AOAC official method 996.06, fat (total, saturated, and unsaturated) in foods. Page 20-24. In Official methods of analysis of AOAC international (17th ed.). Maryland: AOAC International.

Bello-Perez, L.A.; Roger, P.; Baud, B.; & Colonna, P. (1998). Macromolecular features of starches determined by aqueous high-performance size exclusion chromatography. *J. Cereal Sci*. 27, 267-278.

Collins, N.E.; Moran, E.T.; & Stillborn, H.L. (2003). Performance of broilers fed normal and waxy corn diets formulated with chick and rooster derived apparent metabolizable energy values for the grains. *J. Appl. Poult. Res*. 12, 196-206.

Darrah, L.L.; McMullen, M.D.; & Zuber, M.S. (2003). Breeding, genetics, and seed corn production. In P.J. White & L.A. Johnson, (Eds.) *Corn: Chemistry and Technology*, 2nd ed. (pp. 35-68). American Association of Cereal Chemists, Inc., St. Paul, MN.

Deffenbaugh, L.B. & Walker, C.E. (1989). Comparison of starch pasting properties in the Brabender Viscoamylograph and the Rapid Visco-Analyzer. *Cereal Chem*. 66, 493-499.

Denyer, K.; Clarke, B.; Hylton, C.; Tatge, H.; & Smith, A.M. (1996). The elongation of amylose and amylopectin chains in isolated starch granules. *The Plant J*. 10, 1135-1143.

Denyer, K.; Johnson, P.; Zeeman, S.; & Smith, A.M. (2001). The control of amylose synthesis. *J. Plant Physiol.* 158, 479-487.

FAOSTAT. (2012). The Statistics Division of the Food and Agriculture Organization. URL: http://faostat3.fao.org/faostat-gateway/go/to/download/Q/QC/E)

Fergason, V. (1994). High amylose and waxy corns. Pages 55-77. In: *Specialty Corns*, 1st ed., Hallauer, A.R. Eds., CRC Press, Inc., Boca Raton, Florida.

Hanashiro, I.; Itoh, K.; Kuratomi, Y.; Yamazaki, M.; Igarashi, T.; Matsugasako, J.; Takeda, Y. (2008). Granule-bound starch synthase I is responsible for biosynthesis of extra-long unit chains of amylopectin in rice. *Plant Cell Physiol.* 49, 925-933.

Hermansson, A.M.; & Svegmark, K. (1996). Developments in the understanding of starch functionality. *Trends Food Sci. Technol*. 7, 345-353.

Hoseney, R.C.; Zeleznak, K.J.; & Yost, D.A. (1986). A note on the gelatinization of starch. *Starch* 12, 407-409.

Jane, J. (2006). Current understanding on starch granule structures. *J. Appl. Glycosci*. 53, 205-213.

Jane, J. (2007). Structures of starch granules. *J. Appl. Glycosci*. 54, 31-36.

Jane, J. & Chen, J-F. (1992). Effect of amylose molecular size and amylopectin branch chain length of paste properties of starch. *Cereal Chem.* 69: 60-65.

Jane, J.; Chen, Y. Y.; Lee, L. F.; McPherson, A. E.; Wong, K. S.; Radosavljevic, M.; & Kasemsuwan, T. (1999). Effects of amylopectin branch-chain length and amylose content on the gelatinization and pasting properties of starch. *Cereal Chem.* 76, 629-637.

Jiang, H.; Campbell, M.; Blanco, M.; & Jane, J. (2010). Characterization of maize amylose-extender (*ae*) mutant starches: Part II. Structures and properties of starch residues remaining after enzymatic hydrolysis at boiling-water temperature. *Carbohydr. Polym.* 80, 1-12.

Kitahara, K.; Hamasuna, K.; Nozuma, K.; Otani, M.; Hamada, T.; Shimada, T.; Fujita, K.; & Suganuma, T. (2007). Physicochemical properties of amylose-free and high-amylose starches from transgenic sweetpotatoes modified by RNA interference. *Carbohydr. Polym.* 69, 233-240.

Li, L., Jiang, H., Campbell, M., Blanco, M., & Jane, J. (2008). Characterization of maize amylose-extender (*ae*) mutant starches. Part I: Relationship between resistant starch contents and molecular structures. *Carbohydr. Polym*. 74, 396-404.

Miura, H.; Wichramasinghe, M.H.A.; Subasinghe, R.M.; Araki, E.; & Komae, K. (2002). Development of near-isogenic lines of wheat carrying different null Wx alleles and their starch properties. *Euphytica* 123, 353-359.

Sasaki, T.; Yasui, T.; & Matsuki, J. (2000). Effects of amylose content on gelatinization, retrogradation, and pasting properties of starches from waxy and nonwaxy wheat and their F1 seeds. *Cereal Chem*. 77, 58-63.

Schoch, T.J. (1942). Fractionation of starch by selective precipitation with butanol. *J. Am. Chem. Soc*. 64: 2957-2961.

Song, Y.; & Jane, J. (2000). Characterization of barley starches of waxy, normal, and high amylose varieties. *Carbohydr. Polym*. 41, 365-377.

Takeda, Y., & Hizukuri, S. (1987). Structures of rice amylopectins with low and high affinities for iodine. *Carbohydr. Research* 168, 79-88.

Takeda, Y.; Tomooka, S.; and Hizukuri, S. (1993). Structures of branched and linear-molecules of rice amylose. *Carbohydr. Res.* 246, 267-272.

Tester, R.F.; Karkalas, J.; & Qi, X. (2004). Starch – composition, fine structure and architecture. *J. Cereal Sci*. 39, 151-165.

Tsai, C-Y. (1974). The function of the Waxy locus in starch synthesis in maize endosperm. *Biochem. Genetics* 11, 83-96.

USDA ERS. (2015). Corn - Background. (URL: http://www.ers.usda.gov/topics/crops/corn/background.aspx#.Uwt_0IUl8qM)

Wickramasinghe, H.A.M. & Miura, H. (2003) Gene dosage effect of the wheat Wx alleles and their interaction on amylose synthesis in the endosperm. *Euphytica* 132: 303-310.

Yasui, T.; Ashida, K.; & Sasaki, T. (2009). Chain-length distribution profiles of amylopectin isolated from endosperm starch of waxy and low-amylose bread wheat (*Triticum aestivum L.*) lines with common genetic background. *Starch* 61, 677-686.

Yoo, S-H. & Jane, J. (2002a). Structural and physical characteristics of waxy and other wheat starches. *Carbohydr. Polym.* 49, 297-305.

Yoo, S-H. & Jane, J. (2002b). Molecular weights and gyration radii of amylopectins determined by high-performance size-exclusion chromatography.

Table 1. Pedigree, genotype, and waxy gene dosage of the endosperm of the GEM corn samples

	Sample [a]	Pedigree	Genotype of endosperm	Waxy gene dosage
Set 1	wx	DKXL370:N11a20-036-002-B wx	*wxwxwx*	3
	wx × N	DKXL370:N11a20-036-002-B wx × DKXL370:N11a20-036-002-B-B-B-B	*wxwxWx*	2
	N × wx	DKXL370:N11a20-036-002-B-B-B-B × DKXL370:N11a20-036-002-B wx	*wxWxWx*	1
	N	DKXL370:N11a20-036-002-B-B-B-B	*WxWxWx*	0
Set 2	wx	AR16035:S02-615-001-B wx	*wxwxwx*	3
	wx × N	AR16035:S02-615-001-B wx × AR16035:S02-615-001-B-B-B-B	*wxwxWx*	2
	N × wx	AR16035:S02-615-001-B-B-B-B × AR16035:S02-615-001-B wx	*wxWxWx*	1
	N	AR16035:S02-615-001-B-B-B-B	*WxWxWx*	0

[a] wx = waxy corn ; N = normal corn. In each case the female parent line appears first and has the endosperm genotype.

Table 2. Amylose and lipid contents of starch and amylose molecular-weight of the corn starches with different dosages of the *waxy* gene [a]

	Sample	*waxy* gene dosage	Amylose (%)	Relative amylose content	Amylose molecular-weight (DP)	Lipid (%)
Set 1	wx	3	1.6**d**±0.0	6%	N/A [b]	0.24**c**±0.06
	wx × N	2	20.9**c**±0.1	75%	640.5**a**±10.3	0.75**ab**±0.02
	N × wx	1	22.4**b**±0.4	80%	651.3**a**±16.4	0.84**a**±0.05
	N	0	27.9**a**±0.5	100%	629.8**a**±21.4	0.71**b**±0.03
Set 2	wx	3	0.0**d**±0.0	0%	N/A	0.10**c**±0.00
	wx × N	2	20.0**c**±0.1	75%	644.2**a**±8.2	0.74**a**±0.04
	N × wx	1	21.5**b**±0.1	81%	646.1**a**±9.7	0.84**a**±0.07
	N	0	26.6**a**±0.2	100%	637.8**a**±1.8	0.55**b**±0.03

[a] Values are means ± standard deviations of two replicates. Different letters following the mean values within the same columns indicate statistically different mean values within each set of the corn starch samples ($p<0.05$). [b] Not available.

Table 3. Amylopectin molecular-weight and gyration radii of the corn starches with different dosages of the *waxy* gene [a]

	Sample	M_w ($\times 10^8$ g/mol)	R_z (nm)
Set 1	wx	11.8**a**±0.2	380.0±1.4
	wx × N	10.3**b**±0.6	362.3±5.9
	N × wx	9.5**b**±0.2	355.4±1.3
	N	10.1**b**±0.0	363.0±0.8
Set 2	wx	12.4**a**±0.4	387.4±5.6
	wx × N	10.5**a**±0.7	368.2±7.9
	N × wx	11.7**a**±0.6	380.2±15.8
	N	11.1**a**±0.4	376.3±4.9

[a] Values are means ± standard deviations of two replicates. Different letters following the mean values within the same columns indicate statistically different mean values within each set of the corn starch samples ($p<0.05$).

Table 4. Amylopectin branch-chain length distribution of the corn starches with different dosages of the *waxy* gene [a]

	Sample	DP<17	DP17-30	DP30-80	DP>100
Set 1	wx	51.0**a**±0.5	30.0**d**±0.2	17.9**a**±0.2	0.2**d**±0.0
	wx × N	50.4**ab**±0.3	30.8**c**±0.1	17.3**b**±0.1	0.6**c**±0.0
	N × wx	49.8**b**±0.4	31.6**b**±0.2	16.7**c**±0.2	1.0**b**±0.1
	N	47.3**c**±0.2	33.5**a**±0.0	16.2**c**±0.2	2.0**a**±0.0
Set 2	wx	49.9**a**±0.3	31.2**d**±0.1	17.8**a**±0.1	0.3**c**±0.0
	wx × N	49.3**a**±0.3	33.0**c**±0.1	15.6**b**±0.0	1.2**b**±0.0
	N × wx	47.3**b**±0.5	35.6**b**±0.4	14.8**c**±0.0	1.4**b**±0.0
	N	46.1**c**±0.3	37.4**a**±0.3	14.0**d**±0.1	1.8**a**±0.0

[a] Weight averaged. Values are means ± standard deviations of two replicates. Different letters following the mean values within the same columns indicate statistically different mean values within each set of the corn starch samples ($p<0.05$).

Table 5. Starch thermal-properties of the corn starches with different dosages of the *waxy* gene [a]

	Sample	T_o [b] (°C)	T_p (°C)	T_c (°C)	ΔH (J/g)	T_c -T_o (°C)
Set 1	wx	65.7**ab**±0.0	71.8±0.1	77.0**a**±0.4	14.0**a**±0.1	11.2**a**±0.4
	wx× N	66.1**a**±0.1	71.3±0.1	75.9**b**±0.0	12.3**b**±0.1	9.7**b**±0.1
	N × wx	65.2**c**±0.1	69.9±0.1	74.7**c**±0.2	12.0**c**±0.1	9.5**b**±0.3
	N	65.6**b**±0.0	69.7±0.0	74.4**c**±0.1	11.9**c**±0.0	8.8**b**±0.0
Set 2	wx	62.3**a**±0.1	68.9±0.0	74.4**a**±0.0	13.2**a**±0.1	12.1**a**±0.2
	wx × N	62.2**a**±0.1	68.4±0.0	73.5**b**±0.1	11.6**b**±0.0	11.3**b**±0.1
	N × wx	62.3**a**±0.2	67.7±0.1	72.4**c**±0.0	11.6**b**±0.0	10.1**c**±0.3
	N	62.5**a**±0.0	67.4±0.1	72.0**d**±0.1	11.2**c**±0.1	9.5**c**±0.1

[a] Values are means ± standard deviations of two replicates. Different letters following the mean values within the same columns indicate statistically different mean values within each set of the corn starch samples ($p<0.05$). [b] T_o= onset gelatinization temperature, T_p = peak temperature, T_c= conclusion temperature, ΔH= enthalpy change.

Table 6. Starch pasting-properties of the corn starches with different dosages of the *waxy* gene [a]

	Sample	Pasting Temp.(°C)	Peak (RVU)	Hold (RVU)	Final (RVU)	Breakdown (RVU)	Setback (RVU)
Set 1	wx	71.0**b**±0.3	217.3**a**±4.0	78.3±1.6	101.8±2.9	138.9**a**±2.4	23.4**d**±1.3
	wx × N	73.8**a**±0.3	147.8**b**±2.2	73.6±2.4	142.1±2.2	74.2**b**±0.2	68.5**c**±0.2
	N × wx	72.3**ab**±0.6	150.2**b**±2.5	75.1±1.2	148.7±1.5	75.1**b**±1.2	73.5**b**±0.3
	N	71.4**b**±0.3	157.6**b**±1.2	90.4±0.8	182.8±0.6	67.2**c**±1.9	92.5**a**±1.4
Set 2	wx	69.0**c**±0.3	221.0**a**±0.7	72.0±1.7	102.1±0.6	148.9**a**±1.1	30.1**d**±1.1
	wx × N	72.3**a**±0.0	149.9**b**±2.7	74.1±0.6	146.8±1.6	75.8**b**±2.1	72.7**c**±2.2
	N × wx	72.5**a**±0.2	143.6**b**±1.4	84.9±1.7	169.8±2.1	58.7**c**±0.3	84.9**b**±3.8
	N	71.3**b**±0.3	148.3**b**±0.7	95.6±0.4	202.2±2.0	52.5**d**±0.1	106.6**a**±2.4

[a] Values are means ± standard deviations of two replicates. Different letters following the mean values within the same columns indicate statistically different mean values within each set of the corn starch samples ($p<0.05$). RVU = Rapid-visco unit(s).

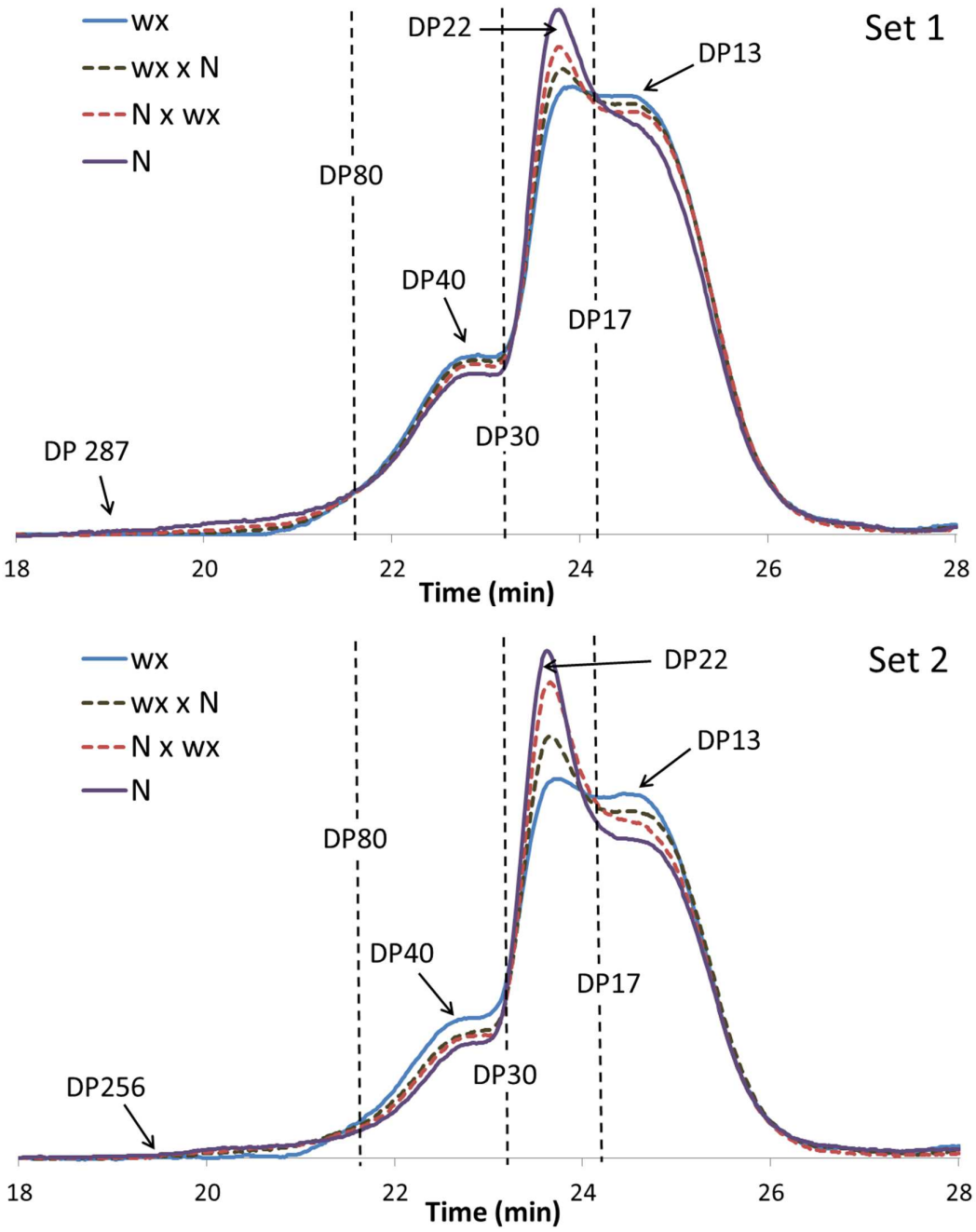

Figure 1. Amylopectin branch-chain length distribution of the corn starches with different dosages of the *waxy* gene.

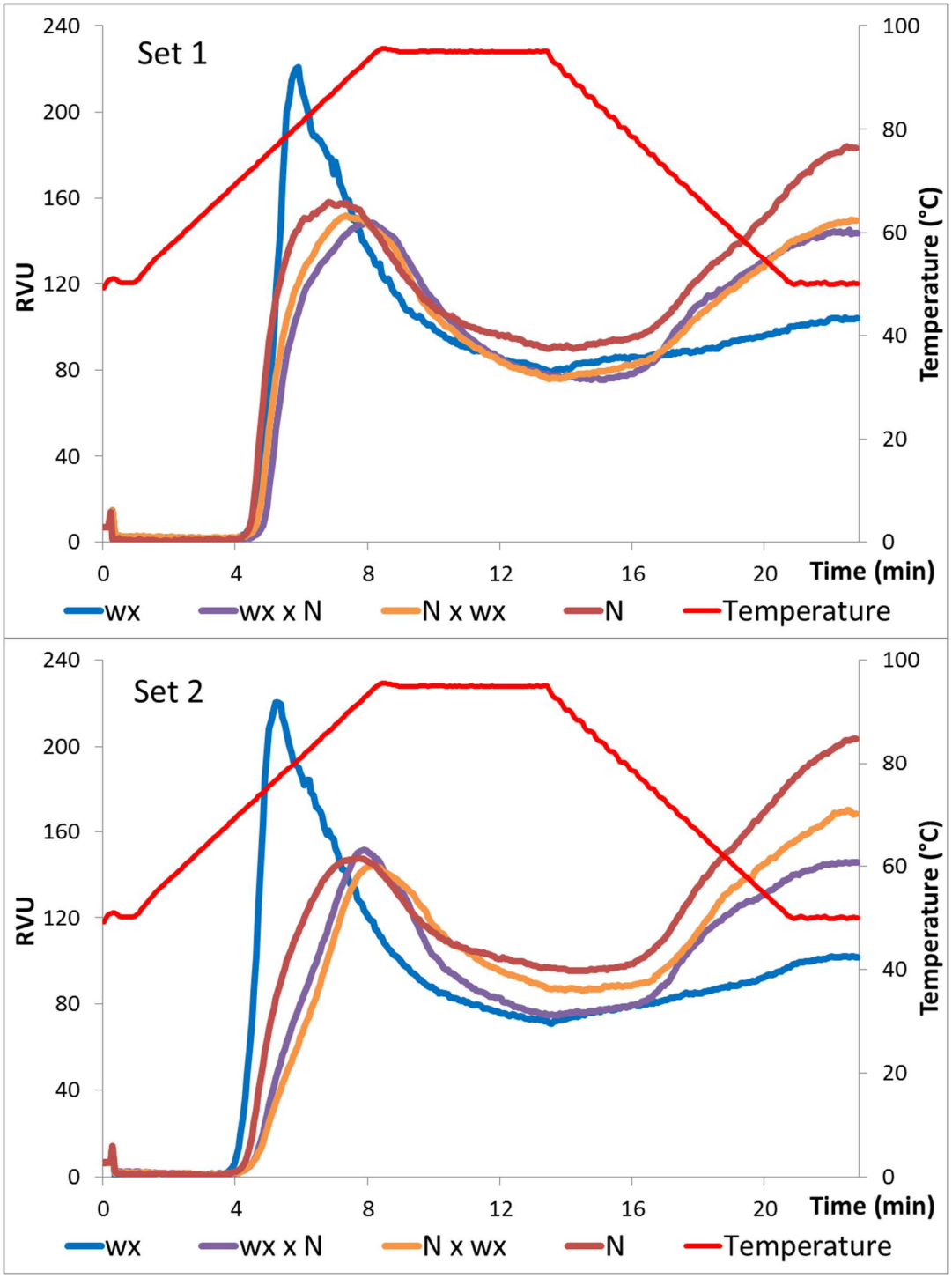

Figure 2. Starch pasting properties of the corn starches with different dosages of the *waxy* gene.

CHAPTER 4

CHARACTERIZATION AND DEVELOPMENT MECHANISM OF *APIOS AMERICANA* TUBER STARCH

A paper submitted to *Carbohydrate Polymers*

Hanyu Yangcheng [a], Vikas Belamkar [b], Steven B. Cannon [c], Jay-lin Jane [a,*]

[a] Department of Food Science and Human Nutrition, Iowa State University, Ames, IA 50011, USA.

[b] Interdepartmental Genetics, Iowa State University, Ames, IA 50011, USA.

[c] USDA-Agricultural Research Service, Corn Insects and Crop Genetics Research Unit, and Department of Agronomy, Iowa State University, Ames, IA 50011, USA.

[*] **Corresponding author**: Jay-lin Jane

Tel: 01 515-294-9892; Fax: 01 515-294-8181;

E-mail address: jjane@iastate.edu (J.Jane)

ABSTRACT

Apios americana is a wild legume-bearing plant with edible tubers. Domestication of *Apios* is in progress because of the superior nutritional value and health benefits of the tuber. Objectives of this study were to: 1) characterize physicochemical properties of *Apios*-tuber starch; and 2) understand differences in starch structures and properties between the mother (seed) and child (progeny) tubers and the mechanism of starch development. Granules of the *Apios*-tuber starch displayed ellipsoidal, rod, or kidney shape with diameter ranges of 1-30 μm. The mother-tuber starches displayed greater percentage-crystallinity, larger gelatinization enthalpy-changes, longer branch-chain lengths of amylopectin, and lower pasting viscosity than their counterpart child-tuber starches. The mother-tuber starch of *Apios* 2127 displayed distinct two peaks of gelatinization, which were attributed to starch granules located at different regions of the tuber having different structures and properties. The mother tuber displayed more active starch biosynthesis in the periphery than in the central region of the tuber.

Keywords: *Apios*; *Child tuber; Mother tuber; Starch; Double thermal-transition*

1. INTRODUCTION

Apios americana, also known as American groundnut or potato bean, is a wild nitrogen-fixing, legume-bearing plant with edible tubers (Belamkar et al., 2015; Wilson, Pichardo, Liuzzo, Blackmon, & Reynolds, 1987). It is native to North America and widely distributed from Canada to southern Florida (Reynolds, Blackmon, Wickremesinhe, Wells, & Constantin, 1990). *Apios* was a food plant for American Indians, and the tubers were an emergency food for the Europeans upon arriving at the American continent in the middle of the nineteenth century (Kinugasa & Watanabe, 1992). Because of the low yield of the wild *Apios* tubers, *Apios* has been cultivated primarily as a garden crop instead of a food crop in recent years (Reynolds et al., 1990).

Recent studies, however, have shown that *Apios* tubers are highly nutritious compared with major food crops, including potatoes, sweet potatoes, and taros. The protein content of *Apios* tubers on the dry-weight basis ranges 11.1-14.0%, which is more than twice of the protein content of potatoes (Wilson et al., 1987; Wilson, Pichardo, Blackmon, & Reynolds, 1990). *Apios*-tuber proteins have excellent and balanced contents of essential amino-acids, including leucine, isoleucine, phenylalanine, threonine, and valine (Wilson et al. 1987). *Apios* tubers contain 4.2-4.6% lipid on the dry-weight basis, and linoleic acid is the dominant (Wilson, Gorny, Blackmon, & Reynolds, 1986). *Apios* tubers are also rich in iron and phosphorus and contain five times the calcium of taros (Kinugasa & Watanabe, 1992). The *Apios* tuber contains a significant amount of isoflavones (Kazuhiro, Nihei, Ogsawara, Koga, & Kato, 2011). Animal-feeding studies have shown that ingestion of *Apios* tubers reduces blood pressure, suggesting its hypertension-preventive function (Iwai & Matsue, 2007).

Product development using *Apios* tubers has also received increasing attention. The tubers are soft and smooth in texture and taste slightly sweet like potatoes, taros, and chestnuts (Kikuta et al., 2011). In Japan, *Apios* tubers are cooked in different ways, including

steaming, boiling, and deep frying, and the *Apios*-tuber flour is used as an ingredient for bakery products, including cookies, donuts, and breads (Kikuta et al., 2011). Chips made from *Apios* tubers displayed a lighter color than potato chips because of the lower reducing-sugar content of the *Apios* tuber, which decreases the Maillard reaction during baking (Reynolds et al., 1990).

Starch is a major component of *Apios* tubers (~68% dry matters) (Ogasawara, Hidano, & Kato, 2006). Physicochemical properties of the *Apios*-tuber starch, however, have not been fully understood (Kikuta et al., 2011). A better understanding of the structures and properties of the starch is important for product developments using *Apios* tubers. It is also important for the starch industry to develop new starch-based ingredients with unique functionalities and good processing properties using alternative crops (Ji et al., 2003).

Hoshikawa (1995) reported the growth patterns of *Apios* tubers growing in the field. The mother (seed) tuber shows a decrease in mass until the full growth of the shoot, followed by an increase in mass thereafter until the end of the plant growth. The growth pattern of the mother tuber of *Apios* is similar to that of the root of sweet potato (Kodama, Nomoto, & Watanabe, 1957), but is different from other tubers, such as potato and Chinese yam (Hoshikawa, 1995). The mother tubers of potato and Chinese yam continue to degenerate during the plant growth. These results suggest that both starch degradation and starch biosynthesis occur in *Apios* mother-tuber. Because of the unique growth pattern of *Apios* tubers, characterization of the starch isolated from mother and child tubers would advance understandings of the mechanism of starch biosynthesis during the development of *Apios* tubers.

Objectives of this study were to 1) characterize physicochemical properties of *Apios*-tuber starch; and to 2) understand differences in starch structures and properties between the mother and child tubers and the mechanism of starch development in the mother tuber.

Results obtained from this study will provide understandings of physicochemical properties of the *Apios*-tuber starch and the mechanism of starch biosynthesis in the mother tuber. Understanding properties of the *Apios*-tuber starch will be useful for the development of value-added applications of the starch.

2. MATERIALS AND METHODS

2.1 Materials

Three breeding lines (LA-898, LA-2127, and LA-2155; abbreviated hereafter as 898, 2127, and 2155) of *Apios* were grown at the North Central Regional Plant Introduction Station (NCRPIS), Ames, IA. The tubers of the three breeding lines harvested in 2012 were planted in 2013, and those harvested in 2013 were planted in 2014 as mother tubers to further grow and produce child tubers. Mother and child tubers harvested in 2013 and 2014 were used in this study. The mother tuber displayed different morphology from the child tuber. The mother tuber was connected to both the stolon and the above-ground stem of the plant. The end of the tuber where the above-ground stem emerged was designated as the bud end, and the opposite end was designated as the distal end. The mother tuber was much larger in size (8-9 cm in diameter) than the child tuber (2-4 cm in diameter) (**Figure S-1**).

Pseudomonas isoamylase (EC 3.2.1.68, 280 U/mg) was purchased from Megazyme International Ireland (Wicklow, Ireland). All other chemicals were reagent grade and were purchased from either Sigma-Aldrich Co. (St. Louis, MO) or Fisher Scientific (Pittsburgh, PA) and used without further treatments.

2.2 Starch Isolation by Wet-Milling

The tubers were peeled and cut into small pieces (1cm × 1cm × 0.5cm). The cut samples were wet-milled using a blender, and starches were isolated following the procedures reported by Li, Jiang, Campbell, Blanco, & Jane (2008).

2.3 Morphology of Starch Granules

Scanning electron micrographs of isolated starch granules were taken using a scanning electron microscope (JEOL 5800, Tokyo, Japan) following the methods previously reported (Ao & Jane, 2007). The average starch granule size was determined by measuring ~200 granules using an Infinity Analyze software (version 6.1.0, Lumenera Corp., Canada).

2.4 Crystallinity of Starch

Starch samples were equilibrated in a chamber with 100% relative humidity for 24 hours. X-ray diffraction patterns of the starch samples were analyzed using a diffractometer (Rigaku Ultima IV, Rigaku Americas, TX, USA) with copper Kα emission. The copper tube was operated at 44 mA and 40 kV, and the scanning region of the two-theta angle (2θ) was from 3° to 35°, with a scanning speed of 1°/min. The crystallinity of the starch was calculated using a MDI JADE software (version 6.5, Materials Data Inc., Livermore, California, USA). Crystallinity of the starch was calculated using the following equation:

Crystallinity (%) = 100% × Ac / $(Ac + Aa)$, where Ac is the crystalline area on the X-ray diffractogram and Aa is the amorphous area.

2.5 Amylose Content of Starch

The amylose content of the *Apios*-tuber starch was determined using an iodine potentiometric-autotitrator (702 SM Titrino, Brinkmann Instrument, Westbury, NY) (Song & Jane, 2000). Starch was defatted using 85% methanol in a Soxhlet extractor for 16 h prior to the analysis. The iodine affinity of amylose used for the calculation was 0.2 (Takeda & Hizukuri, 1987). The amylose content of the starch was calculated using the equation:

Amylose (%) = 100% × IA_s / 0.2, where IA_s was the iodine affinity of the starch.

2.6 Lipid Content of Starch

Lipids of the starch were extracted following the AOAC method 996.06 (2000). The lipid content of the starch was determined gravimetrically after removal of the solvent and calculated using the equation:

Lipid (%) = 100% × Weight of extracted lipids / Weight of the starch (db).

2.7 Branch-chain Length Distribution of Amylopectin

Amylopectin of the starch was separated from amylose and collected using a gel-permeation chromatographic (GPC) column packed with Sepharose CL-2B gel. The isolated amylopectin was debranched using *Pseudomonas* isoamylase (Megazyme International Irelands, Wicklow, Ireland). The branch chains of the debranched amylopectin were labeled with 8-amino-1,3,6-pyrenetrisulfonic acid (APTS) (0.2M APTS in 15% acetic acid), and the branch-chain length distribution was analyzed using a fluorophore-assisted capillary electrophoresis (P/ACE MDQ) (Beckman Coulter, Fullerton, CA) following the methods previously reported (Jiang, Campbell, Blanco, & Jane, 2010; Morell, Samuel, & O'shea, 1998).

2.8 Thermal Properties of Starch

Thermal properties of the isolated starch were analyzed using a differential scanning calorimeter (DSC, Diamond, Perkin-Elmer, Norwalk, CT) following the method of Song & Jane, (2000). Starch gelatinization onset (T_o), peak (T_p), and conclusion temperatures (T_c), and enthalpy change (ΔH) were obtained using a Pyris software (Perkin-Elmer).

2.9 Characterization of Starches Displaying Double Thermal-Transitions of Gelatinization

To characterize starches displaying two peaks of gelatinization, a starch sample was heated in a DSC to 65 ºC (Step 1 heating), the temperature between the two thermal-transition peaks in the original thermogram. The sample was cooled down to 20 ºC, and then

reheated to 110 ºC (Step 2 heating). The thermograms were obtained using a Pyris software (Perkin-Elmer).

2.10 Isolation of Starch Granules with Different Gelatinization-Temperatures

The mother-tuber starch of *Apios* 2127 displaying two peaks of gelatinization were separated to two groups of starch granules: the Group 1 starch gelatinized below 65 ºC and the Group 2 starch gelatinized at temperatures above 65 ºC. The Group 2 starch was isolated by incubating a starch suspension (1%, w/v) at 65 ºC for 20min to gelatinize the Group 1 starch. The un-gelatinized Group 2 starch, which maintained a crystalline structure and had a greater density than the gelatinized Group 1 starch, was isolated by centrifugation at 1,000 *g* after washing with warm water (65 ºC). The process was repeated for five times.

2.11 Pasting Properties of Starch

Pasting properties of the starch were analyzed using a Rapid Visco-Analyzer (Newport Scientific, Sydney, Australia) following the methods of Ao & Jane (2007), with minor modifications. A starch suspension (6%, dsb, w/w) was used for the RVA analysis. The pasting temperature, and the peak, breakdown, and final viscosities were determined using the Thermocline software (Newport Scientific).

2.12 Statistical Analysis

Data were subjected to analysis of variance and Tukey's multiple comparison analysis using PROC ANOA procedure of SAS 9.2 (SAS Institute, Inc., Cary, NC).

3. RESULTS AND DISCUSSION

3.1 Granule Morphology and Crystalline Structures

Images of *Apios*-tuber starch granules obtained using a scanning electron microscope are shown in **Figure 1**. The granules displayed smooth surface with the long-axis diameters ranging 1-30 μm. Granules with diameters larger than 5 μm showed an ellipsoidal, rod, or

kidney shape, whereas granules with diameters smaller than 5 μm showed a spherical or ellipsoidal shape (**Figure 1**). Average granule-diameters and number-percentages of large granules (> 5 μm) are shown in **Table 1**. For the 2013 samples, the child-tuber starches of *Apios* 2127 and 2155 showed significantly ($p<0.05$) smaller granule-size (8.0 and 8.6 μm in diameter, respectively) than their counterpart mother-tuber starches (10.1 and 9.8 μm in diameter, respectively). Child-tuber starches of all the varieties showed smaller number-percentages of large granules (73.0-77.6%) than their counterpart mother-tuber starches (78.0-85.9%). For the 2014 samples, the child-tuber starch of *Apios* 2155 showed smaller granule-size (9.8 μm in diameter) and percentage of large granules (73.7%) than the mother-tuber starch (10.9 μm in diameter and 77.9%, respectively), whereas *Apios* 898 and 2127 showed no significant differences in granule size and percentage of large granules between the child- and mother-tuber starches.

X-ray diffraction analyses of *Apios*-tuber starches showed a typical C-type diffraction pattern with strong peaks at 2θ of 5.5°, 15.0°, 17.0°, and 23.0° (**Figure S-2**). Percentage-crystallinity of the child-tuber starches ranged 23.4-23.9% for the 2013 samples and 23.0-24.4% for the 2014 samples, whereas that of the mother-tuber starches ranged 25.6-26.4% for the 2013 samples and 25.9-26.2% for the 2014 samples (**Table 1**). All the child-tuber starches showed less crystallinity than their counterpart mother-tuber starches.

3.2 Amylose and Lipid Contents of Starch

Amylose contents of *Apios*-tuber starches are shown in **Table 1**. For the 2013 samples, the child-tuber starches of *Apios* 898 and 2127 showed no significant difference in amylose contents (32.1 and 32.2%, respectively) from the mother-tuber starches (31.9 and 32.5%, respectively), whereas the child-tuber starch of *Apios* 2155 showed a significantly smaller ($p<0.05$) amylose content (32.1%) than the mother-tuber starch (33.1%). For the 2014 samples, the child-tuber starch of *Apios* 898 showed no significant difference in the amylose

content (32.5%) from the mother-tuber starch (32.2%), whereas the child-tuber starches of *Apios* 2127 and 2155 showed significantly smaller ($p<0.05$) amylose contents (32.5 and 31.8%, respectively) than their counterpart mother-tuber starches (34.4 and 33.2%, respectively). The mother-tuber starches that had larger granule-size and consisted of more large-granules displayed greater amylose-contents than their counterpart child-tuber starches (**Table 1**). These results agreed with that previously reported for maize starch: the amylose content increased with the increase in starch granule-size during the development of the starch (Li, Blanco, & Jane, 2007; Pan & Jane, 2000).

Lipid contents of the *Apios*-tuber starches ranged from 0.23 to 0.31% for the 2013 samples and from 0.19 to 0.32% for the 2014 samples (**Table 1**). All the samples, except the *Apios* 2155 grown in 2014, displayed a trend that the mother-tuber starch consisted of more lipid than the child-tuber starch, although the differences in lipid contents were not significant.

3.3 Amylopectin branch-chain length

The child-tuber starches showed significantly ($p<0.05$) larger percentages of short branch-chains of amylopectin (DP<12, 20.7-21.1% for 2013 samples and 21.1-21.6% for 2014 samples) than their counterpart mother-tuber starches (19.6-20.0% for 2013 samples and 19.4-21.1% for 2014 samples) (**Table 2**). The child-tuber starches also showed significantly smaller percentages of long branch-chains (DP>37, 17.3-17.9% for 2013 samples and 16.8-18.5% for 2014 samples) than their counterpart mother-tuber starches (17.8-18.8% for 2013 samples and 17.4-19.0% for 2014 samples). As a result, the child-tuber starches showed shorter average branch-chain length (23.4-23.9 DP for 2013 samples and 23.0- 24.1 DP for 2014 samples) than their counterpart mother-tuber starches (24.0- 24.5 DP for 2013 samples and 23.6- 24.5 DP for 2014 samples).

3.4 Starch Thermal Properties

DSC thermograms of *Apios* child- and mother-tuber starches are shown in **Figure 2**, and the data are summarized in **Table 3**. The child-tuber starches showed significantly lower onset gelatinization-temperatures and smaller enthalpy-changes (56.0-57.5 ºC and 14.2-15.2 J/g for 2013 samples and 56.2-57.2 ºC and 14.5-15.0 J/g for 2014 samples, respectively) than their counterpart mother-tuber starches (57.0-59.4 ºC and 14.6-15.7 J/g for 2013 samples and 57.6-58.3 ºC and 15.3-15.9 J/g for 2014 samples, respectively). The onset-gelatinization temperatures of the starches were negatively correlated ($r = -0.78$, $p < 0.01$) with the percentages of the short branch-chains (DP<12, **Table 2**), consistent with that previously reported (Jane et al., 1999; Srichuwong, Sunati, Mishima, Isono, & Hisamatsu, 2005a). The enthalpy change of starch gelatinization reflects the energy required to dissociate the double-helical crystalline structures of starch (Donovan, 1979). The smaller gelatinization enthalpy-changes of the child-tuber starches were consistent with the lower percentage-crystallinity of the child-tuber starches than that of the mother-tuber starches (**Table 1**).

Almost all the *Apios* samples grown in both years showed a second peak, a tail or a shoulder in the DSC thermogram (**Table 3**, **Figure 2**), suggesting segregated thermal-transitions of starch gelatinization. The shoulders, except *Apios* 2127 mother-tuber starch, were present around 75.2-76.2 ºC for the 2013 samples, and around 72.3-75.9 ºC for the 2014 samples. Among all the samples, the mother-tuber starch of *Apios* 2127 grown in 2013 displayed the most distinctly separated peaks in the DSC thermogram, with the first peak (minor peak) at 63.7 ºC and the second peak (major peak) at 72.8 ºC (**Figure 2**). This pattern is rarely observed except for pea starch (C-type polymorph) heated in a salt solution (Bogracheva, Morris, Ring, & Hedley, 1997). The mechanism of the two gelatinization-peaks of *Apios* 2127 mother-tuber starch grown in 2013 was further investigated as follows.

3.5 The Mechanism of Two Gelatinization-Peaks of Starch

The two gelatinization-peaks of starch could result from two independent thermal-transitions of two groups of starch granules with different gelatinization-temperature or two-stage thermal-transition of the same starch granules (Bogracheva et al., 1997; Ji et al., 2003). Bogracheva, et al. (1997) reported two gelatinization-peaks in the DSC thermogram of pea starch (C-type polymorph) when the pea starch was heated in a salt solution. The authors demonstrated that the dissociation of crystalline structures during gelatinization of the pea starch began in the area around the hilum, where the starch had the B-type polymorph, and then propagated radially to the peripheral area, where the starch had the A-type polymorph. The pea starch, therefore, displayed a two-stage thermal-transition of gelatinization.

A two-step heating experiment was conducted using the method described in **Section 2.9** to understand the mechanism of the two-peak gelatinization of *Apios* 2127 mother-tuber starch. After being heated to 65 ºC and the sample was cooled down and reheated, there was only a single peak shown in the thermogram, and the temperature of the peak was consistent with that of the second peak in the original gelatinization-thermogram (**Figure 3 (A)**). After being heated to 65 ºC, some granules showed complete loss of Maltese cross, whereas others retained either intact or partial Maltese cross (**Figure 3 (B)**).These results indicated that the two gelatinization-peaks corresponded to gelatinization of two different groups of starch granules: Group 1 starch gelatinized below 65 ºC and Group 2 starch gelatinized at temperatures above 65 ºC.

The Group 1 and Group 2 starches were separated by gelatinizing and removing the Group 1 starch using the method described in **Section 2.10**. The Group 2 starch was collected and characterized to understand differences in physicochemical properties between the Group 1 and Group 2 starch. The SEM images of the Group 2 starch granules are shown in **Figure S-3**, which displayed intact granular structures. The Group 2 starch showed a substantially

greater number-percentage of large granules (89.6%) and amylose content (34.5%) than the native starch (78.0% and 32.5%, respectively) (**Table 4**). The average branch-chain length and percentage of long branch-chains (DP > 37) of the Group 2 starch (DP 24.2 and 18.1%, respectively) were slightly greater than that of the native starch (DP 24.0 and 17.8%, respectively) (**Table 4**). These results indicated that the Group 2 starch had more large-granules, consisted of more amylose, gelatinized at a higher temperature, and retained Maltese cross after heating at 65 ºC.

3.6 Locations of the Group 1 and Group 2 Starch in the *Apios* Mother Tuber

Starches at different locations of the *Apios* 2127 mother tuber was isolated and characterized to understand where the starch granules of the Group 1 and 2 were located in the tuber after the second-year growth. Starch granules were isolated from the central region and two peripheral regions of the tuber, the bud end that was connected to the stolon and above-ground stem and the distal end that was on the opposite side of the bud end (**Figure S-1**). Morphology of starch granules is shown in **Figure S-3**, and the data of granule size are summarized in **Table 4**. The starch located at the central region of the mother tuber showed significantly ($p<0.05$) larger granule-size (average 10.0 μm in diameter) and greater number-percentage of large granules (79.7%) than the starch located at the bud end (8.8 μm in diameter and 74.0%, respectively) and the distal end (7.2 μm in diameter and 61.7%, respectively). The starch in the central region also consisted of significantly greater amylose content (33.8%) than that at the bud end (30.7%) and the distal end (30.5%) (**Table 4**). Amylopectin branch-chain length distributions of the starches are shown in **Table 4**. The starch in the central region showed a larger proportion of long branch-chains (DP>37, 17.8%) and a longer average branch-chain length (DP 24.0) than the starch at the bud end (17.6% and DP 23.9, respectively) and the distal end (17.5% and DP 23.7, respectively), although the differences were not statistically significant. These results indicated that the Group 1 starch

was mostly located in the peripheral regions, whereas the Group 2 starch was mostly in the central region of the tuber.

The Group 1 starch of *Apios* 2127 mother tuber showed similar gelatinization peak-temperature (63.7 ºC) (**Figure 2**) to the counterpart child-tuber starch (64.2 ºC) (**Table 3**). The child tuber and its starch granules were initiated and developed in the second year of plant growth, displaying smaller granule-size, less amylose content, and lower gelatinization-temperature than the mother-tuber starch that developed for two years (**Table 1**, **Table 3**). The similarity between the Group 1 starch and the child-tuber starch suggested that the Group 1 starch was synthesized during the second-year growth of the mother tuber in the bud end and distal end. On the contrary, the Group 2 starch, located in the central region of the tuber, was likely carried over from the previous growing season, further grew in the second year, and also annealed for two years. Therefore, the Group 2 starch gelatinized at a higher temperature.

3.7 Starch Pasting Properties

The child-tuber starches showed significantly lower ($p<0.05$) pasting temperatures (72.3-74.1 ºC for 2013 samples and 70.9-72.5 ºC for 2014 samples) but higher peak viscosities (99.8-119.8 RVU for 2013 samples and 88.2-112.9 RVU for 2014 samples) than their counterpart mother-tuber starches (75.4-76.0 ºC for 2013 samples and 73.3-75.9 ºC for 2014 samples, and 94.3-97.6 RVU for 2013 samples and 84.5-94.0 RVU for 2014 samples, respectively) (**Table 5**). The differences in pasting properties between the child- and mother-tuber starches could be attributed to the larger amylose and lipid contents of the mother-tuber starches than that of the child-tuber starches (**Table 1**). It is known that amylose-lipid complex intertwines with amylopectin and restricts granule swelling, contributing to a higher pasting temperature and lower viscosity of the starch (Jane et al. 1999; Srichuwong, Sunati, Mishima, Isono, & Hisamatsu, 2005b). In addition, the *Apios* mother tubers were grown in

the field for consecutive two years and went through a longer annealing process. Annealing is known to enhance double-helical crystalline structures of starch, reduce the rate of starch hydration, and restrict granule swelling (Tester, 1997; Tester, Debon, & Sommerville, 2000), which contributes to the higher pasting temperatures and lower viscosities of the mother-tuber starches.

4. CONCLUSIONS

In this study, physicochemical properties of the child- and mother-tuber starches of a new food crop, *Apios americana*, were analyzed, and the mechanism underlying the two-peak gelatinization of *Apios* mother-tuber starch were investigated and illustrated. The mother-tuber starches of *Apios* displayed larger granule sizes in general, greater crystallinity, larger gelatinization enthalpy-changes, longer branch-chain lengths of amylopectin, and lower pasting viscosity than their counterpart child-tuber starches. The mother tubers were growing for two years, and the starch went through a further growth and was subjected to a longer annealing process, resulting in the greater crystallinity, higher pasting temperature, and lower pasting viscosity of the mother-tuber starch. The mother-tuber starch of *Apios* 2127 showed distinct two-gelatinization peaks, which was attributed to two groups of starch granules gelatinizing at different temperatures. The starch granules initiated and synthesized in the second year of planting located at the bud and distal end of the mother tuber gelatinized at a lower temperature, whereas the granules located in the central region of the mother tuber, which were likely carried over from previous year and went through a further growth and a longer annealing process, gelatinized at a higher temperature. These results indicated that starch biosynthesis in the mother tuber during the second year of growth was more active at the bud and distal end than in the central region of the tuber.

ACKNOWLEDGEMENTS

We thank Microscopy and NanoImaging Facility at Iowa State University for the microscopic study.

REFERENCES

AOAC. 2000. AOAC official method 996.06, fat (total, saturated, and unsaturated) in foods. Page 20-24. In Official methods of analysis of AOAC international (17th ed.). Maryland: AOAC International.

Ao, Z.; & Jane, J. 2007. Characterization and modeling of the A- and B-granule starches of wheat, triticale, and barley. *Carbohydr. Polym.* 67, 46-55.

Belamkar, V.; Wenger, A.; Kalberer, S.R.; Bhattacharya, V.G.; Blackmon, W.J.; & Cannon, S.B. 2015. Evaluation of phenotypic variation in a collection of Apios americana: an edible tuberous legume. *Crop Sci*. 55, 712-726.

Bogracheva, T. Y.; Morris. V.J.; Ring, S.G.; Hedley, C.L. 1997. The granular structure of C-type pea starch and its role in gelatinization. *Biopolymers* 45, 323-332.

Donovan, J. W. 1979. Phase transitions of the starch-water system. *Biopolymers* 18, 263-275.

Hoshikawa, K. 1995. The growth of Apios (*Apios Americana* Medikus), a new crop, under field conditions. *Jpn. J. Crop. Sci.* 64, 323-327.

Iwai, K.; & Matsue, H. 2007. Ingestion of *Apios americana* Medikus tuber suppresses blood pressure and improves plasma lipids in spontaneously hypertensive rats. *Nutrition Res.* 27, 218-224.

Jane, J.; Chen, Y.Y; Lee, L.F.; McPherson, A.E.; Wong, K.S.; Radosavljevic, M.; Kasemsuwan, T. 1999. Effects of amylopectin branch chain length and amylose content on the gelatinization and pasting properties of starch. *Cereal Chem*. 76, 629-637.

Ji, Y.; Seetharaman, K.; Wong, K.; Pollak, L.M.; Duvick, S.; Jane, J.; White, P.J. 2003. Thermal and structural properties of unusual starches from developmental corn lines. *Carbohydr. Poly.* 51, 439-450.

Jiang, H., Campbell, M., Blanco, M., & Jane, J. 2010. Characterization of maize amylose-extender (*ae*) mutant starches. Part II: Structures and properties of starch residues remaining after enzymatic hydrolysis at boiling-water temperature. *Carbohydr. Polym.* 80, 1-12.

Kazuhiro, N.; Nihei, K.; Ogsawara, Y.; Koga, H.; Kato, Y. 2011. Novel isoflavone diglycoside in groundnut (*Apios americana* Medik). *Food Chem.* 124, 703-710.

Kinugasa, H. & Watanabe, Y. 1992. Nutritional composition of the tubers of American groundnut (*Apios americana* Medikus). *Sonoda Women's College Sudies* 26, 209-218.

Kikuta, C.; Sugimoto, Y.; Konishi, Y.; Ono, Y.; Tanaka, M.; Iwaki, K.; Fujita, S.; Kawanishi-Asaoka, M. 2011. Physicochemical and structural properties of starch isolated from *Apios americana* Medikus. *J. Appl. Glycosci*. 59, 21-30.

Kodama, T.; Nomoto, T.; & Watanabe, K. 1957. Growth process of sweet potato plants grown directly from seed tubers. (I) Growth of tops and tuberous roots of sweet potato plants. *Proc. Crop Sci. Soc. Japan* 25, 147-148.

Li, L., Blanco, M., & Jane, J. 2007. Physicochemical properties of endosperm and pericarp starches during maize development. *Carbohydr. Poly*. 67, 630-639.

Li, L., Jiang, H., Campbell, M., Blanco, M., & Jane, J. 2008. Characterization of maize amylose-extender (*ae*) mutant starches. Part I: Relationship between resistant starch contents and molecular structures. *Carbohydr. Polym*. 74, 396-404.

Morell, M. K., Samuel, M. S., & O'Shea, M. G. 1998. Analysis of starch structure using fluorophore-assisted carbohydrate electrophoresis. *Electrophoresis* 19, 2603–2611.

Ogasawara, Y.; Hidano, Y.; Kato, Y. 2006. Study on carbohydrate composition of Apios (*Apios americana* Medikus) flowers and tubers. *Nippon Shokuhin Kagaku Kougaku Kaishi*, 53, 40–46.

Pan, D.D. & Jane, J. 2000. Internal structure of normal maize starch granules revealed by chemical surface gelatinization. *Biomacromolecules* 1, 126-132.

Reynolds, B.D.; Blackmon, W.J.; Wickremesinhe, E.; Wells, M.H.; & Constantin, R.J. 1990. Domestication of *Apios americana*. p. 436-442. In: J. Janick and J.E. Simon (eds.), Advances in new crops. Timber Press, Portland, OR.

Song, T. & Jane, J. 2000. Characterization of barley starches of waxy, normal, and high amylose varieties. *Carbohydr. Polym*. 41, 365-377.

Srichuwong, S.; Sunati. T.C.; Mishima, T.; Isono, N.; Hisamatsu, M. 2005a. Starches from different botanical sources I: Contribution of amylopectin fine structures to thermal properties and enzyme digestibility. *Carbohydr. Polym.* 60, 529-538.

Srichuwong, S.; Sunati. T.C.; Mishima, T.; Isono, N.; Hisamatsu, M. 2005b. Starches from different botanical sources II: Contribution of starch structure to swelling and pasting properties. *Carbohydr. Polym.*62, 25-34.

Takeda, Y., & Hizukuri, S. 1987. Structures of rice amylopectins with low and high affinities for iodine. *Carbohydr. Research* 168, 79-88.

Tester, R. F. 1997. Influence of growth conditions on barley starch properties. *Int. J. Biol. Macromo*. 21, 37-45.

Tester, R. F., Debon, S. J. J., & Sommerville, M. D. 2000. Annealing of maize starch. *Carbohydr. Polym*. 42, 287-299.

Wilson, P.W.; Gorny, J.R.; Blackmon, W.J.; & Reynolds, B.D. 1986. Fatty acids in the American groundnut (*Apios americana*). *J. Food Science* 51, 1387-1388.

Wilson, P.W.; Pichardo, F.J.; Liuzzo, J.A.; Blackmon, W.J.; & Reynolds, B.D. 1987. Amino acids in the American groundnut (*Apios americana*). *J. Food Science* 52, 224-225.

Wilson, P.W.; Pichardo, F.J.; Blackmon, W.J.; & Reynolds, B.D. 1990. Protein quality in *Apios Americana* tubers and seeds. p. 443. In: J. Janick and J.E. Simon (eds.), Advances in new crops. Timber Press, Portland, OR.

Table 1. Average granule size, percentage of large granules, amylose and lipid contents, and crystallinity (%) of *Apios*-tuber starches [a]

	Samples		Average granule diameter (μm)	Large granules (%) [b]	Amylose (%)	Lipid (%)	Crystallinity (%)
2013	898	Child	9.8**a**±5.2	77.6	32.1**a**±0.4	0.23**a**±0.00	23.9
		Mother	9.4**a**±4.6	79.1	31.9**a**±0.0	0.28**a**±0.05	25.6
	2127	Child	8.0**b**±3.8	73.0	32.2**a**±0.1	0.24**a**±0.03	23.8
		Mother	10.1**a**±4.9	78.0	32.5**a**±0.1	0.26**a**±0.01	25.7
	2155	Child	8.6**b**±4.4	75.8	32.1**b**±0.3	0.26**a**±0.05	23.4
		Mother	9.8**a**±4.5	85.9	33.1**a**±0.2	0.31**a**±0.00	26.4
2014	898	Child	9.5**a**±5.4	75.7	32.5**a**±0.0	0.27**a**±0.01	24.4
		Mother	9.1**a**±4.9	74.2	32.2**a**±0.5	0.32**a**±0.06	26.2
	2127	Child	9.8**a**±5.8	74.3	32.5**b**±0.5	0.19**a**±0.00	24.4
		Mother	9.9**a**±5.5	75.1	34.4**a**±0.2	0.21**a**±0.00	25.9
	2155	Child	9.8**b**±5.8	73.7	31.8**b**±0.3	0.31**a**±0.02	23.0
		Mother	10.9**a**±6.5	77.9	33.2**a**±0.5	0.29**a**±0.01	26.1

[a] Different letters following the mean values within the same columns and same breeding lines indicate statistically different mean values between the child and mother tuber starches ($p<0.05$).

[b] Number-percentage of the granules with a granule diameter > 5 μm.

Table 2. Amylopectin branch-chain length distribution [a] of *Apios*-tuber starches [b]

	Sample		DP<12	DP13-24	DP25-37	DP>37	Ave.CL
2013	898	Child	20.7**a**±0.0	47.8±0.2	13.9±0.0	17.6**a**±0.1	23.8**a**±0.1
		Mother	19.8**b**±0.1	48.1±0.4	14.2±0.1	17.9**a**±0.2	24.0**a**±0.1
	2127	Child	20.9**a**±0.1	48.0±0.1	13.8±0.0	17.3**b**±0.0	23.4**b**±0.0
		Mother	20.0**b**±0.2	48.3±0.0	13.9±0.2	17.8**a**±0.3	24.0**a**±0.2
	2155	Child	21.1**a**±0.0	47.1±0.0	13.9±0.0	17.9**b**±0.0	23.9**b**±0.0
		Mother	19.6**b**±0.0	47.8±0.2	14.0±0.1	18.8**a**±0.3	24.5**a**±0.2
2014	898	Child	21.6**a**±0.1	46.0±0.3	13.8±0.0	18.5**b**±0.2	24.1**a**±0.2
		Mother	21.1**b**±0.0	46.3±0.1	13.6±0.2	19.0**a**±0.0	24.5**a**±0.2
	2127	Child	21.1**a**±0.1	48.2±0.2	14.0±0.1	16.8**b**±0.2	23.0**b**±0.1
		Mother	19.6**b**±0.2	48.8±0.0	14.3±0.0	17.4**a**±0.1	23.6**a**±0.1
	2155	Child	21.4**a**±0.0	47.6±0.2	14.0±0.2	17.0**b**±0.0	23.3**b**±0.2
		Mother	19.4**b**±0.0	48.1±0.0	14.3±0.0	18.2**a**±0.0	24.0**a**±0.0

[a] Molar basis. [b] Different letters following the mean values within the same columns and same breeding lines indicate statistically different mean values between the child and mother tuber starches ($p<0.05$).

Table 3. Thermal properties of *Apios*-tuber starches [a]

	Samples		T_o [b] (ºC)	Peak 1(ºC)	Peak 2(ºC)	T_c(ºC)	ΔH(J/g)
2013	898	Child	57.5**b**±0.3	67.5±0.0	76.0±0.2	79.9**b**±0.0	14.2**b**±0.0
		Mother	59.4**a**±0.2	69.7±0.1	ND	80.6**a**±0.0	14.6**a**±0.1
	2127	Child	56.1**a**±0.5	64.2±0.7	76.2±0.3	81.0**a**±0.1	14.2**b**±0.1
		Mother	57.0**a**±0.2	63.7±0.2	72.8±0.6 *	80.6**a**±0.8	15.2**a**±0.2
	2155	Child	56.0**b**±0.3	64.0±0.1	75.2±0.0	81.1**a**±0.2	15.2**b**±0.0
		Mother	58.4**a**±0.3	69.4±0.5	76.0±0.1	81.8**a**±0.4	15.7**a**±0.3
2014	898	Child	56.3**b**±0.1	60.3±0.4	72.3±0.0	77.9**b**±0.5	15.0**b**±0.1
		Mother	57.6**a**±0.2	64.5±0.3	74.9±0.2	82.5**a**±0.5	15.7**a**±0.1
	2127	Child	57.2**b**±0.1	62.2±0.5	74.9±0.7	80.2**b**±0.2	14.9**b**±0.2
		Mother	58.1**a**±0.0	62.9±0.1	74.9±0.3	81.1**a**±0.0	15.9**a**±0.2
	2155	Child	56.2**b**±0.2	61.1±0.0	72.8±0.1	79.6**b**±0.3	14.5**b**±0.0
		Mother	58.3**a**±0.1	65.5±0.0	75.9±0.4	82.1**a**±0.0	15.3**a**±0.2

[a] Different letters following the mean values within the same columns and same breeding lines indicate statistically different mean values between the child and mother tuber starches ($p<0.05$). [b] T_o= onset gelatinization temperature, T_c= conclusion temperature, ΔH= enthalpy change. ND = Not detectable. Peak 1 is the major peak and Peak 2 is the minor peak for all the samples except for *Apios* 2127 mother tuber grown in 2013. * Major peak.

Table 4. Granule size, percentage of large granules, amylose content, and amylopectin branch-chain length distribution of *Apios* 2127 mother-tuber starches [a]

Sample	Average granule diameter (μm)	Large granules (%) [b]	Amylose (%)	DP<12	DP13-24	DP25-37	DP>37	Ave.CL [c]
Native	10.1**a**±4.9	78.0	32.5**b**±0.1	20.0**b**±0.2	48.3±0.0	13.9±0.2	17.8**a**±0.3	24.0**a**±0.2
Group 2 granules [d]	10.8**a**±4.5	89.6	34.5**a**±0.6	20.0**b**±0.1	47.9±0.0	14.0±0.0	18.1**a**±0.1	24.2**a**±0.1
Bud end [e]	8.8**b**±4.6	74.0	30.7**c**±0.4	20.1**ab**±0.3	48.1±0.1	14.2±0.0	17.6**a**±0.2	23.9**a**±0.1
Center	10.0**a**±4.9	79.7	33.8**a**±0.1	20.1**ab**±0.0	48.1±0.4	14.0±0.3	17.8**a**±0.1	24.0**a**±0.1
Distal end	7.2**c**±4.1	61.7	30.5**c**±0.3	20.6**a**±0.1	48.0±0.2	13.9±0.0	17.5**a**±0.2	23.7**a**±0.0

[a] Different letters following the mean values within the same columns indicate statistically different mean values ($p<0.05$). [b] Number-percentage of the granules with a granule diameter > 5 μm. [c] Ave.CL: average branch-chain length. [d] Group 2 granules: the group of starch granules of *Apios* 2127 mother tuber that gelatinized at higher temperatures. [e] The starch granules isolated from the bud end, center part, and distal end (opposite to the bud end) of *Apios* 2127 mother tuber.

Table 5. Pasting properties of *Apios*-tuber starches [a]

	Sample		Pasting Temp.(ºC)	Peak (RVU)	Hold (RVU)	Final (RVU)	Breakdown (RVU)	Setback (RVU)
2013	898	Child	72.3**b**±0.1	119.8**a**±2.4	71.5±1.4	124.0±2.8	48.3**a**±1.0	52.5**a**±1.4
		Mother	75.4**a**±0.4	96.5**b**±0.4	64.5±0.2	113.4±1.6	31.9**b**±0.2	48.9**a**±1.5
	2127	Child	74.1**b**±0.3	111.5**a**±1.7	82.0±1.8	144.0±2.1	29.4**a**±0.1	61.9**a**±0.2
		Mother	75.8**a**±0.0	97.6**b**±1.8	72.1±1.6	128.4±1.5	25.5**b**±0.2	56.3**b**±0.1
	2155	Child	73.8**b**±0.3	99.8**a**±2.5	68.8±1.1	123.8±1.1	31.0**a**±1.4	55.0**a**±0.0
		Mother	76.0**a**±0.1	94.3**a**±1.9	73.7±0.8	125.3±1.1	20.6**b**±2.8	51.6**a**±1.9
2014	898	Child	71.4**b**±0.0	112.9**a**±0.9	74.3±1.2	128.2±1.2	38.5**a**±0.3	53.8**a**±0.0
		Mother	75.9**a**±0.0	86.5**b**±0.5	74.0±0.1	124.0±1.1	12.5**b**±0.5	50.0**b**±1.1
	2127	Child	72.5**a**±0.3	88.2**a**±0.2	72.0±0.1	128.8±0.5	16.2**a**±0.4	56.8**b**±0.4
		Mother	73.3**a**±0.3	84.5**b**±0.1	72.5±0.0	134.4±0.6	12.0**b**±0.1	61.9**a**±0.6
	2155	Child	70.9**b**±0.2	102.7**a**±2.8	81.2±0.9	135.3±1.6	21.5**a**±1.9	54.0**a**±2.5
		Mother	75.6**a**±0.0	94.0**b**±1.7	72.1±1.4	117.5±0.1	22.0**a**±0.3	45.5**b**±1.5

[a] Different letters following the mean values within the same columns and same breeding lines indicate statistically different mean values between the child and mother tuber starches ($p<0.05$). RVU = Rapid visco-units.

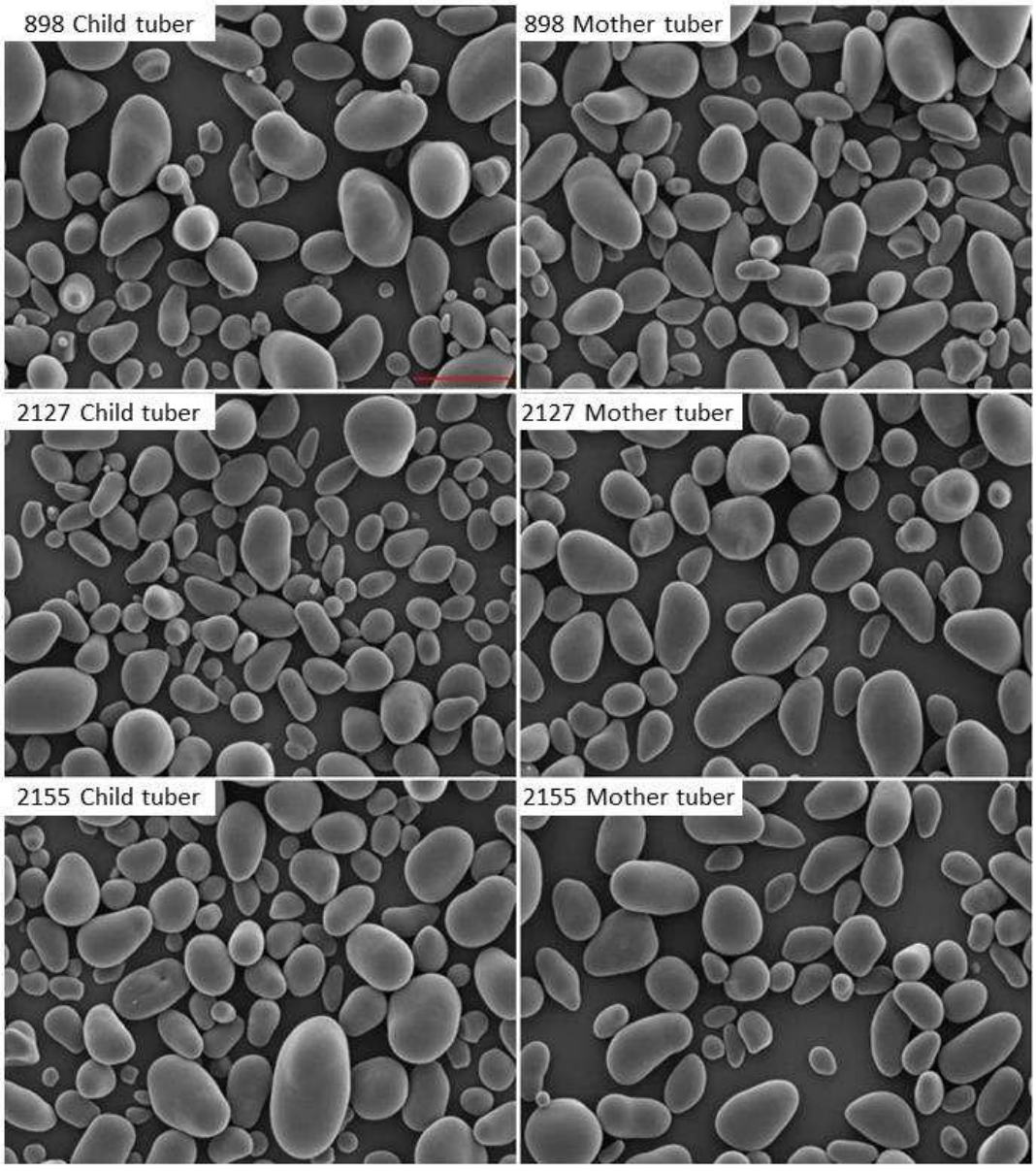

Figure 1. Scanning electron micrographs of *Apios*-tuber starch granules. Scale bar = 20 μm.

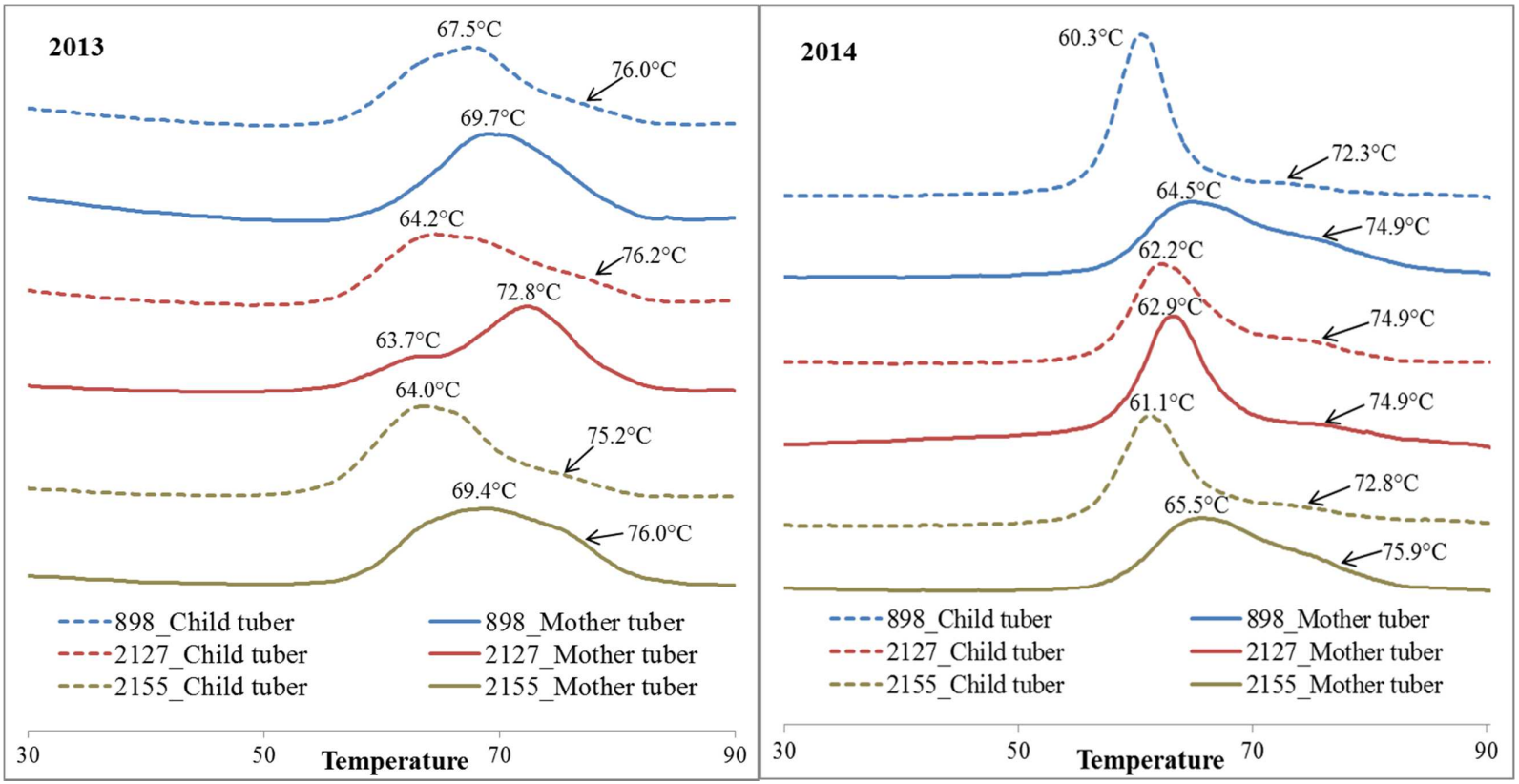

Figure 2. Starch thermographs of *Apios* tubers grown in 2013 and 2014. Peak temperatures of starch gelatinization are labeled above the peak of gelatinization curves. Arrows indicate the shoulders of the gelatinization curves.

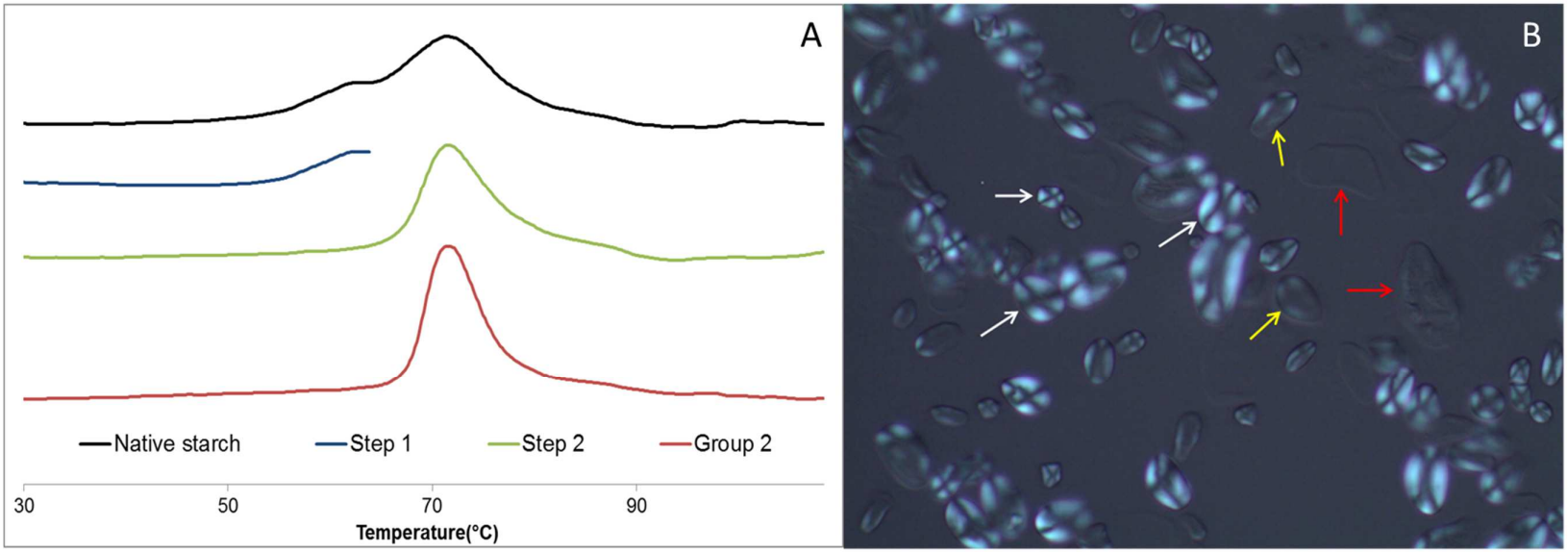

Figure 3. (A): DSC thermograms of *Apios* 2127 mother-tuber starches. The starch with three times of water (w/w) in a DSC pan was heated to 65 ºC (Step 1), cooled down to 20 ºC, and re-heated to 110 ºC (Step 2). Group 2 granules: The group of starch granules of *Apios* 2127 mother tuber that gelatinized above 65 ºC. (B): Micrograph of starch granules of *Apios* 2127 mother tuber under polarized light. The starch suspension (1%, w/v) was incubated at 65°C for 20min prior to the observation under the microscope. White arrows indicate granules that display intact Maltese crosses. Red arrows indicate completely gelatinized granules displaying no Maltese cross. Yellow arrows indicate partially gelatinized granules.

Supplementary Information

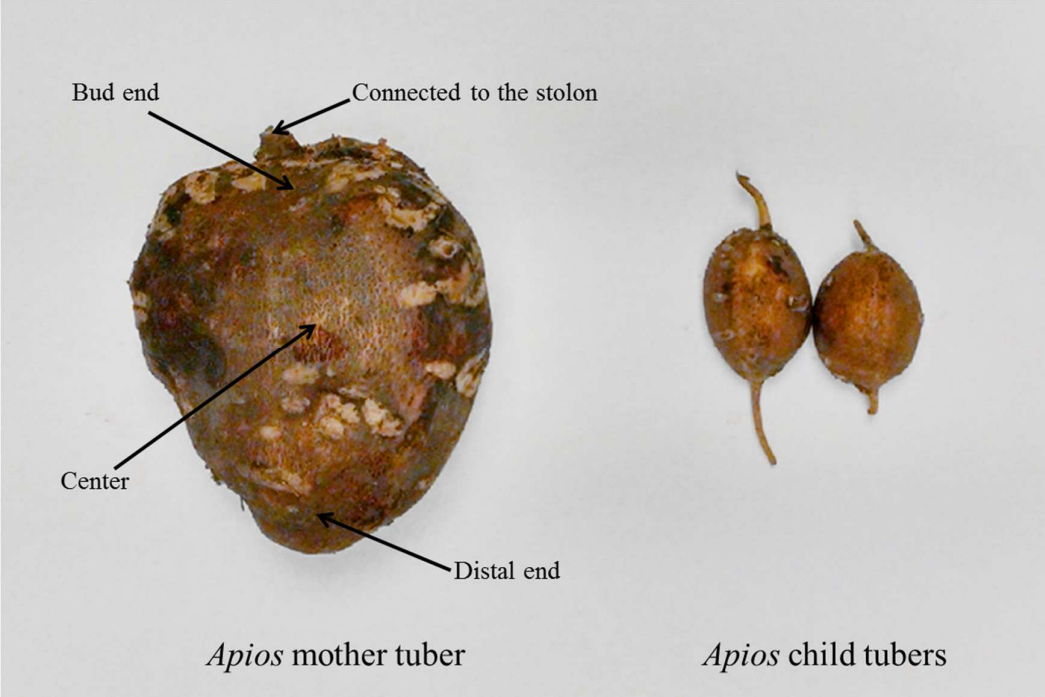

Figure S-1. Photos of *Apios* mother (left) and child tubers (right).

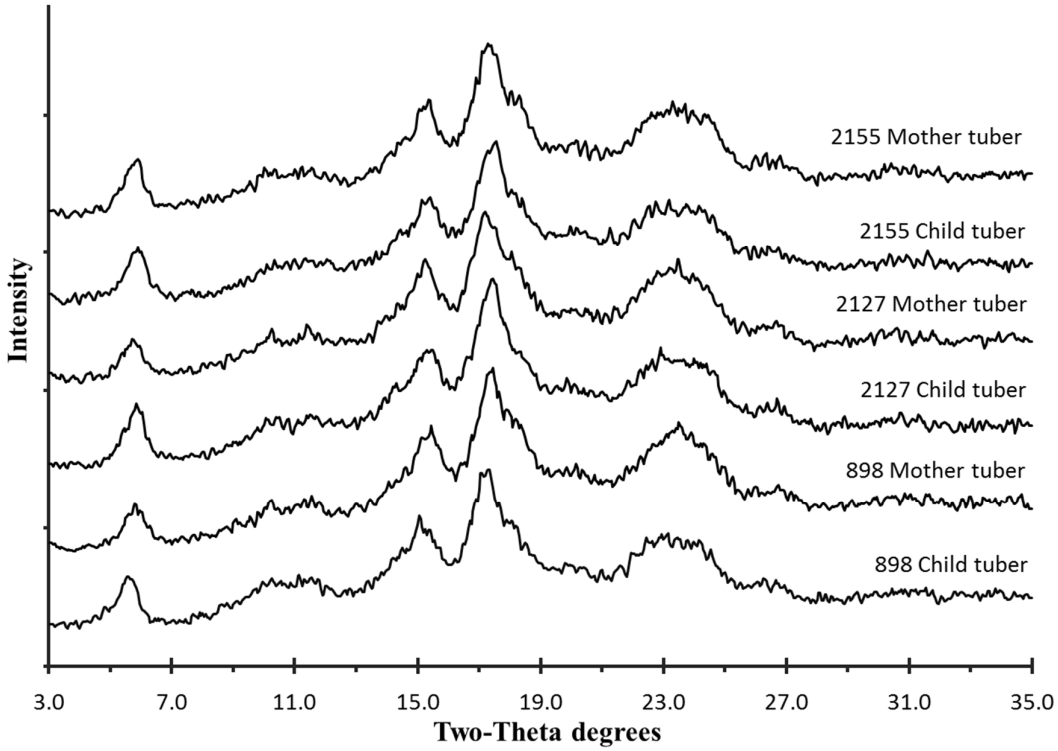

Figure S-2. X-ray diffraction pattern and crystallinity (%) of *Apios*-tuber starches.

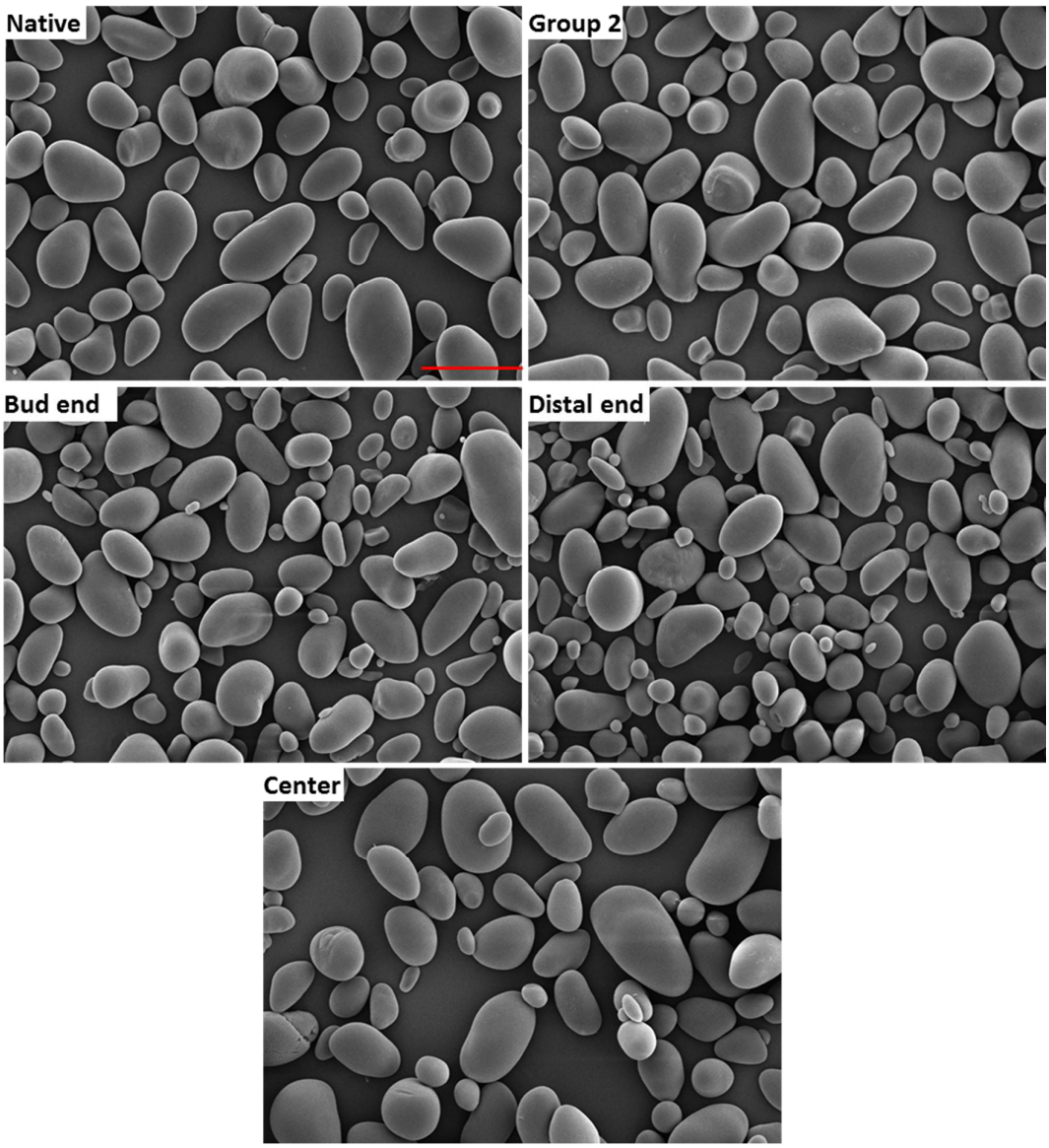

Figure S-3. Scanning electron micrographs of *Apios* 2127 mother tuber starch granules. Scale bar = 20 µm. Group 2 granules: The group of starch granules of *Apios* 2127 mother tuber that gelatinized at higher temperature. Granules of bud end, distal end, and center part: The starch granules isolated from the bud end, distal end (opposite to the bud end), and center part of *Apios* 2127 mother tuber.

GENERAL CONCLUSIONS

This dissertation research reported effects of growing conditions during the development of starch granules and *waxy*-gene dosage on starch structures and properties. Two Tibetan hull-less barley varieties, BQ and KQ, were grown at two locations with different growing temperatures and amount of rainfall. The BQ starches showed lower percentage-crystallinity, lower onset-gelatinization temperature but larger gelatinization-temperature range than the KQ starches. The BQ starches showed significantly greater peak-viscosities (>2.1 folds) than the KQ starches. After removing the lipids from starch by treating starch with 2% sodium-dodecyl-sulfate solution, the starches showed significant decreases in pasting temperatures and increases in peak viscosities, and the KQ starches showed substantially greater increases in peak viscosities than the BQ starches. Annealing of starch and enhanced amylose-lipid complex formation, resulting from higher growing temperatures and more rainfall during the development of the KQ starches, likely contributed to the differences in thermal and pasting properties between the BQ and KQ starches. The cooked KQ starches displayed less rapidly-digestible starch content but more slowly-digestible and resistant-starch contents than the BQ starches, resulting from restricted swelling of the KQ starch granules compared with the BQ starch granules after cooking.

Different dosages of waxy gene (3, 2, 1, 0) in the endosperm of corn were developed by reciprocal crossing of isogenic normal and waxy corn lines. The negative correlation between the *waxy*-gene dosage and the percentage of extra-long branch chains supported that GBSSI was responsible for the biosynthesis of extra-long branch chains. GBSSI also increased the proportion of intermediate chains with DP 17-30 and decreased the proportion of short chains with DP < 17. The *waxy* gene showed dosage effects on the amylose content, but no effects on the molecular weight of amylose. The conclusion gelatinization-temperature and gelatinization temperature-range of the starch were positively correlated with the *waxy*-

gene dosage, indicating that amylose facilitates dissociation of surrounding double-helices of amylopectin.

Apios americana is a new food crop with high nutritional-values and health benefits. The seed (mother) tuber of *Apios* has a unique growing pattern compared with other tubers, such as potato and Chinese yam. The mother-tuber starches of *Apios* displayed larger granule sizes in general, greater crystallinity, larger gelatinization enthalpy-changes, longer branch-chain lengths of amylopectin, and lower pasting viscosity than their counterpart child-tuber starches. The mother-tuber starch of *Apios* 2127 showed distinct two-gelatinization peaks, which was attributed to two groups of starch granules gelatinizing at different temperatures. The Group 1 starch with smaller granule-size and less amylose-content gelatinized at a lower temperature and located more at the bud and distal end of the mother tuber. The Group 1 starch displayed similar granule-sizes and thermal properties to the counterpart child-tuber starch, indicated that the Group 1 starch initiated and synthesized in the second year of growing of the mother tuber. These results indicated that starch biosynthesis in the mother tuber during the second year of growth was more active at the bud and distal end than in the central region of the tuber.